Cosmic String Interactions

MASTER'S THESIS

Roland de Putter

Lorentz Institute of Theoretical Physics
Leiden University

Contents

Introduction

Over the past decade, cosmology, the study of the large scale properties of the universe, has rapidly become accessible to a range of observational tests. This has led to a standard model of cosmology, often referred to as the Concordance Model, in which the universe was formed about 14 billion years ago with the Big Bang. One of the most striking aspects of this model is that only 5 % of the energy content of the current universe consists of the types of matter (mainly baryonic matter) that we are familiar with. The other 95 % consists of Dark Matter (roughly 25 %), matter of which the only notable interaction with ordinary matter is through gravity, and Dark Energy (roughly 70 %), the "energy" responsible for the observed accelerated expansion of the universe. Cosmology can be important for theoretical (particle) physics in two ways. Firstly, any theory that claims to decribe the physics of our universe should be able to explain Dark Matter and Dark Energy. Secondly, the early universe could turn out to be the only setting in which new theories of particle physics can be tested. In particular, there is a lot of interest in so called grand unified field theories (GUT) of particle physics, in which the three fundamental forces (gravity is excluded) are unified into one force. Typically, the differences between a GUT and the current standard model of particle physics will only be observable at very high energy scales (order 10^{15} GeV). It is extremely difficult to reach these energy scales in particle accelerators on earth, but if we look back in time far enough in the early universe, there will be a time at which the typical particle energy is of this order. Hence, any candidate field theory for the description of particle physics could in principle be tested by comparing its predictions on cosmology to observations.

In certain field theories, field configurations may exist in which energy is trapped in a region and cannot dissipate away to infinity due to topological constraints on the evolution of the fields. A particular example of such a so called topological defect solution is the cosmic string. For these solutions, the energy is trapped around a line shaped region. Cosmic strings could be relevant to cosmology because certain grand unified theories of particle physics predict that a network of strings is formed in the very early universe. Such a network typically consists of both closed string loops and infinite strings. While the closed string loops can decay by emission of particles and gravitational radiation, topology prevents this from happening to the infinite strings. This is a potential problem because, if the infinite strings do not lose energy at a sufficiently high rate, they will come to dominate the energy content of the universe soon after the formation of the string network. This is clearly inconsistent with the current cosmological paradigm. A solution is offered by a process called intercommutation, the exchange of ends when two string segments come to intersect. If intercommutation occurs when an infinite string intersects itself, a loop is formed that subsequently decays. This way, the infinite string (network) loses some of its length and energy. It turns out that if the intercommutation probability (the probability for intercommutation to take place when two string segments meet) is of order one, the network can lose energy fast enough for the

existence of strings to be consistent with our current ideas about cosmology based on observation. From the above, it follows that the study of cosmic strings could provide a way to distinguish observationally between different particle physics models. If for example a field theory predicts that the intercommutation probability of strings is equal to zero, this theory probably describes a universe in which strings dominate and therefore cannot be the right theory.

Mainly for the reason explained above, there has been a lot of interest in the intercommutation behavior of cosmic strings ([19, 28]). In this thesis, we will confine our attention to U(1) strings (both local and global). For this type of strings, earlier work suggests that the intercommutation probability is indeed close or equal to one. However, from the literature, it is not entirely clear if strings also intercommute for very high speeds of approach (close to the speed of light) of the string segments. Some papers suggest that for speeds above a certain threshold velocity, strings do not intercommute, but simply pass though each other instead. In our own numerical simulations of string intercommutation for high speeds of approach, which will be presented in this thesis, we find no evidence for the existence of such a threshold velocity. We find that strings intercommute in all cases investigated, where we looked at both global strings and local strings. For local strings, we considered several values of the parameter β, which is the square of the ratio of the Higgs mass to the gauge mass.

The goal of this thesis is twofold. First of all, in the first two chapters, we wish to give a self-contained introduction to cosmic strings and cosmology and explain what the role of cosmic strings in cosmology could be. We will be particularly concerned with the process of intercommutation. Secondly, in the last two chapters of the thesis, we discuss our own numerical simulations of intercommutation and the results following from these simulations.

We will now give a brief overview of the contents of this thesis. In chapter 1, we first introduce the abelian Higgs model (which can be seen as the relativistic version of the Ginzburg-Landau model for superconductors). Then, we will discuss the string solutions occurring in this model and, in particular, the Abrikosov-Nielsen-Olesen solution. Finally, we will devote a section to a more general description of topological defects, of which cosmic strings are an example, in terms of topology. In chapter 2, we start with a brief introduction to cosmology. We will, among other things, discuss how the evolution of the universe depends on the types of matter or energy it contains. We will also describe the Concordance Model. We will discuss how, in certain grand unified theories (GUT) of particle physics, there is a series of phase transitions in the very first moments after this big bang, that can lead to the formation of a network of cosmic strings. Here, the cosmic strings are topologically stable configurations of the fields describing particle physics, i.e. the fields appearing in the GUT. The last part of chapter 2 will then be devoted to the discussion of the evolution of string networks and the interaction of cosmic (U(1)) strings.

In chapter 3, we will describe how we built our simulations of cosmic strings. In these simulations, the interaction of strings is simulated by putting the initial field configuration of two straight strings on a three dimensional lattice and evolving this configuration using the hamiltonian formalism. We will first discuss how the continuous field theory we are interested in is discretized, then we will show in detail how the initial configuration is constructed. Next, we discuss the boundary conditions of our simulations and finally, we will make some remarks about the code we used (codes are available online through `www.lorentz.leidenuniv.nl/~rdeputter`). In chapter 4, we present the results of our simulations. We discuss a particular example of the intercommutation of two local strings and find that the intercommutation process is very fast. During the process, the strings definitely

cannot be described as Nambu-Goto strings. This is consistent with earlier numerical work. We also present simulations of the interaction of strings with very high speeds of approach (close to the speed of light) and find no evidence for the existence of a threshold velocity. Also, we will make some remarks on the formation of a string loop, which sometimes occurs after intercommutation.

Chapter 1

Cosmic strings and the abelian Higgs model

1.1 Introduction

In certain particle physics models, topologically non-trivial "false ground states" may exist as solutions of the (classical) equations of motion. These so called topological defects can be considered ground states because their topology and the demand of continuous field evolution ensure that it takes an infinite amount of energy to evolve to the topologically trivial "real" ground state. For this reason, these solutions are called topologically stable. The word "false" is motivated by the fact that these configurations are not the lowest energy solutions: energy is "trapped" around these defects. We start this chapter (section 1.2) with an introduction to the abelian Higgs model. In particle physics, this model describes the interaction of a Higgs boson with an electromagnetic field. In section 1.3, we will discuss the nature of the topological defect solutions arising in the abelian Higgs model. In two spatial dimensions, these defects are known as vortices. A famous example of such a vortex, the Abrikosov-Nielsen-Olesen vortex, will be discussed in subsection 1.3.1. In three dimensions, vortices generalize to strings. We will end this chapter (section 1.4) with a more general discussion of defect solutions, in terms of topology. Even though strings also exist in other field theories, in this thesis, we will restrict our attention to the strings existing in the abelian Higgs model. The main reason for this, is that the abelian Higgs model seems to be the simplest relevant model to allow strings.

1.2 The abelian Higgs model

The abelian Higgs model describes a complex scalar field ϕ (the Higgs field) and a real vector field A_μ. It can be built up from a model with just a Higgs field by demanding local gauge invariance as follows. We start with the lagrangian density

$$\mathcal{L} = \partial_\mu \phi \, \partial^\mu \phi^* - V(|\phi|). \tag{1.1}$$

Throughout this thesis, we will use the summation convention, unless explicitly stated otherwise. Greek indices are understood to run from 0 to 3 and latin indices run from 1 to 3. The metric is of the form $(+,-,-,-)$ and we work in units with the speed of light $c = 1$ and

Planck's constant $\hbar = 1$, unless explicitly stated otherwise. Clearly, this lagrangian density and hence the action it defines,

$$S = \int \sqrt{-g}\, d^4x\, \mathcal{L}, \tag{1.2}$$

are invariant under global transformations of the form $\phi(x) \to \phi'(x) = e^{ie\alpha}\phi(x)$, where e is a constant that will later play the role of a charge. However, if we let α depend on the space-time coordinate $x = (x^0, x^1, x^2, x^3)$, i.e.

$$\phi(x) \to \phi'(x) = e^{ie\alpha(x)}\phi(x), \tag{1.3}$$

the lagrangian density is no longer invariant because under this transformation $\partial_\mu\phi(x) \to \partial_\mu\phi'(x) = e^{ie\alpha(x)}\partial_\mu\phi(x) + ie(\partial_\mu\alpha(x))e^{i\alpha(x)}\phi(x)$. It is the second term of the expression for $\partial_\mu\phi'(x)$ that spoils the gauge invariance for local transformations. To obtain a model that is not just invariant under global, but also under local gauge transformations, we replace the partial derivatives ∂_μ in the lagrangian density by covariant derivatives

$$D_\mu := \partial_\mu + ieA_\mu, \tag{1.4}$$

where we have introduced a gauge field A_μ, and demand that $D_\mu\phi$ transforms in the same way as ϕ, i.e. $D'_\mu\phi'(x) = e^{ie\alpha(x)}D_\mu\phi(x)$. This means that A_μ has to transform as

$$A_\mu \to A'_\mu = A_\mu - \partial_\mu\alpha. \tag{1.5}$$

The lagrangian density of the abelian Higgs model is now found by adding the standard kinetic energy term of a massless vector field (a mass term would destroy local gauge invariance):

$$\mathcal{L} = D_\mu\phi(D^\mu\phi)^* - \frac{1}{4}F^{\mu\nu}F_{\mu\nu} - V(|\phi|), \tag{1.6}$$

with $F_{\mu\nu} = \partial_\mu A_\nu - \partial_\nu A_\mu$ an anti-symmetric rank two tensor. The gauge field A_μ describes an electromagnetic field with electric field strength[1] $E^i = -F^{0i}$, and magnetic field strength $B^i = -\frac{1}{2}\epsilon^{ijk}F_{jk}$, where ϵ^{ijk} is the anti-symmetric tensor with $\epsilon^{123} = 1$. By construction, this lagrangian density is invariant under local gauge transformations as defined by (1.3) and (1.5).

The model is used in condensed matter physics to describe superconductivity. In this case, the field ϕ describes the order parameter of the superconductor and the model is referred to as the Ginzburg-Landau model. The application that will be relevant for us however, lies in particle physics. Here, the abelian Higgs model is the simplest model to describe the interaction of the Higgs particle with a vector boson. To actually describe particles and their interactions, it is of course necessary to quantize the fields and define a Hilbert space that will contain the particle states. However, for our purpose, namely the study of topological defects, the occupation numbers of the different quantum states are high and it will be sufficient to treat the fields classically. The role of this particle physics model in cosmology, and in particular the (cosmic) strings appearing in it, will be discussed in more detail in the next chapter.

Because of the gauge invariance of the theory, it follows from Noether's theorem that there is a conserved current J^μ such that $\partial_\mu J^\mu = 0$. Using the expression

$$J^\mu := \frac{\delta\mathcal{L}}{\delta\partial_\mu\varphi^i}\frac{\partial\varphi^i_\alpha}{\partial\alpha}\Big|_{\alpha=0}, \tag{1.7}$$

[1] In our conventions, $\vec{E} = (E^1, E^2, E^3)$ and $\vec{B} = (B^1, B^2, B^3)$. Lowering the index introduces a minus sign.

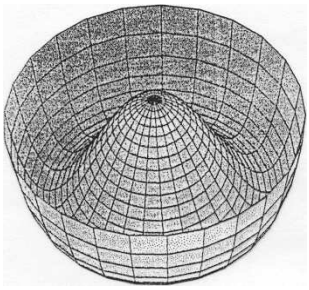

Figure 1.1: The mexican hat potential as a function of the real and imaginary parts of the Higgs field. The minima lie on the circle in the complex plane defined by $|\phi| = \eta$.

where the sum runs over all independent fields (labeled by i) (in this case ϕ, ϕ^* and A_μ) and φ^i_α is defined to be the result of a global gauge transformation working on φ^i, one finds

$$J^\mu = ie\,(\phi(D^\mu\phi)^* - \phi^*(D^\mu\phi)). \tag{1.8}$$

The zeroth component of this current is the charge density and the vector part the charge current. The energy-momentum tensor is given by

$$T^{\mu\nu} = 2\,D^\mu\phi\,(D^\nu\phi)^* - F^{\mu\sigma}F^{\nu}_{\ \sigma} - g^{\mu\nu}\mathcal{L}. \tag{1.9}$$

One example of a potential that gives rise to topological defects, is the Mexican hat potential

$$V(|\phi|) = \frac{\lambda}{4}(|\phi|^2 - \eta^2)^2, \tag{1.10}$$

with $\lambda > 0$. This potential is shown in figure 1.1 and has a degenerate minimum, given by $|\phi| = \eta$. The Euler-Lagrange equations corresponding to (1.6) read:

$$D_\mu D^\mu\phi + \frac{\lambda}{2}(|\phi|^2 - \eta^2)\phi = 0 \tag{1.11}$$

and

$$\partial_\mu F^{\mu\nu} = J^\nu. \tag{1.12}$$

The $\nu = 0$ equation can also be written as

$$\vec{\nabla}\cdot\vec{E} = J^0, \tag{1.13}$$

which is known as Gauss' law.

It is important to realize that the abelian Higgs model, with potential (1.10), has three independent parameters: e, η and λ. As we will show in section 2.4, the mass of the Higgs particle m and the mass of the gauge boson M described by this model, are given in terms of these parameters, by

$$\begin{aligned} m &= \sqrt{\lambda}\eta, \\ M &= \sqrt{2}e\eta. \end{aligned} \tag{1.14}$$

The inverses of these masses are characteristic length scales of the system. It turns out that the fields and distances can be rescaled in such a way that the dynamics of the rescaled system

only depend on one parameter, namely the ratio of the square of the Higgs mass to the square of the gauge mass: $\beta := \frac{m^2}{M^2} = \frac{\lambda}{2e^2}$. The other two degrees of freedom in parameter space only have relevance in that they determine the energy and length/time scales of the system. This is shown explicitly by rescaling the metric by the length naturally defined by the Higgs mass,

$$ds'^2 = m^{-2}\, ds^2 = (\lambda\eta^2)^{-1}\, ds^2, \tag{1.15}$$

rescaling ϕ according to

$$\phi' = \eta^{-1}\, \phi, \tag{1.16}$$

and rescaling the gauge field according to

$$A'_\mu = \frac{e}{m}\, A_\mu = \frac{e}{\sqrt{\lambda}\eta}\, A_\mu. \tag{1.17}$$

The lagrangian density (1.6) with mexican hat potential then becomes

$$\mathcal{L} = \lambda\eta^4 \left[(\partial'_\mu + iA'_\mu)\phi'\, (\partial'^\mu - iA'^\mu)\phi'^* - \frac{\beta}{2} F'^{\mu\nu} F'_{\mu\nu} - \frac{1}{4}(|\phi'|^2 - 1)^2 \right]. \tag{1.18}$$

From this it indeed follows that, scaling of fields and distances aside, the model is fully characterized by β.

As an alternative to the lagrangian formulation, one can also use the hamiltonian formalism to describe the evolution of the fields. In fact, this is the approach we will take later when we perform numerical simulations of the interaction of two strings. In the hamiltonian formalism, we define the conjugate momenta of the fields by taking the partial derivative of the lagrangian density to the time-derivative of the field. The hamiltonian is then constructed by applying a Legendre transformation to the lagrangian

$$L = \int d\vec{x}\, \mathcal{L}. \tag{1.19}$$

This procedure is simplified significantly if we first fix the gauge in a convenient way. Throughout this thesis, we will work in the temporal gauge, which means that $A_0 = 0$. The gauge freedom ensures that we can always make this choice, for if $A_0 \neq 0$, A_0 can be put to zero by a gauge transformation with $\partial_0 \alpha = A_0$. Note that after imposing the temporal gauge, we have an additional gauge freedom left because the gauge is left intact by transformations with $\partial_0 \alpha = 0$. In the temporal gauge, the conjugate momentum of the Higgs field is

$$\pi := \frac{\delta \mathcal{L}}{\delta \partial_0 \phi} = \partial^0 \phi^*, \tag{1.20}$$

while for the gauge field, the conjugate momentum turns out to be equal to the electric field strength,

$$\frac{\delta \mathcal{L}}{\delta \partial_0 A_i} = -F^{0i} = E^i. \tag{1.21}$$

The hamiltonian density now reads

$$\begin{aligned} \mathcal{H} &= \pi\, \partial_0 \phi + \pi^*\, \partial_0 \phi^* + E^i\, \partial_0 A_i - \mathcal{L} \\ &= \frac{1}{2}(\vec{E}^2 + \vec{B}^2) + \pi\pi^* + |\vec{D}\phi|^2 + \frac{\lambda}{4}(|\phi|^2 - \eta^2)^2 \end{aligned} \tag{1.22}$$

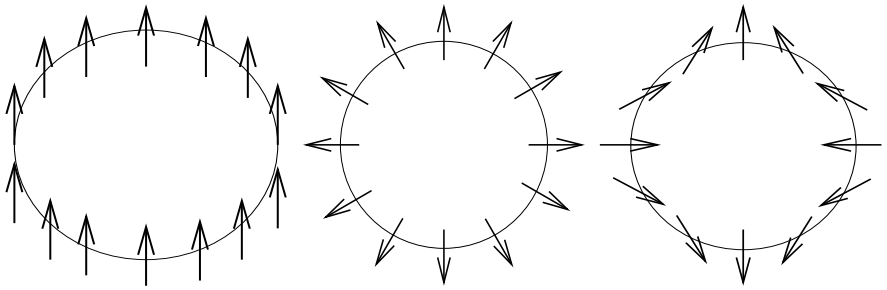

Figure 1.2: Configurations of the Higgs field at spatial infinity with, from left to right, winding number $n = 0$, $n = 1$ and $n = -1$. The arrows indicate the phase of the field. Configurations with non zero winding number correspond to topological defects.

and the energy is given by

$$H = \int d\vec{x}\, \mathcal{H}. \tag{1.23}$$

The resulting hamiltonian equations, $\dot{\phi} = \frac{\delta \mathcal{H}}{\delta \pi}$ and $\dot{\pi} = -\frac{\delta \mathcal{H}}{\delta \phi} + \partial_i \frac{\delta \mathcal{H}}{\delta \partial_i \phi}$, read

$$\begin{aligned} \frac{d\phi}{dt} &= \pi^* \\ \frac{d\pi}{dt} &= -(D_i D^i \phi)^* - \frac{\lambda}{2}(|\phi|^2 - \eta^2)\phi^* \end{aligned} \tag{1.24}$$

and

$$\begin{aligned} \frac{dA_i}{dt} &= -E_i \\ \frac{dE_i}{dt} &= ie(\phi(D_i\phi)^* - \phi^* D_i \phi) + \partial^j(\partial_j A_i - \partial_i A_j), \\ \text{or} \quad \frac{d\vec{E}}{dt} &= \vec{J} + \vec{\nabla} \times \vec{B}, \end{aligned} \tag{1.25}$$

with $\vec{J} = (J^1, J^2, J^3)$ defined in (1.8). This set of equations is equivalent to the Lagrange equations (1.11) and (1.12).

1.3 Defect solutions

The defect solutions of the abelian Higgs model can be most easily understood by first considering the model in two spatial dimensions and then generalizing the results to three dimensions. For a solution to have finite energy, the field must go to a vacuum value, i.e. a value that minimizes the potential V, at spatial infinity. The vacuum manifold will be defined to be the set of all such vacuum values. Since the potential (1.10) attains its minimum for values of the field of the form $\phi = \eta e^{i\psi}$ (ψ real), the vacuum manifold is a circle in the complex plane. Hence, every finite energy solution implies a map from the circle at spatial infinity (a circle because space is two dimensional) to a circle in the complex plane. This map is defined by $\phi(r = \infty, \theta) = \eta e^{i\psi(\theta)}$, with ψ a continuous function of θ. Since ϕ must be continuous, the phase ψ of the field must change by an integer multiple of 2π if we move around the circle

at spatial infinity once, i.e. $\psi(\theta + 2\pi) = \psi(\theta) + n2\pi$. The winding number n can be used to divide the solutions into distinct topological classes. Since gauge transformations can only change the *phase* of the Higgs field, and since this change in phase has to be a continuous function of space (and time), the winding number is a gauge invariant quantity. Moreover, since field evolution has to be continuous and since at spatial infinity the field has to remain in the vacuum, it is imposibible for a configuration to evolve into a configuration with different winding number over time. Hence, the winding number is called a topologically conserved quantity and can be used to classify solutions. An example of a configuration with winding number n is given by

$$\phi(r = \infty, \theta) = \eta e^{in\theta} \tag{1.26}$$

(see figure 1.2) and in fact, any configuration with winding number n can be continuously deformed into a configuration of this form.

Even though locally, because of gauge invariance, the phase of the Higgs field has no physical meaning, there are some quite dramatic differences between solutions with different winding number. Since the energy density (equation (1.22)) is a sum of positive definite terms, it can be easily seen that the vacuum solution (the one with zero energy) has $|\phi| = \eta$ everywhere and can, up to a gauge transformation, be written as $\phi = \eta$, $A_\mu = 0$ and therefore has $n = 0$. For an $n \neq 0$ configuration however, continuity requires that the Higgs field reaches zero somewhere. Hence, the energy of any such configuration will be bigger than 0. The region(s) around the zero(es) of the Higgs field will have non-zero potential energy. These points where topology forces the field to be zero are called topological defects.

1.3.1 The Abrikosov-Nielsen-Olesen vortex

The simplest $n = 1$ vortex solution is the cylindrically symmetric static Abrikosov-Nielsen-Olesen solution ([2],[24]), which in polar coordinates is given by

$$\phi(r, \theta) = \eta X(r) e^{i\theta}, \tag{1.27}$$

$$A_\mu(r, \theta) = \frac{-1}{e}(1 - P(r))\partial_\mu \theta, \tag{1.28}$$

with $X(r)$ and $P(r)$ real functions ([10]). The Higgs field of such a configuration is shown in figure 1.3. At $r = 0$, $X(r) = 0$ and $P(r) = 1$ and the energy density attains a maximum. For $r \to \infty$ the Higgs field approaches its vacuum value ($X(r) \to 1$) and $P(r)$ goes to zero. In between, the profiles $X(r)$ and $P(r)$ are such that the total energy is minimized: on the one hand, the Higgs field "wants" to reach its vacuum value as fast as possible, on the other hand, if this goes too fast, the gradients in the energy density become too high. We will now discuss how the profiles $X(r)$ and $P(r)$ can be found. This discussion gets rather technical, but is included anyway, because it will be of use when we discuss how to construct the initial field configuration for a numerical simulation of string interactions in chapter 3.

The profiles that minimize the total energy can in principle be found by plugging the Abrikosov-Nielsen-Olesen ansatz into the equations of motion:

$$-X'' - \frac{X'}{r} + \frac{XP^2}{r^2} + \frac{\lambda\eta^2}{2}(X^2 - 1)X = 0, \tag{1.29}$$

$$-P'' + \frac{P'}{r} + 2e^2\eta^2 PX^2 = 0. \tag{1.30}$$

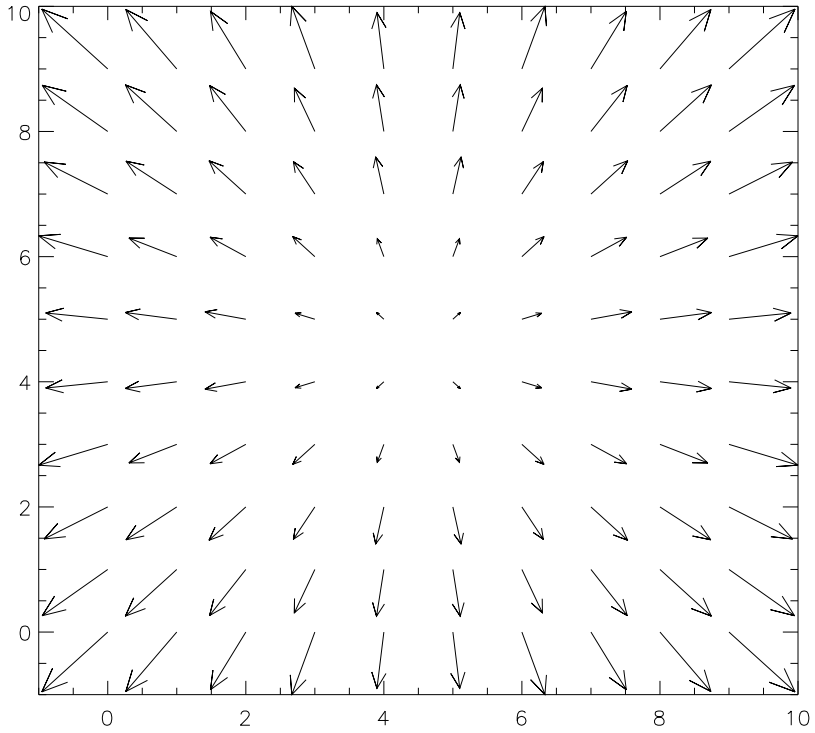

Figure 1.3: Higgs field of an Abrikosov-Nielsen-Olesen vortex. When a path around the center of the vortex is followed, the phase of the fields changes by 2π. Because of this, and because the field has to be continuous, there has to be a point where the field is equal to zero (the center of the vortex). The energy in the region surrounding this point is trapped because of the conservation of winding number.

If we rescale r by the characteristic length m^{-1} set by the Higgs mass,

$$r_{\rm new} = \sqrt{\lambda}\eta\, r_{\rm old}, \tag{1.31}$$

the equations will, in terms of the rescaled coordinate, only depend on the parameter $\beta = \frac{\lambda}{2e^2}$, which was introduced in the previous section. In terms of the rescaled coordinates, the equations read

$$-X'' - \frac{X'}{r} + \frac{XP^2}{r^2} + \frac{1}{2}(X^2-1)X = 0, \tag{1.32}$$

$$-P'' + \frac{P'}{r} + \beta^{-1}PX^2 = 0, \tag{1.33}$$

where primes now denote derivatives with respect to the rescaled distance $r_{\rm new}$. If $\beta = 1$, these equations factor into two (coupled) first order differential equations:

$$r\,X' = XP, \tag{1.34}$$

$$P' = \frac{1}{2}r(X^2-1) \tag{1.35}$$

Unfortunately, these equations cannot be solved analytically. In section 3.3, we will find the profiles numerically by minimizing the energy. In terms of $X(r)$ and $P(r)$ (still working in rescaled coordinates),

$$\mathcal{L} = -\lambda\eta^4\Big(X'^2 + \frac{X^2P^2}{r^2} + \beta\frac{P'^2}{r^2} + \frac{1}{4}(X^2-1)^2\Big), \tag{1.36}$$

such that

$$H = 2\pi\eta^2\int_0^\infty dr\, r\,\Big(X'^2 + \frac{X^2P^2}{r^2} + \beta\frac{P'^2}{r^2} + \frac{1}{4}(X^2-1)^2\Big), \tag{1.37}$$

because for a static solution $\mathcal{H} = -\mathcal{L}$.

This solution trivially generalizes to three dimensions by simply adding an extra coordinate, say z. Now the Abrikosov-Nielsen-Olesen solution corresponds to a straight string on the z-axis. The energy per unit (physical) length $\mu = \frac{dE}{dz}$ is given by

$$\mu = 2\pi\eta^2\int_0^\infty dr\, r\,\Big(X'^2 + \frac{X^2P^2}{r^2} + \beta\frac{P'^2}{r^2} + \frac{1}{4}(X^2-1)^2\Big) \tag{1.38}$$

and can be calculated if the string profiles $X(r)$ and $P(r)$ (still in terms of rescaled coordinates) are known. In three dimensions, the stability of defects is again ensured by the conservation of winding number around circles at spatial infinity. The difference with the two dimensional model is that in three dimensions one has to specify a particular circle (or in general, loop) to be able to speak about winding number in an unambiguous way. In general, if a loop $\mathcal{C}$ at infinity has winding number n, then for any surface $\mathcal{S}$ with boundary $\mathcal{C}$, the magnetic flux (Φ) through it is quantized. The reason for this is that the condition that the energy density at infinity is equal to zero forces A_μ to be such that $D_\mu\phi = (\partial_\mu + ieA_\mu)\eta e^{i\psi(\theta)} = 0$ at $\mathcal{C}$, where we have written $\phi = \eta e^{i\psi(\theta)}$, with $\psi(\theta)$ real as in the first paragraph of section 1.3. This gives $A_\mu(x) = -\frac{1}{e}\partial_\mu\psi(\theta)$, such that

$$\Phi := \int_\Sigma d^2x B_\perp = \oint_{\mathcal{C}}\vec{A}\cdot d\vec{s} = \frac{1}{e}\oint_{\mathcal{C}}\vec{\nabla}\psi(x)\cdot d\vec{s} = n\frac{2\pi}{e}, \tag{1.39}$$

where $B_\perp$ is the component of $\vec{B}$ perpendicular[2] to $\mathcal{S}$ and $\vec{A} = (A^1, A^2, A^3)$.

Not all strings are of course exact Abrikosov-Nielsen-Olesen strings. Strings do not have to be straight and they can have velocities[3] that may depend on the location on the string. The orientation of a string will be defined to be determined from the winding of the Higgs field around it by applying the right hand rule to the direction in which the phase increases by a *positive* multiple of 2π. This is also the direction of the magnetic flux through the string (see equation (1.39)). In figures, we will often indicate this direction by an arrow. As will be discussed in chapter 2, in cosmology entire string networks are studied. These strings are often referred to as cosmic strings and should not be confused with the fundamental strings that appear in string theory. Because of the conservation of winding number, strings cannot just end, so strings are either infinitely long or form loops. The strings in the abelian Higgs model are also often called local strings because they appear in a local gauge theory. If no gauge fields are present (this corresponds to $\beta \to \infty$), the strings are called global strings.

Even though the existence and stability of string configurations can be understood quite well intuitively in the abelian Higgs model, in more complicated models a more formal mathematical approach is necessary. In the next section we will briefly discuss the basic concepts from topology necessary to get an understanding of topological defects in general models. We will also discuss some examples of topological defects that occur in different models, like domain walls and monopoles.

1.4 Topology and topological defects

Whether or not a model allows topological defects and, if so, what kind of defects, all depends on the so called homotopy groups of the vacuum manifold. These homotopy groups are used in topology to provide a classification of topologies. Before we explain what exactly homotopy groups are, it is useful to first discuss some basic topology. A far more complete introduction to topology can be found in [4]. An alternative discussion of the applications of topology in gauge theories can be found in [15]. In this section, we will assume the reader to be familiar with some very basic group theory and to have some basic knowledge of functions. In terms of topology, we tried to make this section as self-contained as possible. We will start with some definitions.

Definition A topological space is a set X equipped with a topology $\mathcal{O}$

Definition A topology $\mathcal{O}$ on a set X is a nonempty collection of subsets of X, called "open sets", such that

1. Any union of open sets is open:
$O_i \in \mathcal{O} \quad \forall i \in I \quad \Rightarrow \quad \bigcup_{i\in I} O_i \in \mathcal{O}$
2. Any finite intersection of open sets is open:
$O_i \in \mathcal{O} \quad \forall i \in \{0, .., n\} \quad \Rightarrow \quad \bigcap_{i=0}^{n} O_i \in \mathcal{O}$
3. Both X and the empty set are open:
$X \in \mathcal{O}$ and $\varnothing \in \mathcal{O}$

[2]The direction of the flux follows from the orientation of the loop by the right hand rule.

[3]The field configuration of a moving straight string is obtained by applying a Lorentz boost to a static Abrokosov-Nielsen-Olesen configuration.

If X is a topological space and $Y \subset X$, the induced topology on Y is simply the collection of open sets in X intersected with Y. So if $\mathcal{O}_X$ and $\mathcal{O}_Y$ are the topologies of X and Y respectively, $\mathcal{O}_Y = \{O \cap Y : O \in \mathcal{O}_X\}$. In this section, all spaces will be assumed to have a topology, even if we do not explicitly call them topological spaces. With the use of open sets, it is possible to formulate the notion of continuity.

Definition A function $f : X \to Y$ is continuous if and only if the inverse image of each open set is open in X.

This definition is a natural generalization of the familiar notion of continuity from real analysis, in which case, the open sets are defined in tems of a distance function or metric. A continuous function is often called a map. A path in a topological space X is a continuous function $\gamma : [0, 1] \to X$. The points $\gamma(0)$ and $\gamma(1)$ are said to be joined by the path γ. An interesting property of topological spaces is whether or not they are path connected.

Definition A space is called path connected if any two of its points can be joined by a path.

Definition A homeomorphism $f : X \to Y$ is a function which is continuous, one-one, onto and has a continuous inverse

If there exists a homeomorphism between two spaces X and Y, they are called homeomorphic and we will write[4] $X \cong Y$. Since, by definition, a homeomorphism provides a one-one onto correspondence between the topologies of X and Y, topologically X and Y can be considered identical. In other words, if $X \cong Y$, all topological results proven for X, automatically also hold for Y.

Much can be learned about the topology of a space by analyzing its homotopy groups. The first homotopy group, also called the fundamental group, is constructed out of the set of loops in a space that begin and end at some specified point. A loop in a space X, based at a point $p \in X$, is defined as a map $\alpha : [0, 1] \to X$, with $\alpha(0) = \alpha(1) = p$. Note that an equivalent definition would be that of a map from the unit circle to X that maps (at least) one point of the circle to p. If two loops can be deformed into each other in a continuous fashion, they are called homotopic to each other. We wish to divide the collection of loops into equivalence classes of loops that can be continuously deformed into each other. Of course, we first need to properly define what it means for two loops, or in general two maps, to be homotopic to each other.

Definition Let $f, g : X \to Y$ be maps. Then f is homotopic to g if there is a map $F : X \times [0, 1] \to Y$ such that $F(x, 0) = f(x)$ and $F(x, 1) = g(x) \quad \forall x \in X$.

If such an F exists, it is called a homotopy. For two loops α and β in X based at point $p \in X$ to be equivalent ($\alpha \sim \beta$), we demand they are homotopic, i.e. there is a homotopy $F : [0, 1] \times [0, 1] \to X$ with $F(x, 0) = \alpha(x)$ and $F(x, 1) = \beta(x) \quad \forall x \in [0, 1]$ but with the extra condition $F(0, t) = F(1, t) = p \quad \forall t \in [0, 1]$. This condition makes sure that for each t, $F(x, t)$ describes a loop with base p. Since F is continuous, the parameter t continuously takes the loop α to β. The equivalence relation defined above divides the collection of loops into equivalence classes denoted by $\overline{\alpha} := \{\text{loops } \beta \quad \text{s.t. } \beta \sim \alpha\}$. A group structure on this collection of equivalence classes naturally arises if we define the product of two loops as:

[4] If two groups are *isomorphic*, we will use "=" to avoid confusion.

Definition The product $\alpha \cdot \beta$ of loops α and β is itself a loop and is defined by

$$(\alpha \cdot \beta)(t) = \left\{ \begin{array}{lll} \alpha(2t) & , & 0 \leq t \leq \frac{1}{2} \\ \beta(2t-1) & , & \frac{1}{2} \leq t \leq 1 \end{array} \right\},$$

In words, the product of α and β is found by starting at p, then first following the loop α, which eventually leads back to p again, and then following β. It is trivial to see that indeed $\alpha \cdot \beta$ is again a loop. It can then be shown that the multiplication on the equivalence classes, $\overline{\alpha} \cdot \overline{\beta} := \overline{\alpha \cdot \beta}$, is well defined and implies a group structure. This group is called the fundamental group of X based at p and is written $\pi_1(X, p)$. A not so nice aspect of this definition is that it still depends on the choice of base point p. However, if a space is path connected, the following theorem states that the definition is independent of the base point.

Theorem 1.4.1 *If X is path connected, then $\pi_1(X, p)$ and $\pi_1(X, q)$ are isomorphic for any two points $p, q \in X$.*

If a space X is not path connected, there are points in X that cannot be connected to p by a path and therefore there can be no loops based at p that go through these points. Hence, these points are completely irrelevant to $\pi_1(X, p)$. Since this means that if X is not path connected, we might as well focus on the subset of X that *can* be connected to p by a path, and since this subset is path connected by definition, we will from now on assume the space we are considering to be path connected. The fundamental group of X is now written $\pi_1(X)$ and is equal to $\pi_1(X, p)$ for any choice of $p \in X$.

From the definition of multiplication on the fundamental group, it follows that, for any base point p, the identity element is given by $e = \{\alpha : \alpha \sim \gamma\}$ with the loop γ given by $\gamma(x) = p$, $\forall x \in [0, 1]$. In other words, the identity element is the set of loops that can be continuously deformed into a point. Hence, the fundamental group is non-trivial if and only if X admits incontractible loops. If for example $X = S^1$, $\pi_1(X) \cong Z$ where the isomorphism relating the two is explicitly given by $n \leftrightarrow \overline{\gamma_n}$, with γ_n given by $\gamma_n(x) = e^{i2\pi nx}$, $x \in [0, 1]$. Note that this is exactly the situation ocurring in the abelian Higgs model. There, the vacuum manifold equals S^1 and saying that a configuration cannot change its winding number is completely equivalent to saying that these configurations correspond to loops in S^1 from different equivalence classes, i.e. they cannot be continuously deformed into each other.

The fundamental group is called first homotopy group because it is constructed using maps from the one dimensional sphere (circle) to X (our loops). We can generalize this method and construct the n-th order homotopy group using maps from the n dimensional sphere to X, i.e. maps of the form $\alpha : [0, 1]^n \to X$, with $\alpha(x) = p$ for all points x at the boundary of $[0, 1]^n$ (it is usually easier to work with maps from $[0, 1]^n$ to X than with maps from S^n to X, but the two definitions are equivalent). The procedure of constructing these groups is equivalent to the construction of π_1. This time the product $\alpha \cdot \beta$ of maps is formed by connecting maps along a common part of the boundary of the n-cube:

$$(\alpha \cdot \beta)(t_1, t_2, ..., t_n) = \left\{ \begin{array}{lll} \alpha(2t_1, t_2, ..., t_n) & , & 0 \leq t_1 \leq \frac{1}{2} \\ \beta(2t_1 - 1, t_2, ..., t_n) & , & \frac{1}{2} \leq t_1 \leq 1 \end{array} \right\},$$

which again yields a group structure on the collection of homotopy equivalence classes, thus making it a group. For instance, $\pi_2(X)$ corresponds to the group found from maps from the

ordinary two dimensional sphere to X and is non-trivial if and only if X admits incontractible spheres. The homotopy groups are so called topological invariants, which means that if two spaces are homeomorphic, their homotopy groups are isomorphic. If for example one wishes to know whether two spaces X and Y are homeomorphic, a good check would be to compare homotopy groups. If for some n, $\pi_n(X) \neq \pi_n(Y)$, X and Y are not homeomorphic. The reverse is not true: if all homotopy groups are equal, it is not necessarily the case that the spaces are homeomorphic.

Whether or not a model allows topological defect solutions depends on the topological structure of the vacuum manifold. The abelian Higgs model, discussed in the previous section, contains one complex scalar field, the Higgs field, and a potential $V(\phi)$. In general, a Higgs field can have more than one component and the potential is a function of all these components. The vacuum manifold, which will be denoted by $\mathcal{V}$, is then defined to be the set of values of the Higgs field for which $V(\phi)$ is minimal. In general, a field theory will be invariant under a group of transformations G, which means that if an element of G transforms the fields, the action is left unchanged. In the abelian Higgs model, $G = U(1)$, the set of phase shifts of the Higgs field. The vacuum manifold $\mathcal{V}$ is mapped into itself by all elements of G. $\mathcal{V}$ can be represented by a group of equivalence classes of transformations as follows. By chosing a particular vacuum expectation value (VEV) $\phi_0 \in \mathcal{V}$ as a starting point, we can define a map f by

$$\begin{aligned} f &: G \to V \\ g &\mapsto g(\phi_0) \end{aligned} \tag{1.40}$$

where $g(\phi_0)$ denotes the result of g working on ϕ_0. In general, this map is not one-one because there could be more than one element in G that has a trivial effect on ϕ_0. If we let $H \subset G$ denote the set of transformations in G that leave ϕ_0 invariant, H is a subgroup of G and defines an equivalence relation on G given by

$$g \sim g' \quad \Leftrightarrow \quad \exists h \in H \quad \text{s.t.} \quad gh = g' \tag{1.41}$$

The set of equivalence classes that follows from this relation is the coset space G/H. The equivalence classes that are the elements of this group are the left cosets of H. They are usually notated by chosing a particular element to represent the entire class: $\overline{g} := gH$. It is this group of left cosets that is homeomorphic to the vacuum manifold. This follows from the fact that the map F that is a trivial generalization of f,

$$\begin{aligned} F &: G/H \to V \\ \overline{g} &\mapsto \overline{g(\phi_0)}, \end{aligned} \tag{1.42}$$

is one-one and onto and both F and its inverse are continuous:

$$\mathcal{V} \cong G/H \tag{1.43}$$

In the abelian Higgs model, the vacuum expectation value is only left invariant by the identity transformation, i.e. $H = 1$, which indeed gives $\mathcal{V} \cong U(1)/1 \cong U(1) \cong S^1$. As said before, this gives rise to stringlike topological defects because $\pi_1(S^1)$ is non-trivial. It may also occur that $\pi_1(G/H)$ is trivial, but $\pi_2(G/H)$ is not. In this case, the defects will be pointlike. This happens, for example, in models where the vacuum manifold is homeomorphic to the two

dimensional sphere S^2. For such a vacuum manifold, it can indeed be found that $\pi_1(S^2) = 0$ and $\pi_2(S^2) = Z$. It is not hard to understand this intuitively: circles on a sphere can always be contracted to a point, while spheres cannot. The pointlike defects that occur in models with a Higgs field coupled to a $U(1)$ gauge field are called monopoles.

Another example of a defect common in field theory, occurs whenever $\pi_0(G/H)$ is non-trivial. Since S^0 is a set of two discrete points, $\pi_0(G/H)$ is non-trivial whenever the vacuum manifold is not path connected, because in that case one can find two points that cannot be continuously moved to each other. The defect ocurring in models with a disconnected vacuum manifold is a two dimensional surface that separates two regions in which the fields are in disconnected parts of the vacuum manifold. These surfaces are called domain walls. We have now seen the three defect types relevant to cosmology. In summary, magnetic monopoles occur whenever $\pi_2(G/H)$ is non-trivial, strings occur whenever $\pi_1(G/H)$ is non-trivial and domain walls are the defects ocurring in models with non-trivial $\pi_0(G/H)$.

So far, the vacuum manifolds we have encountered were n dimensional spheres. For these spaces, we have the useful general results: $\pi_n(S^n) \cong Z$, $\pi_m(S^n) \cong 0, \quad m < n$. For $m > n$, there is no such simple general expression, but these homotopy groups are in general non-trivial. In realistic field theories describing the very early universe, the vacuum manifold G/H can be very complicated. Fortunately, the following theorem can often be used to simplify things.

Theorem 1.4.2 *If $\pi_n(G)$ and $\pi_{n-1}(G)$ are both trivial, $\pi_n(G/H) = \pi_{n-1}(H)$.*

This theorem often makes it possible to tell what kind of defects (if any) a theory admits by analyzing the group that leaves the VEV invariant, the unbroken symmetry H. We will use this in the next section when discussing the existence of defects in field theories describing the particle physics of the early universe.

Chapter 2

Cosmology

2.1 Introduction

The main reason we are interested in topological defects in general and strings in particular, is that they could play an interesting role in cosmology. In the current "standard model" of cosmology, there is a series of phase transitions in the very early universe, a short time after the big bang. During these phase transitions topological defects could be produced. These defects can interact with ordinary matter and radiation and with space-time itself. If defects are indeed formed in the early universe, it is useful to understand their evolution and their effect on the global properties of the universe.

In section 2.2, we will first discuss some basic concepts, like the scale factor and the equations describing its evolution, that are fundamental to cosmology. This discsussion will be quite general. Next, in section 2.3, we will discuss the so called concordance model. This model is supposed to describe our universe and its evolution and is based on observation. We will pay special attention to the earliest stages of the universe. It is thought that the field theory describing particle physics undergoes a series of phase transitions during the first fraction of a second after the big bang. This process and how topological defects might be formed during it, will be the topic of section 2.4. In particular, we will discuss how a cosmic string network might be formed in the early universe. By the end of section 2.4, we will start focusing exclusively on cosmic strings. In section 2.5, we present a discussion of string (network) evolution. It will turn out that a process called intercommutation, the exchange of ends when two string segments come to intersect, plays an important role in string network evolution. This process will be the subjet of section 2.6. The rest of this thesis will then be devoted to the numerical study of intercommutation (at high velocities). Readers interested in a more complete treatment of cosmology than is presented in this chaper, are referred to [7].

2.2 Basic cosmology

Cosmology is the science that studies the properties of the universe and their evolution at the very largest scales. While this makes it observationally a very demanding research field, theoretically, a lot of things are deeply simplified when one does not have to worry about details. The main assumption underlying cosmology is the cosmological principle, which states that the universe is homogeneous (the same at all positions) and isotropic (the same

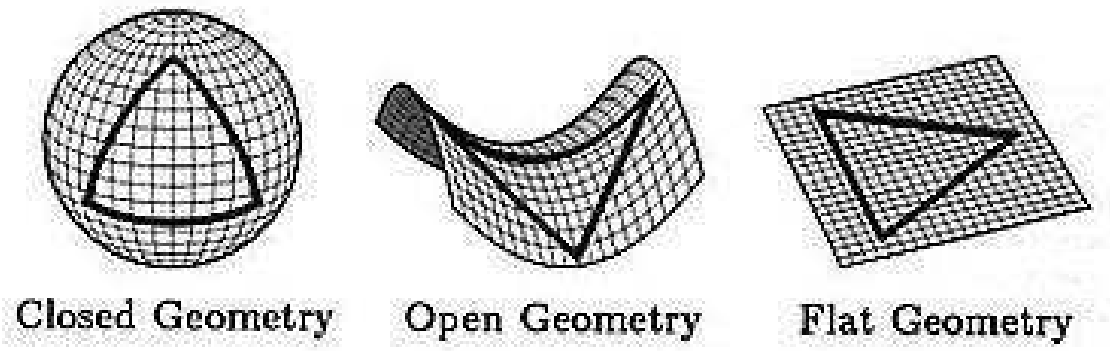

Figure 2.1: The geometry of equal time slices depends on the value of k. For $k = 0$, the universe is flat, for $k = 1$, it is closed and for $k = -1$, the universe is open. Here, the two dimensional analogs of these three dimensional spaces are depicted because the three dimensional spaces are impossible to draw.

in all directions). Of course, if the universe was perfectly homogeneous, there would be no structure whatsoever. There would exist no stars, planets or galaxies and there certainly would be no life. In fact, the universe would be a very boring place. On small scales, say the scale our day to day life takes place at or the scale of galaxies even, the assumption of homogeneity is not even remotely true and the same goes for isotropy. However, when we start looking at the large scales of galaxy clusters and superclusters and forget about the rich, complicated structures the universe contains on smaller scales, the cosmological principle is actually a fairly good approximation of what our universe looks like. We therefore use the cosmological principle to describe the universe at the most basic level. This homogeneous and isotropic universe is then used as a background against which we can study the deviations from the cosmological principle, like the formation of large scale structure (LSS).

We assume that, except in very extreme circumstances (to which we will come back briefly later), space-time can be described by general relativity (GR). In GR, the geometry of the space-time manifold is described by the metric. The most general space-time that respects the cosmological principle is the Robertson-Walker metric, given by the line element (still in units with the speed of light $c = 1$)

$$ds^2 = dt^2 - a^2(t)\Big(\frac{dr^2}{1-kr^2} + r^2(d\theta^2 + sin^2\theta\, d\phi^2)\Big), \tag{2.1}$$

with $r \geq 0$, $0 \leq \theta < \pi$ and $0 \leq \phi < 2\pi$. $a(t)$ is called the scale factor and has to be positive, while for suitably chosen coordinates the curvature k takes on the values $k = -1, 0, 1$. The coordinates used here are called comoving coordinates. In this metric, worldlines of constant spatial coordinates are geodesics and t is the proper time along these worldlines. An observer at constant spatial coordinates is called a comoving observer. Note that this form of the metric seems to imply that the origin O, given by $r = 0$, is a special point. However, the metric has the same form regardless of which origin is chosen. If this was not the case, the homogeneity condition would have been violated. The proper (spatial) distance between two comoving observers, assuming without loss of generality that one is at $r = 0$ and the

coordinates of the other are $(r, \theta = 0, \phi = 0)$, is given by

$$d(r) = a(t) \int_0^r \frac{dr'}{\sqrt{1 - kr'^2}}. \tag{2.2}$$

Since the integral written above is independent of time, we can express the distance between comoving observers in terms of the distance at some particular time t_0 as folows:

$$d(t) = \frac{a(t)}{a_0} d_0, \tag{2.3}$$

whith $a_0 = a(t_0)$ and $d_0 = d(t_0)$ and the coordinate r has been suppressed. This shows that proper distances between comoving observers are proportional to $a(t)$, thus justifying the name scale factor. From (2.3), it follows that the relative radial velocity is given by

$$v(t) = \dot{d}(t) = \frac{\dot{a}(t)}{a_0} d_0 = \frac{\dot{a}(t)}{a(t)} \frac{a(t)}{a_0} d_0 = \frac{\dot{a}(t)}{a(t)} d(t). \tag{2.4}$$

This is exactly Hubble's law[1] $v(t) = H(t)\, d(t)$ with the Hubble parameter given by $H(t) = \frac{\dot{a}(t)}{a(t)}$. This law was first formulated by Hubble in 1929 based on observations of galaxy velocities. The conclusion was that galaxies move away from each other at a speed that is proportional to their relative distance, i.e. $H > 0$. The actual value of H has since been modified significantly, but the main conclusion remains: we live in an expanding universe. Let us now discuss the meaning of the curvature k. The curvature does not depend on space or time and is thus a parameter of the model. For $k = 1$, the space described by the spatial part of the metric (2.1) is a three dimensional sphere with radius $a(t)$ (closed universe). This can be seen by applying the coordinate transformation $r = \sin \rho$, which renders the spatial part of the metric dl^2, defined as $-ds^2$ with $dt = 0$, in the form

$$dl^2 = a^2(t) \Big(d\rho^2 + \sin^2 \rho \, d\theta^2 + \sin^2 \rho \, \sin^2 \theta \, d\phi^2 \Big), \tag{2.5}$$

which is the metric of a 3-sphere. For $k = 0$, the equal time slices correpond to ordinary flat space because in this case the spatial part of the metric gets the form

$$dl^2 = a^2(t) \Big(dr^2 + r^2 (d\theta^2 + \sin^2 \theta \, d\phi^2) \Big), \tag{2.6}$$

Finally, the spatial part of the Robertson-Walker metric with $k = -1$ is a hyperboloid, a space with constant negative curvature (open universe). This follows from the coordinate transformation $r = \sinh \rho$, such that

$$dl^2 = a^2(t) \Big(d\rho^2 + \sinh^2 \rho (d\theta^2 + \sin^2 \theta \, d\phi^2 \Big), \tag{2.7}$$

which is the hyperboloid metric. The $k = -1$ and $k = 0$ spaces are both infinite while the 3-sphere is curved into itself and has a finite volume. In figure 2.1, the two dimensional analogs of the three dimensional spaces described above are sketched.

As stated above, the only thing that was used to find the metric (2.1) is the cosmological principle. To determine the complete form of the metric, we need to know the value of the

[1]Here, we used the Robertson-Walker metric to derive Hubble's law, but it can even be derived without the specific form of the metric, using only the homogeneity and isotropy of space.

scale factor as a function of (comoving) time. In GR, the metric is determined by the Einstein equations. These equations relate the metric to the energy content of the universe. Hence, in order to find equations for $a(t)$, we need to know the energy-momentum tensor $T^{\mu\nu}$. For a homogeneous, isotropic perfect fluid with (rest) energy density ρ and pressure p, the energy momentum tensor takes the form

$$T^{\mu\nu} = (\rho + p)u^\mu u^\nu - p\, g^{\mu\nu}, \tag{2.8}$$

with $u^\mu = \frac{dx^\mu}{ds}$ the four velocity of the fluid. Here s is the proper time of an observer in the rest frame of the fluid. Even though, in general, there are ten independent Einstein equations, the symmetry of our model ensures that if we plug the energy momentum tensor (2.8) in the Einstein equations, we end up (after some manipulation) with only two independent equations. One of them is the Friedmann equation, which reads

$$\Big(\frac{\dot{a}}{a}\Big)^2 = \frac{8\pi G\rho}{3} - \frac{k}{a^2} + \frac{\Lambda}{3}, \tag{2.9}$$

with G the gravitational constant (in SI units $G = 6.7 \cdot 10^{-11}\mathrm{Nm^2kg^{-2}}$). The constant Λ that suddenly appears in this equation is the famous cosmological constant. It will turn out to have the effect of accelerating the expansion of the universe. It was introduced into the equations by Einstein to make a static universe consistent with GR. However, when it turned out that the universe is not static, but is in fact expanding, the cosmological constant was omitted from the equations and Einstein famously called the introduction of a cosmological constant the greatest blunder of his career. More recently however, the cosmological constant was reinstated to explain the observed *accelerated* expansion of the universe, but the nature of the physics behind this constant is not well understood to say the least. It is not even sure that Λ should be a constant. As we will later see, accelerated expansion might also be explained by introducing a matter field with an unorthodox equation of state, in which case the effective cosmological "constant" may depend on time. The phenomenon reponsible for the accelerated expansion is generally referred to as dark energy and it is one of the main challenges of cosmology to understand its nature. The second equation is called the fluid equation and is analogous to the continuity equation that appears in ordinary newtonian fluid dynamics,

$$\dot{\rho} + 3\Big(\frac{\dot{a}}{a}\Big)(\rho + p) = 0. \tag{2.10}$$

This last equation can also be derived directly from the general relativistic version of energy conservation, namely $\nabla_\mu T^{\mu\nu} = 0$. Another equation often found in the literature is the acceleration equation,

$$\ddot{a} = -\frac{4\pi}{3}G(\rho + 3p)a + \frac{\Lambda}{3}. \tag{2.11}$$

This equation is implied by the Friedmann equation and the fluid equation and therefore contains no extra information. However, the acceleration equation can be very insightful because it gives a direct expression for the second time derivative of the scale factor. This will turn out to be useful when studying the history of the universe.

Returning to the Friedmann equation (2.9) and ignoring the cosmological constant for a moment, we see that the energy density necessary for the universe to be flat ($k = 0$) is $\rho_c = \frac{3H^2}{8\pi G}$. This energy density is called the critical density and depends on time because the

Hubble parameter depends on time. The energy density of the universe is often expressed relative to this critical density, using the density parameter

$$\Omega := \frac{\rho}{\rho_c}. \tag{2.12}$$

$\Omega = 1$ corresponds to a flat universe, $\Omega > 1$ means the universe has positive curvature and $\Omega < 1$ implies a universe with negative curvature. The equivalent quantity for Λ is $\Omega_\Lambda := \frac{\Lambda}{3H^2}$ such that we can write the Friedmann equation in a dimensionless form by dividing both sides by $H^2 = (\frac{\dot{a}}{a})^2$:

$$1 + \frac{k}{a^2H^2} = \frac{8\pi G}{3H^2}\rho + \frac{\Lambda}{3H^2} = \Omega_{\text{matter}} + \Omega_\Lambda. \tag{2.13}$$

Hence, in a flat universe the density parameters of the cosmological constant and the matter content of the universe should add up to one (at all times).

The energy density ρ appearing in the equations above is the total energy density of all types of matter present in the universe. Here the word matter is used in the broadest sense of the word, including both radiation and matter consisting of particles with mass. To solve the equations (2.9) and (2.10), we need to know the relation between energy density and the pressure of all types of relevant matter. The relation $p = p(\rho)$ is called the equation of state and is usually assumed to be of the form

$$p = \omega\rho, \tag{2.14}$$

where $\omega \leq 1$ is a constant that depends on the type of matter we are discussing. Inserting (2.14) into the fluid equation (2.10) and multiplying by $a^{3(1+\omega)}$, yields

$$\dot{\rho}\, a^{3(1+\omega)} + 3(1+\omega)\, a^{2+3\omega}\, \dot{a}\, \rho = \frac{d}{dt}[\rho a^{3(1+\omega)}] = 0. \tag{2.15}$$

This means that the quantity in brackets is a constant and we can write

$$\rho = \rho_0 \left(\frac{a}{a_0}\right)^{-3(1+\omega)}, \tag{2.16}$$

with ρ_0 and a_0 the density and scale factor at a particular time t_0. This result can be used to find the scale factor as a function of time from the Friedmann equation. Let us now discuss some examples of equations of state.

To a good approximation, a non relativistic fluid or gas can be considered pressureless, the reason being that the typical thermal energy of particles is much smaller than their rest energy. Matter with this property is usually called dust and is described by $\omega = 0$. Since for such models the total energy per unit comoving volume should be constant, we expect the energy density to be inversely proportional to the scale factor cubed. From (2.16) and $\omega = 0$ it indeed follows that

$$\rho = \frac{\rho_0 a_0^3}{a^3}. \tag{2.17}$$

In a flat universe filled with dust with no cosmological constant, the equation (2.9) combined with (2.17) now gives

$$a(t) = a_0 \Big(\frac{t}{t_0}\Big)^{2/3} \tag{2.18}$$

and

$$\rho(t) = \rho_0 \Big(\frac{t}{t_0}\Big)^{-2}. \tag{2.19}$$

The equation of state for radiation (or any other type of fluid of relativistic particles) in thermal equilibrium is given by $\omega = 1/3$, which gives

$$\rho = \frac{\rho_0 a_0^4}{a^4}. \tag{2.20}$$

The 4-th power of a can be understood by noting that whille the number density of photons scales with a^{-3}, like in the case of dust, there is the additional effect of redshift when we are dealing with radiation, which throws in an extra factor of a^{-1}. From the Friedmann equation, it follows that a radiation dominated flat universe with no cosmological constant is described by

$$a(t) = a_0 \Big(\frac{t}{t_0}\Big)^{1/2}, \tag{2.21}$$

such that

$$\rho(t) = \rho_0 \Big(\frac{t}{t_0}\Big)^{-2}. \tag{2.22}$$

We conclude that the energy density in a flat radiation dominated universe has the same time dependence as in a dust dominated universe.

If the only relevant component of the universe is the cosmological constant, again assuming flatness, the time evolution of the scale factor follows directly from the Friedmann equation (2.9) with $k = 0$ and $\rho = 0$:

$$a(t) = a_0 e^{\pm\sqrt{\frac{\Lambda}{3}}(t-t_0)}. \tag{2.23}$$

This means that a cosmological constant dominated universe, also called a de Sitter universe, expands exponentially (in case of a "+"-sign in (2.23)). We mentioned earlier that accelerated expansion can also arise from certain types of matter with unconventional equations of state. We can see this from the acceleration equation (2.11). For $\Lambda = 0$, the condition for $\ddot{a}$ to be negative is

$$\rho + 3p > 0. \tag{2.24}$$

This is called the strong energy condition. Since the equation of state implies that $\rho + 3p = (1 + 3\omega)\rho$, we find that the universe will decelerate if the matter in it fulfills $-\frac{1}{3} < \omega \leq 1$. However, there are models, making use of a scalar field, that have $\omega < -\frac{1}{3}$. As we will show, a matter component with $\omega = -1$ has exactly the same effect as a cosmological constant. For matter with $\omega = -1$, we have, from (2.16), $\rho_\omega =$ constant. Looking at equation (2.9), we see that this corresponds to a cosmological constant given by $\frac{\Lambda}{3} = \frac{8\pi G}{3}\rho_{\omega=-1}$ or $\Lambda = 8\pi G \rho_\omega$. The advantage of describing dark energy with a matter field is that we can also create a dynamical cosmological "constant". For example, inflation, a short phase of very strong acceleration in the early universe, can be described by a scalar field with ω (temporarily) smaller than $-1/3$. We will say a little bit more about inflation in the next section.

After having discussed three specific, relatively simple cosmologies ($\omega = -1, 0, 1/3$), we now wish to make some more general remarks before we discuss the so called concordance model, the model that is suggested by observation to describe the universe we live in, in the next section. First of all, we know since the early twentieth century that the universe is expanding. This leads in all realistic models to the conclusion that at some time in the

past the scale factor must have been zero[2] for if we go back in time when the scale factor was smaller, we can ignore the cosmological constant and the acceleration equation (2.11) says that (using that both matter and radiation obey the strong energy condition) $\ddot{a} < 0$. Hence, in earlier times the universe was decelerating, i.e. the further we look back in time, the faster its expansion. Hence, the scale factor must have been zero a finite time ago. This "event" is what is usually referred to as the Big Bang. Form the above argument, it follows that the age of the universe, i.e. the time passed since the big bang, must be of order H^{-1}. Models in which the scale factor reaches zero a finite time ago are called Big Bang models. In the three cosmologies discussed above, it was relatively easy to find the solutions of the equations for a and ρ because we limited ourselves to models with $k = 0$. Fortunately, in a Big Bang model we can at early times describe the universe as if it were flat. The reason for this is that as $a \to 0$, the density parameter will tend to one, which means that the curvature term $\frac{k}{a^2H^2} = 1 - \Omega$ can be ignored. Such a model with $k = 0$ is called an Einstein-de Sitter universe. In the following argument, we will assume the universe to be dominated by a type of matter with equation of state $\omega > -1/3$. For $a \to 0$, this assumption is justified as long as the universe contains at least one such type of matter. Equation (2.16) then makes sure that for a small enough scale factor, this type of matter will dominate the energy content of the universe. From (2.16) and the definition of the density parameter (2.12), it can be derived that

$$H^2 = H_0^2\Big(\frac{a}{a_0}\Big)^{-2}\Big(\Omega_0\Big(\frac{a}{a_0}\Big)^{-(1+3\omega)} + (1 - \Omega_0)\Big), \tag{2.25}$$

and

$$\rho = \rho_0\Big(\frac{a}{a_0}\Big)^{-3(1+\omega)} = \frac{3H_0^2}{8\pi G}\,\Omega_0\,\Big(\frac{a}{a_0}\Big)^{-3(1+\omega)}. \tag{2.26}$$

Equation (2.12) now becomes

$$\Omega = \frac{\Omega_0\Big(\frac{a}{a_0}\Big)^{-3(1+\omega)}}{(1 - \Omega_0) + \Omega_0\Big(\frac{a}{a_0}\Big)^{-3(1+\omega)}}. \tag{2.27}$$

It is now clear that for $a \to 0$, the density parameter goes to one, meaning that the universe becomes flat.

An important concept in cosmology is the particle horizon. It comes up when we ask which part of space could have been in contact with a particular point in space O up to a certain time t. The size of this region can be found by noting that no signal can travel faster than the speed of light. This means that the comoving radius of the region described above is found by calculating the (comoving) distance a light ray travels between $t = 0$ and t. The particle horizon $R_H(t)$ is defined as the physical radius the region has at time t and thus can be found by multiplying the comoving radius by the scale factor at t:

$$R_H(t) = a(t)\int_0^t \frac{dt'}{a(t')}. \tag{2.28}$$

In addition to the particle horizon, there is a handful of other cosmological horizons that can be found in the literature. The significance of the particle horizon is that two points

[2]When a approaches zero, there will be a point in time where the laws of physics we know break down, so we cannot really make any claims about what happens before that time and technically we do not know if a goes all the way to zero.

separated by a distance larger than $R_H(t)$ have not had the time to send any kind of signal to each other. Until the distance between them gets smaller than the horizon, the two points are in completely separate parts of the universe. In this thesis, we will only be interested in the order of magnitude of $R_H(t)$, which is about $R_H(t) \sim t$.

2.3 The Concordance Model

The concordance model is the cosmology currently thought to descibe the universe best. It is supported by a broad spectrum of observations, ranging from galaxy cluster counts to measurements of the anisotropies in the cosmic background radiation (CMB). In this section, we will present the basic properties our universe is thought to have without going into their experimental justification. Readers who wish to know more about that subject are referred to, for example, [7].

In the concordance model, the universe was formed about 13.7 billion years ago with the Big Bang. We will start by describing the current properties of the universe and then work our way back in time towards the Big Bang. Since the uncertainty in the Hubble parameter has for a long time been rather large, H_0 (its value at the present time t_0) and quantities depending on H_0 are often expressed in terms of the dimensionless parameter h, defined by $H_0 = 100\,h\,\mathrm{kms}^{-1}\mathrm{Mpc}^{-1}$, of which for a long time not much more was known than that it lies in the interval $0.5 < h \leq 1.0$. We now now with reasonable certainty that $h = 0.7$. Furthermore, the universe is flat, i.e. $k = 0$, and it is dominated by the cosmological constant (or some other form of dark energy): $\Omega_\Lambda \approx 0.7$. Of the rest of the energy content, the majority is made up by an unknown type of matter that cannot be observed directly. The presence of this dark matter, as it is called, is only betrayed by its gravitational effects. About 25 % of the energy content of the universe is thought to be in the form of cold dark matter (CDM): $\Omega_{CDM} = 0.25$. The rest of the energy in the universe (about 5 %) mostly consists of non-relativistic matter, mainly baryonic, and radiation. At present, the energy density in non-relativistic matter greatly exceeds that in radiation. It is interesting to realize that of the ordinary matter that is present, only a small part can be considered (optically) visible matter. We must conclude that visible matter only plays a marginal role in our universe. The density parameter of all types of matter combined shall be written $\Omega_M \approx 0.3$. Note that because the universe is flat, the density parameters add up to one (see equation (2.13)): $\rho = \rho_c \approx 1.9 \cdot 10^{-26} h^2\,\mathrm{kg\,m}^{-3}$. The model described above is often referred to as a Λ-CDM model, for reasons that should now be clear.

If we extrapolate this situation to the future, the cosmological constant will dominate more and more and eventually, the universe will be a de Sitter universe. We will now walk through the different periods the universe went through in the past by discussing some crucial points in time. From now on, we define the scale factor to be equal to one at the present time[3]. Points in the history of the universe will be characterized by redshift, $z = 1/a - 1$, by temperature T, which roughly scales with a^{-1}, and cosmic time t (the time passed since the big bang). As we come closer to $t = 0$, these quantities will become increasingly uncertain.

0. **Now**; $z = 1,\ T \approx 3$ K, $\ t \approx 13.7 \cdot 10^9$ yrs.

[3]We can do this because the universe is flat. For $k \neq 0$, the curvature sets a typical scale and we cannot in general define our coordinates such that the scale factor is one at present unless we allow $|k|$ to take on other values than one.

1. **Matter - Λ equivalence**; $z < 2$.

Looking back in time, Λ will start to matter less and less because its energy density is constant while the matter density goes like a^{-3} and the radiation density like a^{-4}. It is remarkable that the time when the matter component and the dark energy component were exactly equal is very close to the present time. A straightforward calculation shows that this must have been somewhere between now and the time at which the scale factor was half the current size. Before this time, the universe was dust dominated. It seems that we live in a rather special time in the history of the universe, which is always reason for some concern in science.

2. **Decoupling**; $z \approx 10^3,\ T \approx 3 \cdot 10^3$ K, $t_{\mathrm{D}} \approx 3 \cdot 10^5$ yrs.

Before this time, the density is so high that atoms are not stable. This means the universe is filled with a plasma of (among other things) unbound protons and electrons. The timescale relevant for the interaction of photons with particles is much smaller than the characteristic expansion timescale and thus matter and radiation are coupled. Hence, matter and radiation are in thermal equilibrium and a single temperature T can be used to describe it. After protons and electrons join to form atoms (a process called recombination), the photons decouple from matter and can virtually move freely. The subset of space-time corresponding to $t = t_{\mathrm{D}}$ is called the last scattering surface and had a temperature of about $3 \cdot 10^3$ K. The radiation released from the last scattering surface is seen now as cosmic background radiation and has cooled to a mere 3 K due to the expansion of the universe.

3. **Matter - radiation equivalence**; $z \approx 10^4,\ T \approx 3 \cdot 10^4$ K, $t_{\mathrm{eq}} \approx 10^4$ yrs.

Since the energy density in radiation grows faster than the energy density in matter as the scale factor gets smaller, eventually the universe will be radiation dominated as we move back in time. The time that marks the transition between a dust dominated and a radiation dominated universe is t_{eq}. Before t_{eq}, the universe is radiation dominated all the way down to the big bang except, possibly, for a brief period of inflation which will be discussed later.

4. **Quark - hadron transition**; $z \approx 10^{12},\ T \approx 200 - 300$ MeV, $t_{\mathrm{qh}} \approx 10^{-5}$ s.

Another important moment is the time at which quarks start to be confined t_{qh}. Before this time, the temperature is so high that quarks can exist freely, while after t_{qh}, quarks only appear in bound states called baryons. Since we are now entering the realm of rather high energy scales, temperatures will from now be expressed in units of energy (eV). The energy scale corresponding to a certain temperature is found by multiplying the temperature by Boltzmann's constant k_B, which, in SI units, is given by $k_B = 1.38 \cdot 10^{-23} JK^{-1}$. The quak-hadron transition occurs when the temperature reaches $T \approx 200 - 300$ MeV.

5. **Electroweak transition**; $z \approx 10^{15},\ T \approx 10^2$ GeV, $t_{\mathrm{EW}} \approx 10^{-11}$ s.

For $t > t_{\mathrm{EW}}$, apart from gravity, physics is governed by three distinct fundamental forces: the strong nuclear force, the weak nuclear force and electromagnetism. The electromagnetic

force is described by a $U(1)$ invariant gauge theory and is mediated by a massless vector boson, the photon, whereas the vector bosons that carry the weak nuclear force have very high mass, which is why this force is so short ranged. However, for high enough temperature, electromagnetism and the weak interaction are unified into one force. The gauge group describing this so called electroweak interaction is[4] $(SU(2) \times U(1))/Z_2$. Since the gauge group describing the strong interaction is $SU(3)$, the symmetry group of the full lagrangian is now $G = (SU(3) \times SU(2) \times U(1))/Z_6$. The electroweak (phase) transition, i.e. the transition between the phase where there is one unified electroweak force and the phase where electromagnetism and the weak interaction are separate forces, occurs at a temperature $T \approx 10^2$ GeV, corresponding to $z \approx 10^{15}$. In general, the process of the relevant symmetry group getting smaller ("breaking down") as the temperature drops, is called spontaneous symmetry breaking, which will be the topic of the next section.

On energy scales beyond the energy scale corresponding to the electroweak transition, physics becomes highly speculative. Therefore, our discussion of the following period in the history of the universe should be treated accordingly.

6. **The GUT time**; $z \approx 10^{28}$, $T \approx 10^{15}$ GeV, $t_{\mathrm{GUT}} \approx 10^{-37}$ s.

It is assumed that at $t = t_{\mathrm{GUT}}$, there is a phase transition to a theory with an even bigger symmetry group in which there is only one fundamental force (in addition to gravity). Such a theory is called a grand unified theory (GUT) because it unifies the strong and the electroweak force into one force, but a realistic GUT has not yet been found. For that reason, also the energy, and correspondingly the time, at which it occurs is not known exactly. A popular candidate GUT is described by the symmetry group $G_{\mathrm{GUT}} = SU(5)$, which breaks down at $E_{\mathrm{GUT}} \approx 10^{15}$ GeV. However, it should be noted that the GUT described by $SU(5)$ predicts that protons decay at a rate too high to be consistent with observation and can therefore not be the GUT we are looking for. In general, it may be that the transition from G_{GUT} to $(SU(3) \times SU(2) \times U(1))/Z_6$ is achieved by a series of phase transitions between t_{GUT} and t_{EW}. Clearly, when talking about this period in the history of the universe, we have to leave a lot of room for uncertainty.

The GUT time is also the time around which a period of inflation is thought to have occurred. This is a period of accelerated expansion in which the scale factor grows extremely rapidly within a short period of time. Inflation became popular in the early eighties because it can eliminate a number of big problems in cosmology, most notably the horizon problem (the fact that, in a model without inflation, at recombination, the universe was virtually homogeneous on scales much larger than the cosmic horizon at that time) and the flatness problem (the fact that the geometry of the universe is extremely close to being flat). It might also explain why monopoles do not dominate the energy density at the present time (the monopole problem). Another important feature of inflation is that it can explain the small deviations from homogeneity, needed for structure formation to occur later, as quantum fluctuations that were blown up by inflation to macroscopic size. The predictions about the nature of these density perturbations agree very well with the observed anisotropies in the CMB. For these reasons, inflation is now a rather important part of the cosmological "standard model".

[4]Both $SU(2)$ and $U(1)$ have $Z_2 = \{-1, 1\}$ as a subgroup. Hence, in order to not double count this group, it is divided out. In general, $SU(n)$ has the subgroup Z_n in common with $U(1)$ and this group needs to be divided out when the product $SU(n) \times U(1)$ is considered.

7. **The Planck time**; $z \approx 10^{32},\ T \approx 10^{19}$ GeV, $t_{\rm P} \approx 10^{-43}$ s.

So far, it was possible to treat physics on small scales and physics on large scales separately: the physics on large scales was described purely by general relativity, while physics on small scales was described purely by quantum physics. However, if we go back in time far enough, the energy density becomes so big, and the cosmic horizon size so small, that the cosmological scales on which gravity is important and the scales on which the quantum theory of the three other fundamental forces should be applied, coincide. At this point, a theory of everything (TOE) is needed that unifies gravity with the other fundamental forces.

The Planck mass, $m_{\rm P}$, can be defined as the mass for which a particle's Schwarzschild radius $l_{\rm S}$ is of the same order as its Compton length l_C. If these two lengths are approximately the same, it is clear that both gravity and quantum effects need to be taken into account to describe the particle. In the following discussion, we will use units with c and $\hbar$ not necessarily equal to one. The relation $l_{\rm C} = l_{\rm S}$ gives $\frac{\hbar}{mc} = \frac{2Gm}{c^2}$, and hence we define

$$m_{\rm P} := \left(\frac{\hbar c}{G}\right)^{1/2} \approx 2.5 \cdot 10^{-8} kg. \tag{2.29}$$

The Planck energy is then defined to be the energy corresponding to this mass $E_{\rm P} := m_{\rm P}c^2 = \left(\frac{\hbar c^5}{G}\right)^{1/2} \approx 10^{19} GeV$, the Planck time is $t_{\rm P} := \frac{\hbar}{m_{\rm P}c^2} = \left(\frac{\hbar G}{c^5}\right)^{1/2} \approx 10^{-43} s$ and the Planck length is $l_{\rm P} := ct_{\rm P} = \left(\frac{\hbar G}{c^3}\right)^{1/2} \approx 2 \cdot 10^{-35} m$.

On dimensional grounds, when the age of the universe is roughly $t_{\rm P}$, the energy $k_B T$ corresponding to the temperature of the universe, roughly equals the Planck energy. This means that, at this time, the energy of a typical particle is about $E_{\rm P}$ and its Schwarzschild radius and Compton length are equal, namely about $l_{\rm P}$. Moreover, the cosmic horizon size $R_{\rm H}$ is also about equal to the Planck length, since it is roughly equal to ct. In other words, the scale on which gravity is important and the scale on which quantum physics is important, are the same. Hence, a TOE will be necessary to describe the universe for $t \lesssim t_{\rm P}$. A candidate for such a theory is string theory, which describes all particles and interactions in terms of excitations of fundamental strings. Unfortunately, this theory is mathematically very challenging and is still far from being fully understood. Another problem with string theory is that it will be hard to come up with realistic experiments to test it. At present, we have to admit that we simply do not know anything (yet) about what happens at energies above the Planck energy. Fortunately, the Planck time is extremely small and a large part of history *can* be understood.

2.4 Spontaneous symmetry breaking and cosmic topological defects

The phase transitions at $t_{\rm EW}$ and $t_{\rm GUT}$ correspond to a process called spontaneous symmetry breaking. It is through this process that topological defects might have formed in the early universe. In this section, we will first explain the process of spontaneous symmetry breaking in the context of the abelian Higgs model discussed in section 1.2. This can then easily be generalized to symmetry breaking in GUT's. We will discuss the conditions on the symmetry breaking process, under which the formation of topological defects occurs and find that, in

certain GUT's, cosmic strings are indeed formed in the early universe. A more extensive discussion of string formation and evolution in the early universe can be found in [13].

In the abelian Higgs model, given by the lagrangian (1.6), with a potential given by

$$V(|\phi|) = \alpha\,|\phi|^2 + \beta\,|\phi|^4 \quad \alpha, \beta > 0, \tag{2.30}$$

The vacuum expectation value (VEV) ϕ_0 of the Higgs field, i.e. the value of ϕ that minimizes the potential, is $\phi_0 = 0$ and has the same symmetry as the lagrangian, i.e. $G = U(1)$. In perturbative quantum field theory, the significance of the VEV is that the field is suppposed to be expanded around it. The perturbations around the VEV can then be considered as the real physical fields with the usual particle interpretations. In general, this means that if ϕ_0 is a VEV, we write

$$\phi = \phi_0 + \sigma \tag{2.31}$$

and express the lagrangian in terms of the "physical" field σ. The field σ will now be considered to represent a particle and one can apply ordinary perturbation theory. In case of the potential (2.30), $\sigma = \phi$ and the group of transformations on σ that leaves the lagrangian unchanged is exactly the same as the group of transformations on ϕ that leaves the lagrangian unchanged, namely $G = U(1)$.

However, if the potential is the mexican hat potential (1.10) (corresponding to $\alpha < 0$ in (2.30)), the VEV has to be of the form $|\phi_0| = \eta$. Even though the set of possible VEV's now still has the symmetry G, any particular choice of ϕ_0 does not. In this model, the only element of G that will leave a particular VEV invariant is the identity element. The group that leaves a particular VEV invariant is the broken group H which we encountered in section 1.4. When the field is expanded around a VEV as in (2.31), H is the group of transformations on σ that will leave $\mathcal{L}$ unchanged. The process of the Higgs field acquiring a non-zero VEV is called spontaneous symmetry breaking. From the point of view of someone interested in topological defects, the most important aspect of symmetry breaking is the fact that the gauge group gets maller ($G \to H$). However, from a particle physics point of view, there is another very important effect of symmetry breaking, namely that the gauge field acquires a mass. Noting that, without loss of generality, we may choose $\phi_0 = \eta$ such that $\phi = \eta + \sigma$, the gauge mass follows from

$$D_\mu\eta\,(D^\mu\eta)^\dagger = e^2\eta^2 A_\mu A^\mu = \frac{1}{2}M^2 A_\mu A^\mu, \quad M = \sqrt{2}e\eta. \tag{2.32}$$

In addition, the real part of the (new) Higgs field $Re(\sigma)$ also acquires a mass because the potential

$$\frac{\lambda}{4}(|\phi|^2 - \eta^2)^2 = \frac{\lambda}{4}(|\sigma|^2 + 2\eta Re(\sigma))^2 \tag{2.33}$$

contributes the term

$$\lambda\eta^2 Re(\sigma)^2 = m^2 Re(\sigma)^2, \quad m = \sqrt{\lambda}\eta \tag{2.34}$$

to the lagrangian. In general, the excitations of the Higgs field, i.e. the deviations of ϕ from ϕ_0, within the vacuum manifold are massless because these excitations are in the direction of constant potential V. The massless particles corresponding to these excitations are called Goldstone bosons. However, these components of the field can be put to zero by a suitably chosen gauge transformation. The gauge fields corresponding to the excitations of the Higgs field described above acquire a mass in this process. The excitations of the Higgs field perpendicular to the vacuum manifold also acquire a mass because they increase the potential energy, i.e. in these directions the potential has positive second partial derivatives. The

process of gauge particles acquiring a mass through spontaneous symmetry breaking is called the Higgs mechanism. It is through this mechanism that the vector bosons that mediate the weak interactions get their mass in the standard model.

The two situations described above are static in the sense that either the symmetry is always unbroken (if the potential is given by (2.30) with $\alpha > 0$) or it is always broken (if the potential is given by 2.30) with $\alpha < 0$ or (1.10)). Evolution from the unbroken phase to the broken phase may occur if the potential changes with temperature T. For finite T, the VEV ϕ_0 is found by minimizing the so called *effective* potential[5] $V(\phi, T)$ (see for example [11]), which is constructed by making temperature dependent (and ϕ dependent) corrections to the zero temperature potential $V(\phi)$. Let us assume the effective potential is given by

$$V(|\phi|, T) = \alpha(T)\,|\phi|^2 + \beta(T)\,|\phi|^4, \quad \beta > 0. \tag{2.35}$$

For $\alpha < 0$, this potential has a non-zero minimum given by $|\phi|^2 = \frac{\alpha(T)}{2\beta}$, while for $\alpha(T) \leq 0$ there is only one minimum, namely $\phi = 0$. If we now assume that there is a critical temperature T_c such that for $T > T_c$, $\alpha(T) > 0$ and hence the symmetry unbroken, and for $T < T_c$, $\alpha(T) < 0$, and hence the symmetry broken, we have found a way to obtain a phase transition from the symmetric to the broken phase.

In a GUT, the lagrangian of course consists of many more fields than in the abelian Higgs model used above. In particular, there may be more than one Higgs field. However, the phase transitions within a GUT can be explained in the same way as in the abelian Higgs model. Again, there will be a temperature dependent effective potential $V = V(|\phi|, T)$. For temperatures $T > T_{\text{GUT}}$, the effective potential is such that the VEV has the same symmetry as the complete lagrangian, in analogy with (2.35) for $\alpha(T) \leq 0$, and the gauge group describing the field theory is G_{GUT}. Now for $T < T_{\text{GUT}}$, the potential will be such that spontaneous symmetry breaking takes place. The theory is now described by the unbroken symmetry group H that leaves the new VEV invariant. As was mentioned in the previous section, several such phase transitions may take place from T_{GUT} down to T_{EW}. The last phase transition is the electroweak transition at T_{EW} leading from $(SU(3)\times SU(2)\times U(1))/Z_6$ to the group describing the standard model that is still "operational" at present, $(SU(3)\times U(1))/Z_3$. This gives a sequence $H_1 \subset H_2 \subset ... \subset H_n$ of groups with $H_1 = (SU(3) \times U(1))/Z_3$, $H_2 = (SU(3) \times SU(2) \times U(1))/Z_6$ and $H_n = G = G_{\text{GUT}}$.

Whether or not topological defects can exist at a certain time when the relevant symmetry group is H_i ($i \in \{1, ..., n\}$), depends on the homotopy groups of the vacuum manifold G/H_i at that time, as was explained in section 1.4. Monopoles are allowed to exist if $\pi_2(G/H_i)$ is non-trivial. If we make the assumption that G has no incontractible spheres or loops (this is definitely the case for the GUT described by $SU(5)$), theorem (1.4.2) tells us that $\pi_2(G/H_i) = \pi_1(H_i)$. Since H_i must contain $U(1)$, any GUT for which the modest assumptions made above hold, predicts the possible[6] existence of magnetic monopoles. Cosmic strings are allowed to exist if $\pi_1(G/H_i)$ is non-trivial. Hence, if we assume that G is connected and has no incontractible loops, theorem (1.4.2) tells us that cosmic strings can arise if $\pi_1(G/H_i) = \pi_0(H_i)$ is non-trivial. In other words, H_i needs to be disconnected for strings to be able to exist. Hence, if the assumptions made about G hold, there will be no topologically

[5] We use the same letter, namely V, for both the effective and the "ordinary" zero temperature potential. The two can be distinguished because for the effective potential we explicitly write the temperature dependence.

[6] We use the word possible because the existence of monopole configurations does not necessarily mean that these configurations are realized in nature.

stable strings after the phase transition leading to H_1. Finally, domain walls may exist if the vacuum manifold is disconnected, i.e. $\pi_0(G/H_i)$ needs to be non-trivial. To determine whether or not there can be domain walls, there is no theorem like theorem (1.4.2) to make things easier. One really needs to know the full group G.

Once it has been established whether or not a field theory allows topological defect solutions after a certain phase transition, the next question is whether or not these defects are actually formed in nature. The answer appears to be yes. If the phase transition is of second order, then, at the time of the phase transition, the field will tend to a VEV $\phi_0 \in \mathcal{V}$ at every point in space and the values of ϕ_0 will be correlated over large distances. However, points separated by a distance larger than the horizon size $R_H(t)$ cannot be correlated at all, because of causality. Hence, on super horizon scales, ϕ_0 is not correlated and topologically non-trivial configurations enclosing defects will exist. For the example of the abelian Higgs model from section 1.2, the process described above is illustrated in figure 2.2. A non-zero VEV is reached everywhere, dividing space into regions with roughly the same phase. The strings form at the boundaries between these regions around which there is a non-zero winding number. If the phase transition is of first order, the field will go to its new VEV in a different way, but the same result holds, namely the formation of uncorrelated regions with defects trapped between them (see for example [13]). In conclusion, if at some time in the history of the universe, the topology of the vacuum manifold allows defect configurations, these configurations probably actually exist at that time.

Even though we have shown that GUT's may also predict monopoles and domain walls, we will from now on focus exclusively on strings. It turns out that it is very hard to make the existence of monopoles or domain walls consistent with observation. The reason for this is that, unless they form at relatively late times, these defects would come to dominate the energy density of the universe rather soon after they come into existence. This is clearly inconsistent with observation because we would not even exist if this had happened.

Assuming that cosmic strings form at some point, it is important to understand the details of their formation and subsequent behavior. This behavior of course depends on the details of the GUT they appear in. For instance, in certain models, there exist so called superconducting strings, which have very different properties than the strings that we know from the abelian Higgs model. If, after a certain phase transition characterized by a critical temperature T_c, the unbroken group H_i is such that the vacuum manifold G/H_i allows for the existence of cosmic strings, the symmetry breaking process described above creates a network of strings that will subsequently evolve. An important parameter for the description of cosmic string networks is the characteristic length scale ξ, which is a measure for the typical separation of cosmic strings. It is formally defined such that a volume ξ^3 contains a total string length ξ. Remembering from section 1.3.1 that μ is the string energy per unit length, we can write this in the alternative form

$$\rho_s = \frac{\mu}{\xi^2}, \tag{2.36}$$

where ρ_s is the energy density of the string network. From the discussion about string formation, it is clear that at the time of formation, we must have $\xi < R_H \approx t$ and probably even $\xi \ll r_H \approx t$. The details of string formation have been investigated numerically by, among others, [29]. It was found that the majority (about 80 %) of the total string length was part of infinite strings and the rest was part of string loops. Other simulations give similar conclusion, although the exact numbers may differ. Around the time the universe reaches $T = T_c$, the universe is dominated by (high energy) radiation. Hence, right after

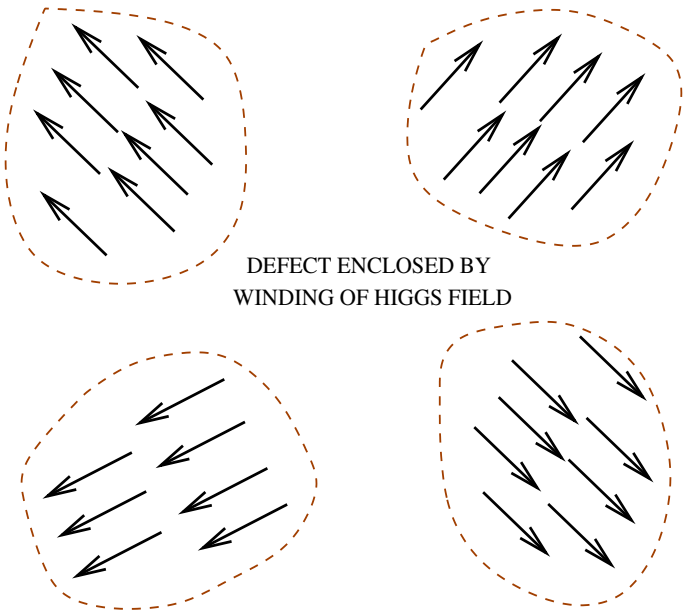

Figure 2.2: During a (second order) cosmic phase transition, the VEV's of the fields move to a value on the new vacuum manifold everywhere at the same time. Points in space that are separated by a distance larger than the horizon size have never been in contact in any way and therefore, after the phase transition, the VEV's at these points will be completely independent. This means that, if the topology of the vacuum manifold allows it, topologically non-trivial configurations enclosing defects will be formed. The figure illustrates this in the case of the abelian Higgs model. The arrows indicate the phase of the VEV of the Higgs field and the regions enclosed by the dashed lines are assumed to have a size of the same order as the cosmic horizon size and to be separated by a distance (slightly) larger than the horizon size. Within these regions, the phase of the Higgs field is about the same, but the phase in any region is independent of the phase in any other region. Hence, a configuration with non-zero winding number can be formed. In the figure, the winding number happens to be equal to one. Therefore, somewhere in between the regions, the Higgs field must thus be equal to zero. In other words, a cosmic string passes through this central region.

string formation, string motion is heavily damped by the surrounding radiation. This causes the string network to lose energy and (equivalently) the characteristic length ξ to grow. It can be shown (see for example section 5.3 of [13]) that this will soon (for $T_c = T_{\mathrm{GUT}}$, it will occur around $t \sim 10^{-31}$ s) cause ξ to become of the same order as the horizon size t, regardless of the value of ξ at the time of string formation. The typical string radius will then be negligible compared to ξ. Not long after this, as the universe cools further, the friction with radiation will become irrelevant because the energy density in radiation becomes too small. The strings will then practically become independent of anything else in the universe. How the string network evolves from here will be the topic of the next section.

We conclude this section by noting that, for a while, the string network was considered a possible explanation of the existence of structure (i.e. deviations from perfect homogeneity and isotropy) in the universe. A string network has an inhomogeneous energy distribution and therefore perturbs the metric of the universe. These perturbations might have acted as the seeds of the current inhomogeneity of the universe. However, this scenario has by now been abandoned in favor of the scenario based on inflation, which agrees very well with the anisotropy observed in the CMB and other observations. Still, it may be possible that the string network accounts for a small fraction of density perturbations. The current upper bound is about 10 % ([25]).

2.5 String evolution

Starting at a time t_0 with a network of characteristic length scale $\xi \sim t$ that (virtually) does not interact with the other types of matter in the universe, we wish to know how this network will evolve in an expanding universe. It is known that the string loops can decay by emission of particles and gravitational radiation. Infinite strings on the other hand are not allowed to disappear because of conservation of winding number. An important question is how the infinite string energy density evolves with time. Let us start answering this question assuming the network of infinite strings does not lose any energy at all. In that case, the evolution of the string energy density is completely determined by the expansion of the universe. Hence, the characteristic length ξ will be proportional to the scale factor a, i.e. the strings are stretched by the expansion of the universe, and consequently the energy density expressed in terms of quantities at $t = t_0$ will, from equation (2.36), be given by

$$\rho_s = \rho_{s,0}\Big(\frac{a}{a_0}\Big)^{-2}, \quad \rho_{s,0} = \frac{\mu}{\xi_0^2}, \tag{2.37}$$

which goes like t^{-1} in a radiation dominated universe. Since the radiation energy density scales with a^{-4} and the matter density scales with a^{-3}, this means that if there is no energy loss mechanism, the universe will eventually be dominated by the string network. Since the energy density in radiation in a radiation dominated universe ($a \sim \sqrt{t}$) is roughly given by $\rho \approx \frac{3}{32\pi G t^2}$ from the Friedmann equation, the ratio of the energy density in the string network to the energy density in radiation is given by

$$\frac{\rho_s}{\rho} \approx \frac{32\pi}{3}\,\frac{\mu G}{\xi_0^2}\,t_0\,t \approx \frac{30\mu G}{t_0}\,t. \tag{2.38}$$

For realistic values of μ and t_0, (2.38) implies that strings will come to dominate the universe relatively soon after they come into existence, which is apparently the same problem as with

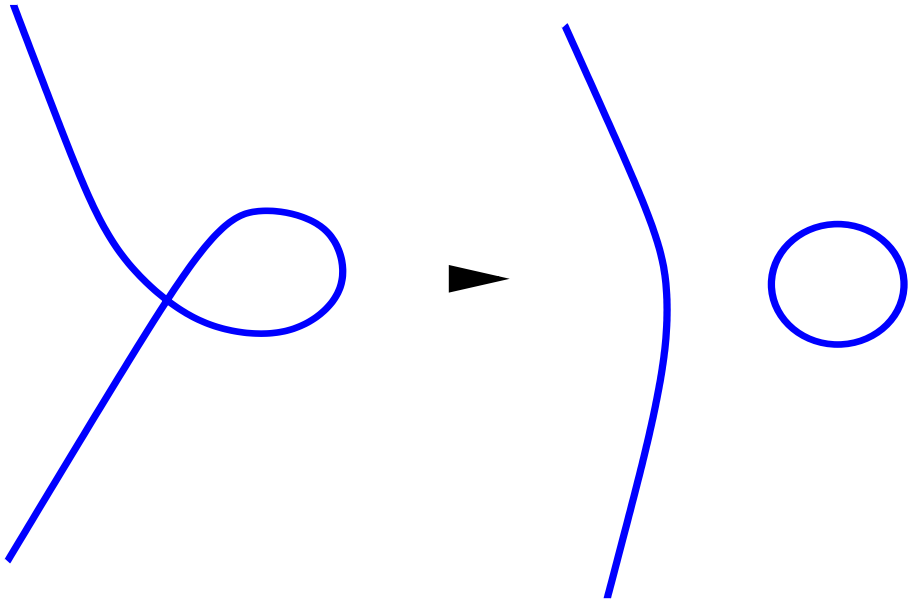

Figure 2.3: When an abelian higgs string comes to intersect itself, there are two possible outcomes. Either the string simply passes through itself, or a loop is formed. The latter process is sketched here. The loop that is formed decays by emitting particles and gravitational radiation and hence loop formation is a possible way the string network can lose energy.

monopoles and domain walls. This would be a big problem because clearly, today, we see no trace of strings ever having dominated the universe. In fact, to be consistent with observations, only a small fraction of the total energy density of the universe could have consisted of cosmic strings at any time during the history of the universe. To make things more quantitative, let us explicitly write the network scale ξ as a function of t:

$$\xi(t) = \gamma(t)\, t. \tag{2.39}$$

Since the "ordinary" energy density in both a matter and a radiation dominated universe scales like t^{-2}, equation (2.36) tells us that $\gamma(t)$ should either approach a constant as time goes by, or it should keep growing. If instead $\gamma(t)$ keeps getting smaller, ρ_s will fall off slower than t^{-2} and will eventually dominate the total energy density, which is inconsistent with observations. However, causality tells us that ξ cannot grow faster than (a constant times) t because otherwise, the characteristic length will grow much larger than the horizon size. Hence, the only remaining option that is consistent with cosmology is that $\gamma(t)$ approaches a constant, say γ, i.e. for large enough time, $\xi = \gamma t$. Such a solution is called a scaling solution and once γ has indeed reached a constant, the network is said to be in the scaling regime. Since we have shown that if the infinite strings do not lose energy, their energy density scales like t^{-1}, we must conclude that, if strings have indeed formed, there has to exist a mechanism through which infinite strings can lose energy and it must be strong enough for the string network to reach a scaling solution. Furthermore, the string energy density in this scaling solution must be small compared to the energy density of ordinary matter/radiation.

Luckily, such a mechanism seems to exist. Strings are expected to lose energy by forming string loops, as we will explain here. Since the strings in a typical network will not be

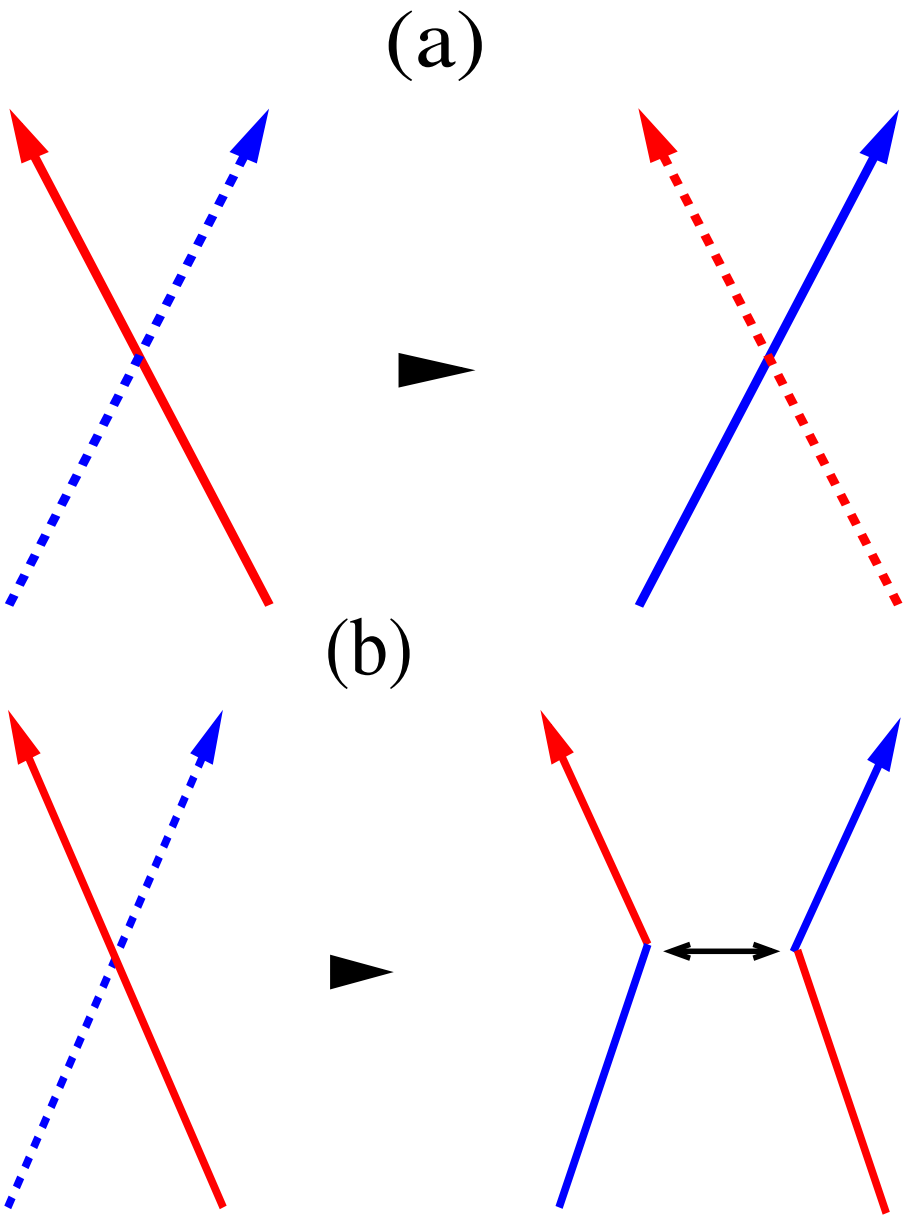

Figure 2.4: The process of loop formation as shown in figure 2.3 can be understood in terms of the interaction of two (segments of) strings. When two (abelian higgs) string segments intersect, they either pass through each other (a), or they exchange ends (b). The latter process is called intercommutation and results in loop formation if a string intersects *itself*. In the figures, if a string lies behind the other string, it is represented by a dashed line.

straight, but instead rather wiggly, strings will often self intersect. When a string intersects itself, two things can happen. The first possibility is that the intersecting string segments move through each other and the string keeps its original shape. The other[7] possibility is the more interesting one (see 2.3). It may happen that the string segments exchange ends. In this process, string orientation, defined by the handedness of the winding of the Higgs field, should be conserved. If this happens, a loop is formed and the remaining infinite string loses some of its length. The loop that thus comes into existence then decays by emitting particles and gravitational radiation. The end result of this process is that the infinite string, and therefore the string network, loses some of its length/energy. The process of two string segments exchanging ends (see figure 2.4), as opposed to simply passing through each other, is called intercommutation or reconnection. Whether or not two string segments intercommute when they intersect of course depends on many things, like the velocities of the segments and their relative angle, but, when dicussing network evolution, we are mainly interested in the so called intercommutation probability, p, which is simply the likelihood that a random intersection in a network leads to intercommutation. As one might expect, the efficiency of loop formation as an energy loss mechanism depends directly on this intercommutation probability. It can be shown by analytic arguments that if p is of order one, a scaling solution consistent with cosmology may be reached. In [28], this is done using a simple one-scale model. More complex models have also been used, but yield the same qualitative result. Readers interested in these analytic models of network evolution are referred to [16] or, more recently, [20, 17, 18]. We will see later that in the cases investigated so far, indeed $p \approx 1$. It is imporant to realize that, in the abelian Higgs model, the intercommutation probability only depends on the parameter β. As was shown in section 1.2, the two other degrees of freedom in parameter space only have relevance in that they are necessary to determine the energy and length/time scales of the system. However, once the evolution of the rescaled fields, which only depends on β, has been determined, changing the overall energy or length scale of the system has no effect on whether or not intercommutation has taken place. With cosmic strings, we will from now on mean the strings ocurring in the abelian Higgs model (given by the lagrangian (1.6)). For finite β, we speak of local strings and for $\beta \to \infty$, we speak of global strings. In the latter case, the gauge fields can be ignored and the lagrangian is given by (1.1). We by no means claim that all strings can be described as abelian Higgs strings. Non-abelian strings can for example have some completely different properties.

There are two types of simulations of cosmic string networks that we wish to briefly discuss, both of which seeming to confirm that scaling solutions consistent with cosmology exist. The first type is desribed in [1] (see also [5]) and approximates all infinite strings as infinitely thin strings that undergo free motion as long as they do not intersect. The free motion of strings is found using an effective action, found by integrating over the world sheet of a string. This so called Nambu-Goto action and corrections to it are discussed quite clearly in [3]. When strings intersect, the strings intercommute with probability p, which is a parameter of the simulations that needs to be put in by hand. If they do not intercommute, they simply move through each other. Either way, after the interaction the strings move freely again. Obviously, for this type of simulation it is crucial to have a good estimate of the value of p. A big advantage of this type of simulation is that it is computationally not so demanding.

[7] There is actually a third possibility. For non-abelian strings it may also happen that the two string segments get entangled. In this thesis, this possibility will not be relevant because we will not discuss strings arising in non-abelian gauge theories.

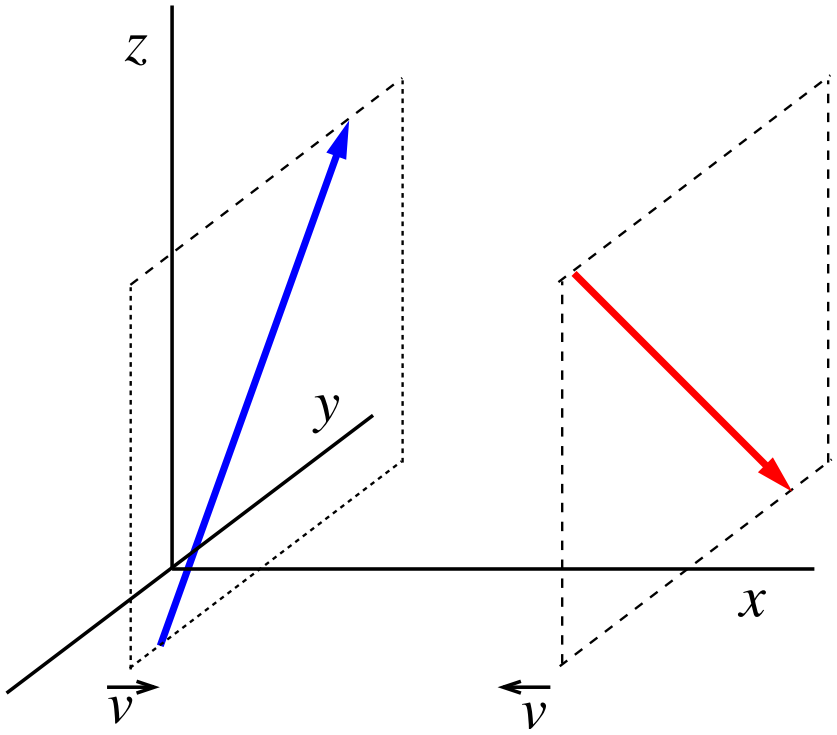

Figure 2.5: The typical initial configuration for a simulation of the interaction of two strings. Both strings lie in a plane of constant x. The string on the left (string 1) moves in the positive x-direction with velocity v and the string on the right (string 2) moves in the negative x-direction with the same speed. The orientation of the strings is indicated by arrows.

The disadvantage is that a lot of assumptions about the dynamics of strings need to be made. The second type of simulation we would like to discuss does not have this problem.

In these simulations (see for example [18, 20]), the exact evolution of the fields is calculated using a lattice field theory approach. The intercommutation probability does not have to be put in by hand and for a fixed background cosmology and fixed initial situation, the evolution basically only depends on β. However, all simulations of this type that we know of, use $\beta = 1$. Hence, it would still be useful to have knowledge of p as a function of β, as this would give us a quick way to estimate how the network evolution depends on β (using the dependence of network evolution on p known from the first type of simulation and from analytic models).

Another reason we would like to know more about the intercommutation behavior of cosmic strings is simply that it is a very fundamental property of cosmic strings. In the next section we will go into the current state of knowledge about intercommutation.

2.6 String intercommutation

Intercommutation is usually studied by asking what will happen when two straight strings approach each other. Without loss of generality, we will assume the strings to lie in planes of constant x and to approach each other in the x-direction with equal speeds (see figure 2.5 and figure 2.6). If a system of two straight strings does not look like this, a Lorentz

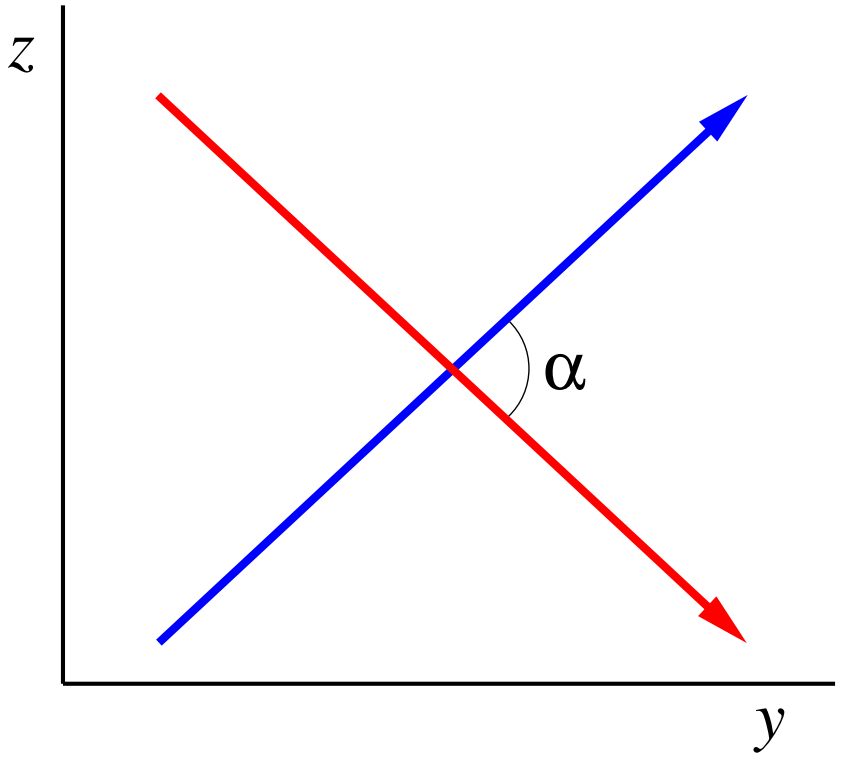

Figure 2.6: The configuration from figure 2.5 projected on the yz-plane. The orientation of the strings is indicated by arrows and α is defined to be the angle between the strings. Whether or not intercommutation takes place depends on this angle and on the speed v.

transformation can be applied such that the sytem does fit the above description. Such a system can be described by only two parameters: the speed $v > 0$ that each string has in the direction of the other string (i.e. string 1 has velocity v and string 2 has velocity $-v$), and the angle α between the two strings when they are projected on the yz-plane. Since local strings have a finite width, we can in principle always make the initial seperation of the two strings big enough for the strings initially not to notice each other's presence. This means that as long as the initial separation exceeds twice the string radius, the interaction will be independent of the initial separation. Global strings on the other hand have an infinite width (the fields around a global string never reach zero energy density because there is no gauge field to compensate the gradients in the Higgs field). This means that, in principle, the result of a global string simulation does depend on the initial separation. This dependence might be removed by using as parameters the velocity and angle at the time (or just before) the strings intersect instead of the initial velocity and angle. In the following discussion, we will not explicitly mention any dependence on initial separation.

Two questions naturally arise. The first is whether or not, with the initial configuration described above, the strings will at some time meet and intersect. If the strings do not repel this will certainly happen, but it might be that the strings repel and never come to overlap. The second question arises if the strings indeed meet: will they exchange ends (intercommute) or will they pass through each other? Ideally, we would like to know for all combinations of α and v whether or not intercommutation takes place. As we explained in the previous section, this may depend on β. It can be conveniently expressed in terms of the "step function" $P_\beta(\alpha, v)$, which is defined to be equal to one if intercommutaton takes place and equal to zero if it does not. Note that $P_\beta(\alpha, v)$ only takes on these two values because we are talking about a classical deterministic process, which for fixed initial conditions always gives the same result. The intercommutation probability p can be obtained by taking a weighted average of the step function over parameter space ($0 \leq \alpha \leq \pi$ and $0 < v < 1$). The step function has been investigated by putting the fields corresponding to the situation described above on a lattice and evolving this configuration numerically. These simulations are easiest to carry out if the strings are either exactly parallel or exactly anti-parallel, because in this case, the system is effectively two dimensional.

2.6.1 Interaction of vortices in two dimensions

The two dimensional system of (anti-)parallel strings is equivalent to a system of two (anti-) vortices in a superconductor and has been studied extensively. In two dimensions, two strings cannot really intersect in one point because they are always either parallel or anti-parallel. It is therefore meaningless to speak about exchanging ends. Rather, vortices in two dimensions are said to collide. When the vortex cores are still separated by a non-zero distance but close enough for the vortices to overlap at least a little bit, an important and well known fact (see for example [23]) is that parallel strings repel for[8] $\beta > 1$ (corresponding to vortices in type-I superconductors), and attract for $\beta < 1$ (type-II superconductors). Exactly anti-parallel strings always attract. Strings with $\beta = 1$ are called critically coupled strings and do not exert a force on each other when they are parallel. The next question is what happens when the separation between (anti-)vortex cores somehow becomes zero, i.e. when two (anti-)vortices collide entirely. In [21], strings were made to interact on a two dimensional lattice. The main

[8]This means that parallel global strings repel because they are described by $\beta \to \infty$.

result is that, regardless of the value of β, if two parallel strings collide head-on, they scatter at an angle of 90 degrees. In [23], a more extensive survey of parameter space was carried out. It was found that when two anti-parallel strings collide head-on, they annihilate, but that if their energy was sufficiently high, they reemerge after annihilation, either both continuing in the same direction or both turning around depending on the value of β. In section 4.5, we will briefly come back to this phenomenon of reemergence. We will argue that, in three dimensions, the reemergence of a vortex anti-vortex pair in a two dimensional slice of space, corresponds to the formation of a string loop in three dimensions.

2.6.2 String intercommutation in three dimensions

The two dimensional results can be used to argue that, in three dimensions, intercommutation takes place whenever two strings intersect. To see this, we focus on two perpendicular planes through the point of intersection. First of all, in the plane that bisects the angle α between the strings, the orientations of the strings are opposite, i.e. one string intersects this plane "coming from below" and the other intersects it "coming from above". Hence, in this plane, the strings have opposite winding number. This is similar to the two dimensional case of a vortex anti-vortex pair described above and we expect annihilation to take place in this plane. If this is indeed the case, the strings are forced to exchange ends. The plane perpendicular to the plane just discussed, provides us with a second argument. Both strings have the same orientation in this plane and their interaction is therefore expected to be similar to the two dimensional case of a vortex vortex pair described above, i.e. we expect 90 degree scattering. This would again correspond to intercommutation. A third argument follows from energy considerations. For strings that are not (anti-)parallel, intercommutation is a way to reduce the total string length and therefore string energy. However suggestive these arguments may be, they do not prove that intercommutation takes place. In principle, it could for example be that, for high velocities, the strings do not have time to intercommute and simply pass through each other instead. To find out what really happens, we again need to rely on lattice simulations, this time in three dimensions.

Three dimensional lattice simulations indeed show that intercommutation takes place in most cases. In the case of global strings, the only paper known to us that extensively investigates intercommutation in three dimensions, is the classic paper [28]. Their result is that, for fixed α, strings intercommute for all velocities up to some threshold velocity $v(\alpha)$. This threshold velocity turns out to be very high such that intercommutation is expected in most cases and hence $p \approx 1$. When the step function is expressed in terms of the velocity right before the interaction (instead of the initial velocity), the threshold velocity appears to be independent of α and has a value of about 0.97. The existence of a (high) threshold velocity, seems to be supported by analytic arguments in [12] and, more recently, [8], although the behavior of the threshold velocity as a function of α predicted in these papers differs from the results in [28]. We will discuss the analytic arguments in these two papers in some detail in section 4.4.

The numerical results in [28] might be used to argue that also for local strings, there must be a threshold velocity, albeit a high one. The analytic arguments in [8] and [12] also point in this direction. However, it has not been confirmed (nor ruled out) by simulations. In [19], to our knowledge the most complete intercommutation survey for local strings, simulations with different values of α and with velocities up to 0.9 are described for a fixed value of β close to one. Except in the case of exactly anti-parallel strings, in which case annihilation

occurs, intercommutation is found in all cases. However, this does not necessarily mean that there is no threshold velocity. It may simply have a value higher than 0.9. This is not totally unlikely, keeping in mind the threshold velocity of $v \approx 0.97$ found in [28] for global strings.

In chapter 4, we will present simulation results of our own that show that intercommutation occurs for speeds up to (at least) $v = 0.99$ for both local and global strings. We will also use simulations to discuss in some detail what the process of intercommutation typically looks like. Even though our results do not exclude the possibility that there is a threshold velocity with value larger than $v = 0.99$, study of the evolution of the Higgs field during the interaction of strings, together with what we know from two dimensional simulations, at least suggests that this is not the case and that, in fact, for velocities larger than $v = 0.99$, strings still intercommute. We do find that, in some cases, strings can intercommute a second time (for sufficiently high initial velocities) so that the net result looks as if the strings simply passed through each other. We will also suggest possible explanations for why the results in [8], [12] and [28] seem to contradict our results.

In this thesis, we will only be concerned with simulations of the high velocity behavior of strings, even though for low velocities, it may also occur that strings do not intercommute. For example, strings do not intercommute if they simply never come to intersect because of repulsion between them. Another possibility, again relevant for low approach velocities, is that the two strings attract and form a bound $n = 2$ state ([6]). This will only happen when $\beta < 1$, because otherwise such a state is unstable. Particularly for values of β very different from one, these effects might have an important effect on the intercommutation probability. This is definitely worth investigating. However, we will not pursue this course in this thesis.

Chapter 3

Simulations

3.1 Introduction

To investigate the intercommutation behavior of strings numerically, we simulated the interaction of two strings on a lattice. We did this by first placing an initial field configuration, corresponding to two strings approaching each other, on the lattice and then evolving the fields using the hamiltonian formalism. The initial strings are straight Abrikososov-Nielsen-Olesen strings and the only parameters necessary to characterize the interaction are the center of mass velocity v and the relative angle α (see previous section). Even though real space is supposed to be continuous, on a computer we need to represent space by a discrete lattice. Hence, some modifications need to be made to our field theory in order for it to be simulated on a lattice. This will be the topic of the next section and it will turn out that this can be done in a natural way that preserves gauge invariance, albeit in a slightly different form ([9, 14]). In section 3.3, we will describe how the initial configuration is constructed. We will discuss the boundary conditions of our simulation in section 3.4 and in section 3.5 we will finally discuss our code. A particular useful reference for us in setting up our simulation was [22].

3.2 Lattice gauge theory

In lattice gauge theory, space-time is approximated by a discrete set of points in space-time, the lattice. These points will be called vertices and the lines connecting neighboring vertices will be referred to as links. The goal is to set up the discretized theory in such a way that the resulting field theory aproximates field theory in continuous space-time. For this reason, the lattice spacing, defined as the separation between neighboring vertices, should be small compared to the relevant physical scales of the system. The discretization will be set up in such a way that in the limit of the lattice spacing approaching zero, the continuous theory will be recovered. Although it is possible to create a four dimensional lattice including time[1], we will only put the d spatial dimensions on the lattice[2]. Time will later be discretized in the sense that the fields on the lattice are evolved in finite time steps, using the hamiltonian formalism. The geometry of the lattice may in principle be chosen at will, but in our simulations, we

[1] When one wishes to include quantum effects, a common approach is to perform Monte Carlo simulations. In this case, all four dimensions of space-time need to be put on a lattice.

[2] We will perform both two and three dimensional simulations, i.e. both $d = 2$ and $d = 3$ will be of use.

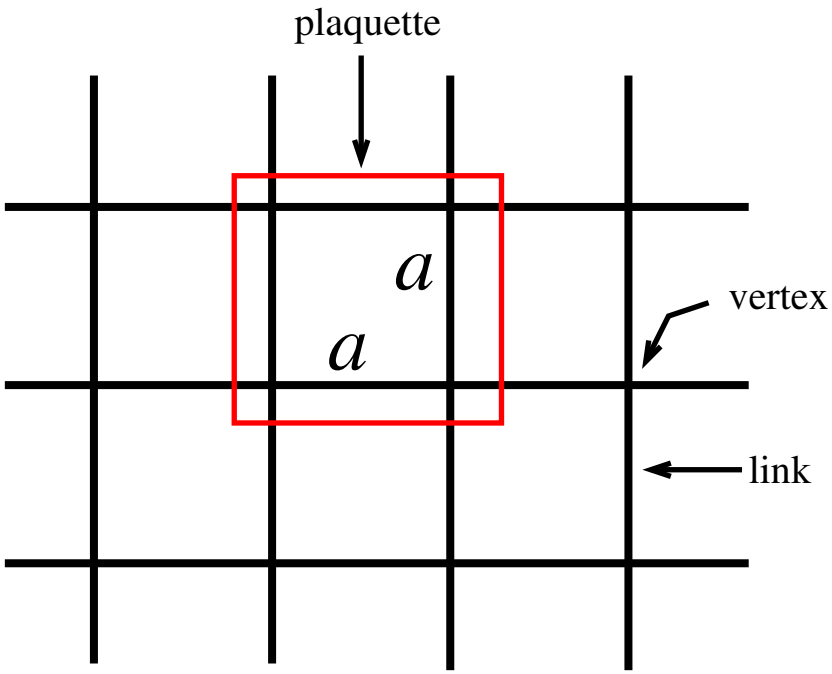

Figure 3.1: We study the interaction of strings by putting the fields on a lattice that represents space. In particular, a three dimensional cubic lattice with sides a is chosen. Here, we show a two dimensional slice of such a lattice. The Higgs field (and its conjugate momentum) is attributed to the vertices of this grid and the gauge fields (and its conjugate momenta) define parallel transport between the vertices and are therefore attributed to the links. A single square with sides a is called a plaquette.

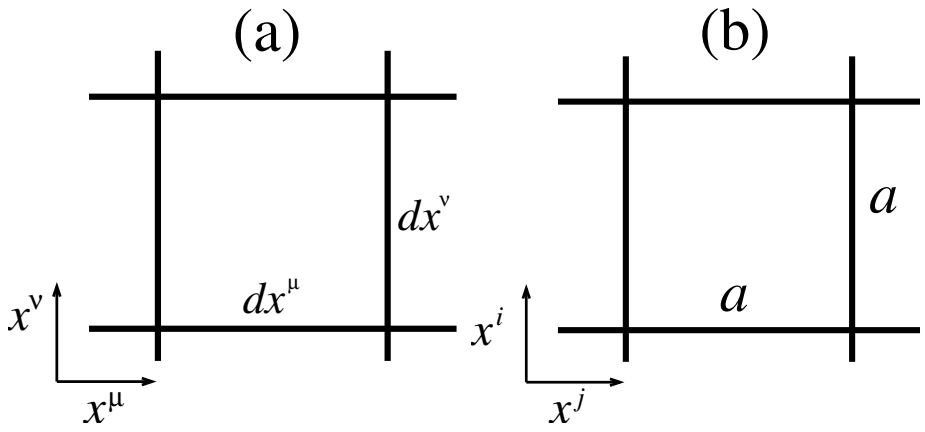

Figure 3.2: In the continuous case, the field strength $F_{\mu\nu}$ ($\mu \neq \nu$) is a measure of the phase change of the Higgs field upon transport over an infinitesimal rectangle with sides dx^μ and dx^ν in the $x^\mu x^\nu$-plane (a). In the lattice formulation of field theory, the analog of a spatial component of the field strength F^{ij} is a measure of the phase change of the Higgs field upon transport over a (finite) plaquette in the $x^i x^j$-plane (b).

will use a cubic lattice because this is the easiest lattice to work with (see figure 3.1). In particular, we will assume vertex coordinates to be given by $\vec{x} = \vec{x}_0 + a\vec{n}$, with $\vec{n} \in N^d$, and $a > 0$ the lattice spacing. The obtained results can be transferred to general lattice geometries relatively straightforwardly. Throughout this section, we will assume the fields are in the temporal gauge, which was discussed in section 1.2.

Our approach will be to define a discretized lagrangian, in terms of field variables defined on the lattice, that reduces to the continuous lagrangian in the limit of vanishing lattice spacing. This new lagrangian will be referred to as the lattice lagrangian. The resulting discrete system has a finite number of degrees of freedom, namely the values of the field on different lattice positions. We will find the conjugate momenta of the fields and derive the equations of motion and the hamiltonian. The equations of motion will turn out to reduce to the continuous equations of motion ((1.24) and (1.25)) in the limit of vanishing lattice spacing.

If the field theory consists of only the Higgs field and no gauge fields, the discretization procedure is very simple. To every vertex with position x, there will be attributed a field value $\phi(x) \to \phi_x$. The main change when going to the discrete formalism is that in the lagrangian, ordinary spatial partial derivatives need to be replaced by lattice derivatives defined in terms of finite differences. If $\hat{\imath}$ is the unit vector in the i-direction, we get

$$\partial_i \phi \to (\phi_{x+a\hat{\imath}} - \phi_x)/a. \tag{3.1}$$

Since time is not a lattice coordinate, time derivatives do not need to be redefined.

In the *abelian* Higgs model, which is the model we are interested in, one also needs to deal with the gauge field. The original lagrangian,

$$L = \int d\vec{x}\mathcal{L}, \quad \mathcal{L} = D_\mu\phi\,(D^\mu\phi)^* - \frac{1}{4}F^{\mu\nu}F_{\mu\nu} - V(|\phi|), \tag{3.2}$$

contains the covariant derivative D_μ, given by (1.4). There is a geometric interpretation to this partial derivative. In the same way that the connection coefficients in GR define a

rotation of the local reference system, the gauge field can be seen to define a rotation of the reference frame within some internal symmetry space. The field at a point x is transported over an infinitesimal distance to a point $x + dx$ by

$$\phi(x) \to U\,\phi(x), \quad U = e^{-ieA_\mu dx^\mu}, \tag{3.3}$$

where it is assumed that $dx^\mu > 0 \quad \forall \mu$ (the position dependence of A_μ is suppressed in the notation, but because of the infinitesimal nature of the transformation, we could use the value of A_μ at any point between x and $x + dx$). If we use this definition of transport to define the partial derivative (w.r.t. x^μ) in terms of differences in the field evaluated in the same (internal) reference frame, we indeed end up with covariant differentiation according to (1.4), as can be seen from

$$\lim_{a\to 0} \frac{e^{ieaA_\mu}\phi(x + a\hat{\mu}) - \phi(x)}{a} = \lim_{a\to 0} \frac{\phi(x + a\hat{\mu}) - \phi(x)}{a} + ieA_\mu\phi(x) \equiv D_\mu\phi(x). \tag{3.4}$$

In the continuous theory, the transformation given by (3.3) is over an infinitesimal distance dx^μ (we used this in (3.4)). On the lattice, spatial covariant partial derivatives are simply defined by generalizing (3.3) to finite distances a. Transport over a link in the positive μ-direction is given by

$$\phi_x \to U_{i,x}\,\phi_x, \quad U_{i,x} = e^{-ieA_{i,x}a}, \tag{3.5}$$

and the lattice analog of the spatial covariant derivative now reads

$$D_i\phi(x) \to D_i\phi_x, \quad D_i\phi_x := \frac{e^{ieaA_{i,x}}\phi_{x+a\hat{\imath}} - \phi_x}{a}, \tag{3.6}$$

where we use the same notation for the lattice derivative as for the continuous derivative. From the context, it will always be clear which one we are talking about. Since in the lattice theory, the gauge fields define covariant transport along a link, they are considered to "live" on the links and not on the vertices like the Higgs field. The gauge field on the link between x and $x + a\hat{\mu}$ is written $A_{\mu,x}$. The definition of the (spatial) covariant derivative on the lattice was chosen in such a way that if we define local gauge transformations on the lattice according to

$$\begin{aligned} \phi_x &\to e^{ie\alpha_x}\,\phi_x \\ A_{i,x} &\to A_{i,x} - (\alpha_{x+a\hat{\imath}} - \alpha_x)/a \end{aligned} \tag{3.7}$$

(cf. (1.3) and (1.5)), the covariant derivative transforms in the same way as the field itself: $D_i\phi_x \to e^{ie\alpha_x} D_i\phi_x$. The final thing that we need in order to be able to construct the lattice lagrangian, is a discrete analog of the kinetic energy term of the gauge field $-\frac{1}{4}F_{\mu\nu}F^{\mu\nu}$. Since we are working in the temporal gauge ($A_0 = 0$) and time is (for now) left continuous, the discretization of the terms with at least one index equal to zero is trivial. The term $-\frac{1}{4}F_{ij}F^{ij}$ needs some special attention though. In the continuous theory, the field strength $F_{\mu\nu} = \partial_\mu A_\nu - \partial_\nu A_\mu$ is a measure of the rotation of the internal reference frame after parallel transport over an infinitesimal square p with sides dx^μ and dx^ν (see figure 3.2),

$$U = e^{ieF_{\mu\nu}dx^\mu dx^\nu} \tag{3.8}$$

(no summation over μ and ν). Equation (3.5) implies that parallel transport around a plaquette in the $\hat{\imath}$- and $\hat{\jmath}$-direction on the lattice, i.e. a finite sized square with sides a as depicted in figure 3.2, is given by

$$U_p = e^{iea((A_{j,x+a\hat{\imath}}-A_{j,x})-(A_{i,x+a\hat{\jmath}}-A_{i,x}))}. \tag{3.9}$$

The integral of $-\frac{1}{4}F^{ij}F_{ij}$ in the continuous lagrangian should now be replaced by a sum over all plaquettes in terms of U_p in such a way that in the continuous limit the original lagrangian is retrieved. This can in principle be done in many ways, but we will choose

$$\begin{aligned} &-\int d^3x \frac{1}{4}F^{ij}F_{ij} \to -a^3 \sum_p \frac{1}{e^2a^4}(1 - Re(U_p)) \\ &= -\frac{1}{2e^2a}\sum_x \sum_{i\neq j}[1 - \cos(ea[(A_{j,x+a\hat{\imath}} - A_{j,x}) - (A_{i,x+a\hat{\jmath}} - A_{i,x})])], \end{aligned} \tag{3.10}$$

where the first sum is over all plaquettes. The full discrete lagrangian can now be written

$$\begin{aligned} L = a^3 \sum_x \Big[&|\partial_0 \phi_x|^2 - \sum_{i=1}^{3} |D_i \phi_x|^2 + \sum_{i=1}^{3} \frac{1}{2}(\partial_0 A_{i,x})^2 \\ &- \frac{1}{2e^2a^4}\sum_{i\neq j}\Big(1 - \cos ea(A_{j,x+a\hat{\imath}} - A_{j,x} - A_{i,x+a\hat{\jmath}} + A_{i,x})\Big) \\ &- \frac{\lambda}{4}(|\phi_x|^2 - \eta^2)^2\Big]. \end{aligned} \tag{3.11}$$

The degrees of freedom of this system are the values of the Higgs field on the vertices $\{\phi_x\}$ (and its conjugates) and the set of values of the gauge fields on the links $\{A_{i,x}\}$. To get rid of the factor a^d in front of the summation in (3.11), the lagrangian is rescaled by this factor, i.e. $L \to a^{-d}L$. This of course does not change the dynamics of the system. The conjugate momenta can be obtained in the standard way by taking the derivative of the (rescaled) lattice lagrangian to the time derivative of the field. The result is basically the same as (1.20) and (1.21), namely[3]

$$\pi_x = \partial_0 \phi_x^* \tag{3.12}$$

and

$$E_{i,x} = -\partial_0 A_{i,x}. \tag{3.13}$$

The rescaled hamiltonian is found to be

$$\begin{aligned} H = \sum_x \Big[&|\pi_x|^2 + \sum_{i=1}^{3} \frac{1}{2}(E_{i,x})^2 + \sum_{i=1}^{3} |D_i \phi_x|^2 \\ &+ \frac{1}{2e^2a^4}\sum_{i\neq j}\Big(1 - \cos ea(A_{j,x+a\hat{\imath}} - A_{j,x} - A_{i,x+a\hat{\jmath}} + A_{i,x})\Big) \\ &+ \frac{\lambda}{4}(|\phi_x|^2 - \eta^2)^2\Big], \end{aligned} \tag{3.14}$$

[3]For the fields and momenta on the lattice, we use the same conventions with respect to the raising and lowering of indices as for the fields and momenta in the continuous case, i.e. $\vec{E}_x = (E_x^1, E_x^2, E_x^3) = (-E_{1,x}, -E_{2,x}, -E_{3,x})$, etc.

and the hamiltonian equations, $\dot{\varphi} = \frac{\partial H}{\partial \pi_\varphi}$ and $\dot{\pi}_\varphi = -\frac{\partial H}{\partial \varphi}$ (for al fields φ, i.e. ϕ and A_μ, and their conjugate momenta), now become

$$\begin{aligned}
\frac{d\phi_x}{dt} &= \pi^*_x \\
\frac{d\pi_x}{dt} &= \frac{1}{a^2}\sum_i [e^{ieaA_{i,x-a\hat{\imath}}}\phi^*_{x-a\hat{\imath}} + e^{-ieaA_{i,x}}\phi^*_{x+a\hat{\imath}}] - \frac{2d}{a^2}\phi^*_x - \frac{\lambda}{2}(|\phi_x|^2 - \eta^2)\phi^*_x, \quad (3.15)
\end{aligned}$$

for the Higgs field and

$$\begin{aligned}
\frac{dA_{i,x}}{dt} &= -E_{i,x} \\
\frac{dE_{i,x}}{dt} &= \frac{1}{ea^3}\sum_{j\neq i}[\sin(ea(A_{j,x+a\hat{\imath}} - A_{j,x} - A_{i,x+a\hat{\jmath}} + A_{i,x})) \\
&\quad - \sin(ea(A_{j,x-a\hat{\jmath}+a\hat{\imath}} - A_{j,x-a\hat{\jmath}} - A_{i,x} + A_{i,x-a\hat{\jmath}}))] \\
&\quad - \frac{ie}{a}(\phi^*_x e^{ieaA_{i,x}}\phi_{x+\hat{\imath}} - \phi^*_{x+\hat{\imath}} e^{-ieaA_{i,x}}\phi_x) \quad (3.16)
\end{aligned}$$

for the gauge fields. Note that in the limit $a \to 0$, we get[4] the equations (1.24) and (1.25). These equations will be used to evolve the fields by taking finite timesteps of size Δt using a leapfrog algorithm. In section 3.5 this will be discussed in more detail. Note that the discretization procedure described above consisted of first constructing a lattice hamiltonian, for which gauge invariance holds as defined by (3.7), and then deriving the exact equations of motion of the system described by this hamiltonian. The big advantage of this approach is that, as long as time is left continuous, the symmetries of the discrete system described by the lattice hamiltonian are preserved exactly and therefore the corresponding quantities, like the energy, are conserved exactly. An alternative approach would have been to directly look for any set of equations that reduces to the continuous equations of motion in the limit $a \to 0$, but in that case, it is not guaranteed that the discrete analogs of the conserved quantities in the continuous theory are exactly conserved.

3.3 Initial configuration

Before we can start our simulation, we need to put the field values corresponding to the desired initial configuration on the lattice. Eventually, we wish to simulate two Abrikosov-Nielsen-Olesen strings approaching each other in the x-direction (see figure 3.3 and 3.4). One string (string 1) will initially lie entirely in the $x = x_1$ plane and the other one (string 2) will lie in the $x = x_2 > x_1$ plane. The angle between the strings will be α, i.e. if α_i is the angle that string i makes with the z-axis, α is the difference between α_2 and α_1. The central point of the box, i.e. the point where the strings will intersect, has coordinates (x_0, y_0, z_0), with $x_0 = (x_1 + x_2)/2$ (see figure 3.3) and y_0 and z_0 as defined in figure 3.4.

If the initial separation is large enough, the field configuration corresponding to the two string system described above, can be approximated very well by superposing the configurations of the two strings individually. If ϕ_i, $A_{\mu,i}$, π_i and $\vec{E}$ are the fields and momenta corresponding to a system with one of the strings (string i) described above, the fields and

[4] We explicitly checked this.

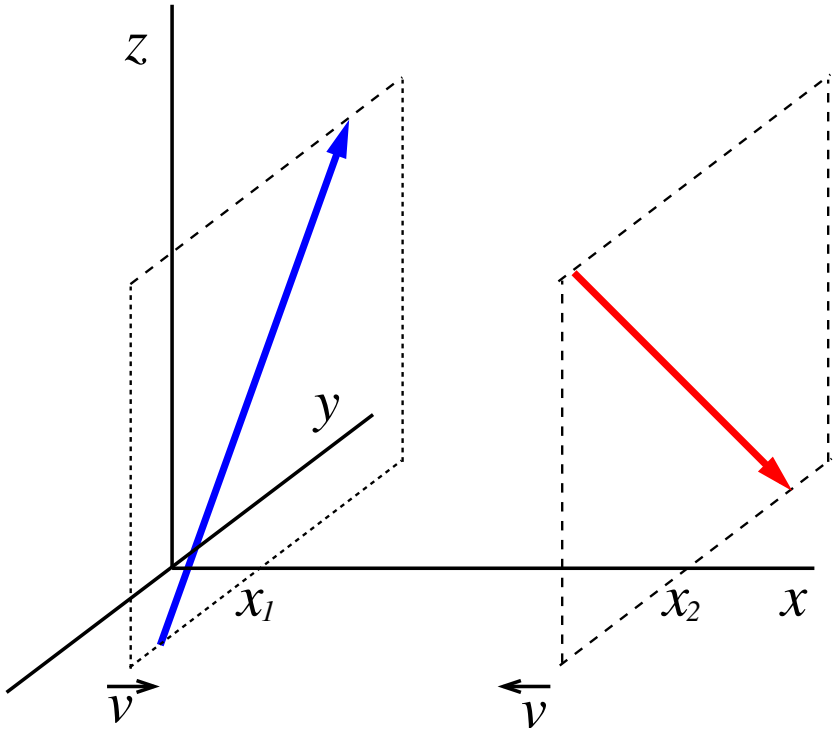

Figure 3.3: The typical initial configuration for a simulation of the interaction of two strings. By applying a proper Lorentz transformation, any system of two straight strings approaching each other can be brought in this form. x_1 is the initial x-coordinate of string 1 and x_2 is the initial x-coordinate of string 2. The initial distance between strings is equal to $x_2 - x_1$. String 1 moves in the positive x-direction with speed v and string 2 moves in the opposite direction with the same speed. The arrows indicate the orientations of the strings: rotation around a string in the direction found using the right hand rule increases the phase of the Higgs field by 2π.

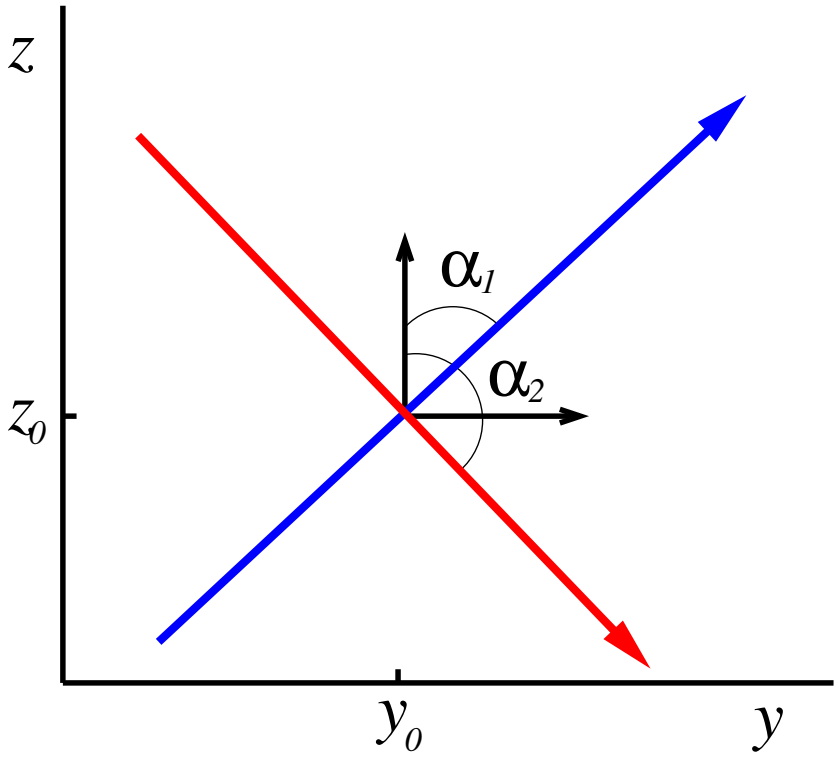

Figure 3.4: The typical initial configuration projected on the yz-plane. α_1 is the angle string 1 makes with the z-axis in the yz-plane and α_2 is this angle for string 2. The angle α between the strings is the difference between α_2 and α_1. Typically, we will choose $\alpha_1 = \frac{\pi}{2} - \frac{\alpha}{2}$ and $\alpha_2 = \frac{\pi}{2} + \frac{\alpha}{2}$. This means that intercommutation corresponds to annihilation of a vortex anti-vortex pair in the $z = z_0$ plane. The coordinates of the point where the strings will come to intersect are (x_0, y_0, z_0), with $x_0 := (x_2 + x_1)/2$. Whether or not intercommutation takes place depends on α and on the speed v.

momenta of the composite system are taken to be

$$\begin{aligned} \phi &= \phi_1 \cdot \phi_2 \\ \pi &= \pi_1 \cdot \phi_2^* + \pi_2 \cdot \phi_1^* \\ A_\mu &= A_{\mu,1} + A_{\mu,2} \\ \vec{E} &= \vec{E}_1 + \vec{E}_2. \end{aligned} \tag{3.17}$$

This expression is exact in the limit of the distance between the strings going to infinity. Hence, to construct an initial configuration, we need to know what the field configuration of a straight Abrikosov-Nielsen-Olesen string, with velocity v in the x-direction and angle α with the z-axis, is. From section 1.3.1, we know that the configuration of a string that stands still and is parallel to the z-axis, is given by (1.27) and (1.28). The equations (1.29) and (1.30) for the profiles $X(r)$ and $P(r)$ cannot be solved in terms of known functions and therefore the profiles need to be found numerically. The code we used to do this is available online through `www.lorentz.leidenuniv.nl/~rdeputter` under the name `profiles.c`. It is also available in postscript format (`profiles.ps`). The program described by this code finds the profiles to any desired accuracy by minimizing the energy, given by

$$H = 2\pi\eta^2 \int_0^\infty dr\, r \left(X'^2 + \frac{X^2 P^2}{r^2} + \beta \frac{P'^2}{r^2} + \frac{1}{4}(X^2-1)^2 \right), \tag{3.18}$$

where we have expressed everything in terms of the rescaled r, as given by (1.31). Once these profiles have been found, the profiles in terms of physical (non-rescaled) coordinates are found by replacing r by $rm^{-1} = r/(\sqrt{\lambda}\eta)$.

In order to find the profiles ([10]), we represent the profiles by their values at a discrete set of equally spaced points in the range $0 \leq r \leq R$. The distance between points, Δr, is chosen small enough for the array of values to represent a continuous function. R must be large enough to represent $r = \infty$, i.e. it is chosen such that the solution does not change much if we make R bigger. The values are labeled by an index i such that $X_i = X(i\Delta r)$ and $P_i = P(i\Delta r)$, and put in an array. The total number of elements for each array is $N+1 \equiv \frac{R}{\Delta r} + 1$. Since we know that $X(0) = 0$, $P(0) = 1$, $X(\infty) = 1$ and $P(\infty) = 0$ (see for example [10]), we keep the values of the first and last element of each array fixed: $X_0 = P_N = 0$, $X_N = P_0 = 1$. Also, we will restrict the array values to satisfy $0 \leq X_i$ and $P_i \leq 1 \quad \forall i$, because we know from the profile equations that the solutions must be bounded by 0 and 1. In terms of the grid values of the profiles, we calculate the hamiltonian by summing over the points halfway between grid points (the points given by $r_{i+\frac{1}{2}} = (i+\frac{1}{2})\Delta r$). The field profile values at $r_{i+\frac{1}{2}} = (i+\frac{1}{2})\Delta r$ are considered to be given by $X((i+\frac{1}{2})\Delta r) = \frac{X_i + X_{i+1}}{2}$ and $P((i+\frac{1}{2})\Delta r) = \frac{P_i + P_{i+1}}{2}$, and the derivatives are $X'((i+\frac{1}{2})\Delta r) = \frac{X_{i+1} - X_i}{\Delta r}$ and $P'((i+\frac{1}{2})\Delta r) = \frac{P_{i+1} - P_i}{\Delta r}$, such that

$$H = 2\pi\eta^2 \sum_{i=0}^{N-1} r_{i+\frac{1}{2}} \left((X'(r_{i+\frac{1}{2}}))^2 + \frac{X^2(r_{i+\frac{1}{2}}) P^2(r_{i+\frac{1}{2}})}{r_{i+\frac{1}{2}}} + \beta \frac{(P'(r_{i+\frac{1}{2}}))^2}{r_{i+\frac{1}{2}}^2} + \frac{1}{4}((X^2(r_{i+\frac{1}{2}}))^2 - 1) \right). \tag{3.19}$$

The gradients of this energy with respect to X_i and P_i are now given by

$$\begin{aligned} \frac{\partial H}{\partial X_i} = \quad & 2\pi\eta^2 \Big[r_{i+\frac{1}{2}} \Big(-\tfrac{2}{\Delta r} X'(r_{i+\frac{1}{2}}) + \tfrac{X(r_{i+\frac{1}{2}}) P^2(r_{i+\frac{1}{2}})}{r_{i+\frac{1}{2}}^2} + \tfrac{1}{2}(X^2(r_{i+\frac{1}{2}}) - 1) X(r_{i+\frac{1}{2}}) \Big) \\ & + r_{i-\frac{1}{2}} \Big(\tfrac{2}{\Delta r} X'(r_{i-\frac{1}{2}}) + \tfrac{X(r_{i-\frac{1}{2}}) P^2(r_{i-\frac{1}{2}})}{r_{i-\frac{1}{2}}^2} + \tfrac{1}{2}(X^2(r_{i-\frac{1}{2}}) - 1) X(r_{i-\frac{1}{2}}) \Big) \Big], \end{aligned} \tag{3.20}$$

and

$$\frac{\partial H}{\partial P_i} = 2\pi\eta^2\Big[r_{i+\frac{1}{2}}\Big(\frac{X^2(r_{i+\frac{1}{2}})P(r_{i+\frac{1}{2}})}{r^2_{i+\frac{1}{2}}} - 2\beta\frac{P'(r_{i+\frac{1}{2}})}{\Delta r r^2_{i+\frac{1}{2}}}\Big) + r_{i-\frac{1}{2}}\Big(\frac{X^2(r_{i-\frac{1}{2}})P(r_{i-\frac{1}{2}})}{r^2_{i-\frac{1}{2}}} + 2\beta\frac{P'(r_{i-\frac{1}{2}})}{\Delta r r^2_{i-\frac{1}{2}}}\Big)\Big]. \tag{3.21}$$

Before we start minimizing the energy, we first fill the arrays with a trial function. In principle, any smooth function satisfying the constraints described above may be used, but we chose

$$X(r) = \sin(\pi r/2R),$$
$$P(r) = \cos(\pi r/R).$$

Starting from this trial function, the energy is now minimized by going through all values of $i \in \{1, ..., N-1\}$ one by one and changing X_i and P_i according to $X_i \to X_i - \delta\frac{\partial H}{\partial X_i}$ and $P_i \to P_i - \delta\frac{\partial H}{\partial P_i}$, with δ a small, positive number. The derivatives $\frac{\partial H}{\partial X_i}$ and $\frac{\partial H}{\partial P_i}$ are always calculated using the current sets of values $\{X_i\}$ and $\{P_i\}$. Once all array elements (except of course the ones with $i = 0$ and $i = N$) have been evolved this way, the whole procedure can be repeated for a desired number of *rounds*. In the end, the energy of the resulting profile is calculated. If δ is chosen small enough and the number of rounds large enough, the profiles converge to the lowest energy solution. By making Δr smaller, we can approximate the continuous profiles as accurately as we wish.

The values of Δr, δ, the number of rounds and especially of R that give satisfacory profiles, depend on the value of β because β is a measure of the size of the gauge core relative to the size of the Higgs core. As an example, for $\beta = 1$, it was sufficient to choose $R = 10$ and $\Delta r = 0.025$, giving $N = 400$. The solutions were reached using δ in the order of 10^{-5} and the number of rounds in the order of 10^6. The total running time was a few minutes. For other values of β, the parameters had similar values, the most important difference being that R needs to be increased with β. The profiles for $\beta = 1$ can be found in figure 3.5. From now on, the functions $X(r)$ and $P(r)$ will be the profiles in terms of physical, non-rescaled distance and X' and P' will be the derivatives of these functions with respect to that distance.

The field configuration of a single straight Abrikosov-Nielsen-Olesen string with velocity v in the x-direction and angle α with the z-axis, can be obtained from (1.27) and (1.28). If we call our coordinate system S, we may apply a Lorentz boost on the x and t coordinates over a velocity v, given by

$$\begin{pmatrix} t \\ x \end{pmatrix} \to \begin{pmatrix} t' \\ x' \end{pmatrix} = \begin{pmatrix} \gamma(v) & -v\gamma(v) \\ -v\gamma(v) & \gamma(v) \end{pmatrix} \begin{pmatrix} t \\ x \end{pmatrix}, \tag{3.22}$$

followed[5] by a rotation in the $y - z$ plane over an angle α given by

$$\begin{pmatrix} y \\ z \end{pmatrix} \to \begin{pmatrix} y' \\ z' \end{pmatrix} = \begin{pmatrix} \cos\alpha & -\sin\alpha \\ \sin\alpha & \cos\alpha \end{pmatrix} \begin{pmatrix} y \\ z \end{pmatrix} \tag{3.23}$$

[5]Applying the rotation first, and then applying the boost would give the same result. The order in which the transformations are performed is irrelevant because they work on different coordinates.

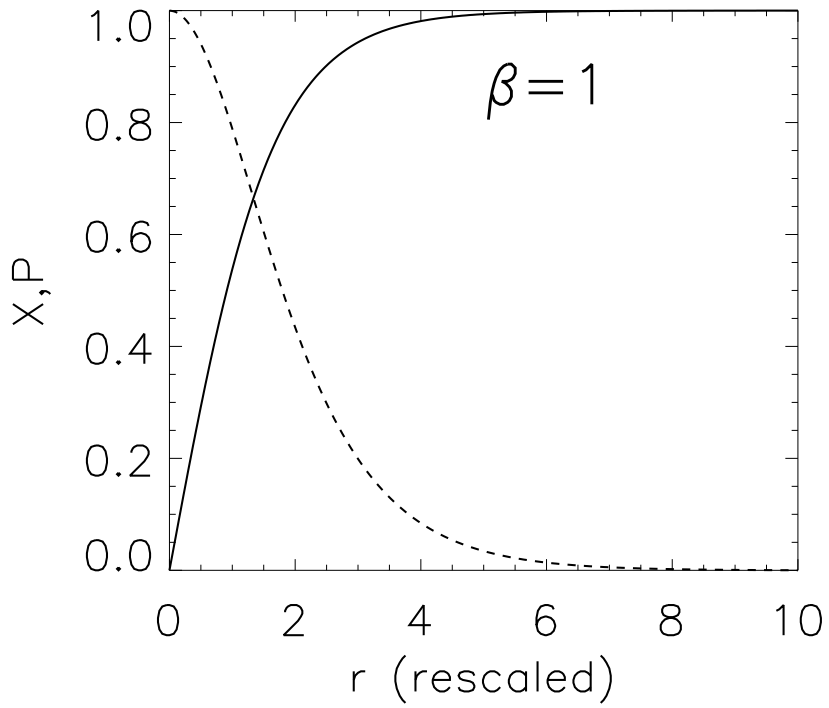

Figure 3.5: Profiles of a critically coupled Abrikosov-Nielsen-Olesen string ($\beta = 1$). X (continuous line) determines the behavior of the Higgs field and P (dotted line) the behavior of the gaugefield. The profiles were found numerically and the distances on the x-axis are in units m^{-1}, where $m = \sqrt{\lambda}\eta$ is the Higgs mass (see equation (1.31)).

to the system S' in which the string is parallel to the z-axis and has zero velocity. In this system, the fields $\phi'(t',\vec{r}')$ and $A'_\mu(t',\vec{r}')$ might in principle be read off directly from (1.27) and (1.28), i.e.

$$\phi'(t',\vec{r}') = \eta X(r')e^{i\theta'}, \tag{3.24}$$

and

$$A'_\mu(t',\vec{r}') = \frac{-1}{e}(1-P(r'))\begin{pmatrix} 0 \\ -\frac{y'}{r'^2} \\ \frac{x'}{r'^2} \\ 0 \end{pmatrix}, \tag{3.25}$$

with $x' = r'\cos\theta'$ and $y' = r'\sin\theta'$. The desired fields $\phi(t,\vec{r})$ and $A_\mu(t,\vec{r})$ can then be found by transforming $\phi'(t',\vec{r}')$ and $A'_\mu(t',\vec{r}')$ back to S with

$$\phi(t,\vec{r}) = \phi'(t',\vec{r}'), \tag{3.26}$$

and

$$\begin{pmatrix} A_0(t,\vec{r}) \\ A_1(t,\vec{r}) \end{pmatrix} = \begin{pmatrix} \gamma(v) & -v\gamma(v) \\ -v\gamma(v) & \gamma(v) \end{pmatrix}\begin{pmatrix} A'_0(t',\vec{r}') \\ A'_1(t',\vec{r}') \end{pmatrix} \tag{3.27}$$

and

$$\begin{pmatrix} A_2(t,\vec{r}) \\ A_3(t,\vec{r}) \end{pmatrix} = \begin{pmatrix} \cos\alpha & \sin\alpha \\ -\sin\alpha & \cos\alpha \end{pmatrix}\begin{pmatrix} A'_2(t',\vec{r}') \\ A'_3(t',\vec{r}') \end{pmatrix}. \tag{3.28}$$

However, since the boost mixes the 0- and 1-component of the gauge field, thus creating a non-zero 0-component, this configuration would not be in the temporal gauge. This problem is solved if, before we transform back to S, we apply a gauge transformation to the fields in the S'-frame that renders $A'_1(t',\vec{r}')$ to zero. The gauge transformation that achieves this is given by

$$\alpha(x',y') = \frac{1}{e}y'I_2(x',y'), \quad I_2(x,y) = \int_0^x \frac{1-P(\sqrt{\xi^2+y^2})}{\xi^2+y^2}\,d\xi. \tag{3.29}$$

After transformation of the fields back to S by (3.26), (3.27) and (3.28) , the fields have the form

$$\begin{aligned}
\phi(t',\vec{r}') &= \eta X(r')e^{i(\theta'+y'I_2(x',y'))} \\
A_\mu(t',\vec{r}') &= -\frac{1}{e}\Big(\frac{x'}{r'^2}(1-P(r')) + \partial_{y'}(y'I_2(x',y'))\Big)\begin{pmatrix} 0 \\ 0 \\ \cos\alpha \\ -\sin\alpha \end{pmatrix} \\
&= -\frac{1}{e}\Big(\frac{x'}{r'^2}(1-P(r')) + I_2(x',y') + \frac{y'^2}{x'}\Big(\frac{1-P(r')}{r'^2} - \frac{1-P(|y'|)}{y'^2}\Big) + y'^2 I_4(x',y')\Big)\begin{pmatrix} 0 \\ 0 \\ \cos\alpha \\ -\sin\alpha \end{pmatrix},
\end{aligned} \tag{3.30}$$

with

$$I_4(x,y) := \int_0^x \frac{1}{\xi^2}\Big(\frac{1-P(\sqrt{\xi^2+y^2})}{\xi^2+y^2} - \frac{1-P(|y|)}{y^2}\Big)\,d\xi \tag{3.31}$$

and the coordinates $t',\vec{r}'$ given in terms of the coordinates t and $\vec{r}$ by (3.22) and (3.23).

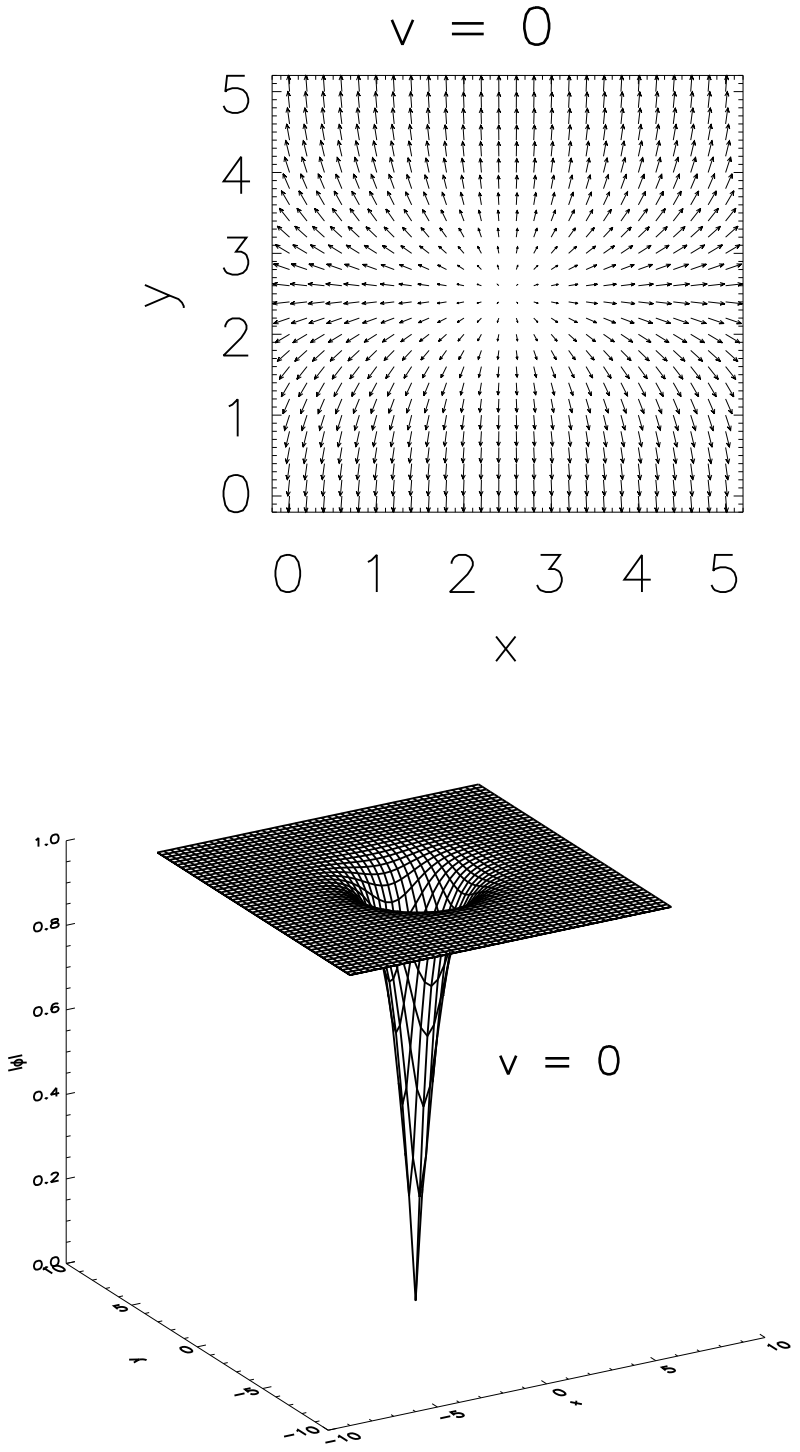

Figure 3.6: The field configuration of an Abrikosov-Nielsen-Olesen string in the gauge with $A_x = 0$ (described in the text). A slice of constant z is shown of a vertical straight string. In the first image, the Higgs field around the string center is represented by arrows and the second image shows the absolute value of the Higgs field. Since ϕ is a scalar field and since $A_t = A_x = 0$, the only difference in the fields between the shown Higgs configuration of a static string and that of a string with $v \neq 0$ is that, in the latter case, there is a Lorentz contraction in the direction of motion. Another difference between the $v = 0$ and the $v \neq 0$ case is that for $v \neq 0$, the *momenta* are non-zero (see figure 3.8 and 3.9). The configuration above corresponds to a model with $e = \eta = 1$ and $\lambda = 2$. The units of the coordinates on the axes are physical (non-rescaled) units ($m^{-1} = 1/\sqrt{2}$ physical units).

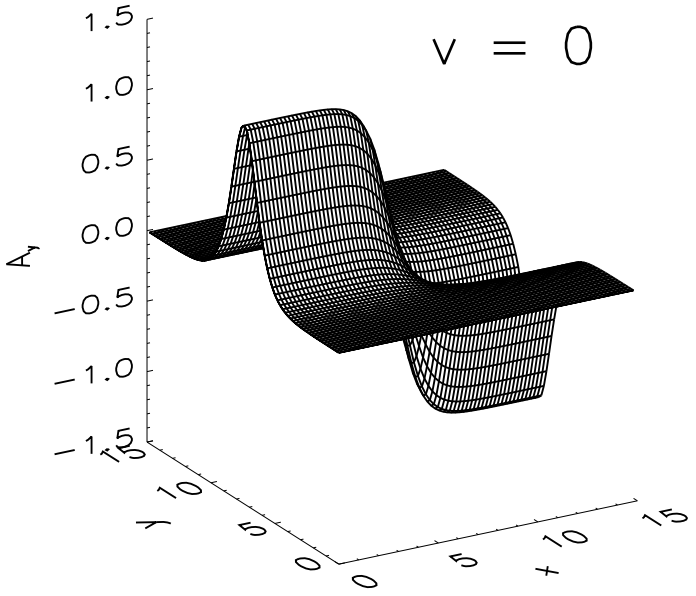

Figure 3.7: The y-component of the gauge field of a static string parallel to the z-axis. We show the field in a slice of constant z. The other components of the gauge field are zero in this particular gauge (see text). To find the gauge field of a string that is not parallel to the z-axis, a rotation needs to be applied to the gauge field given here. The configuration above corresponds to a model with $e = \eta = 1$ and $\lambda = 2$. The units of the coordinates on the axes are physical (non-rescaled) units ($m^{-1} = 1/\sqrt{2}$ physical units).

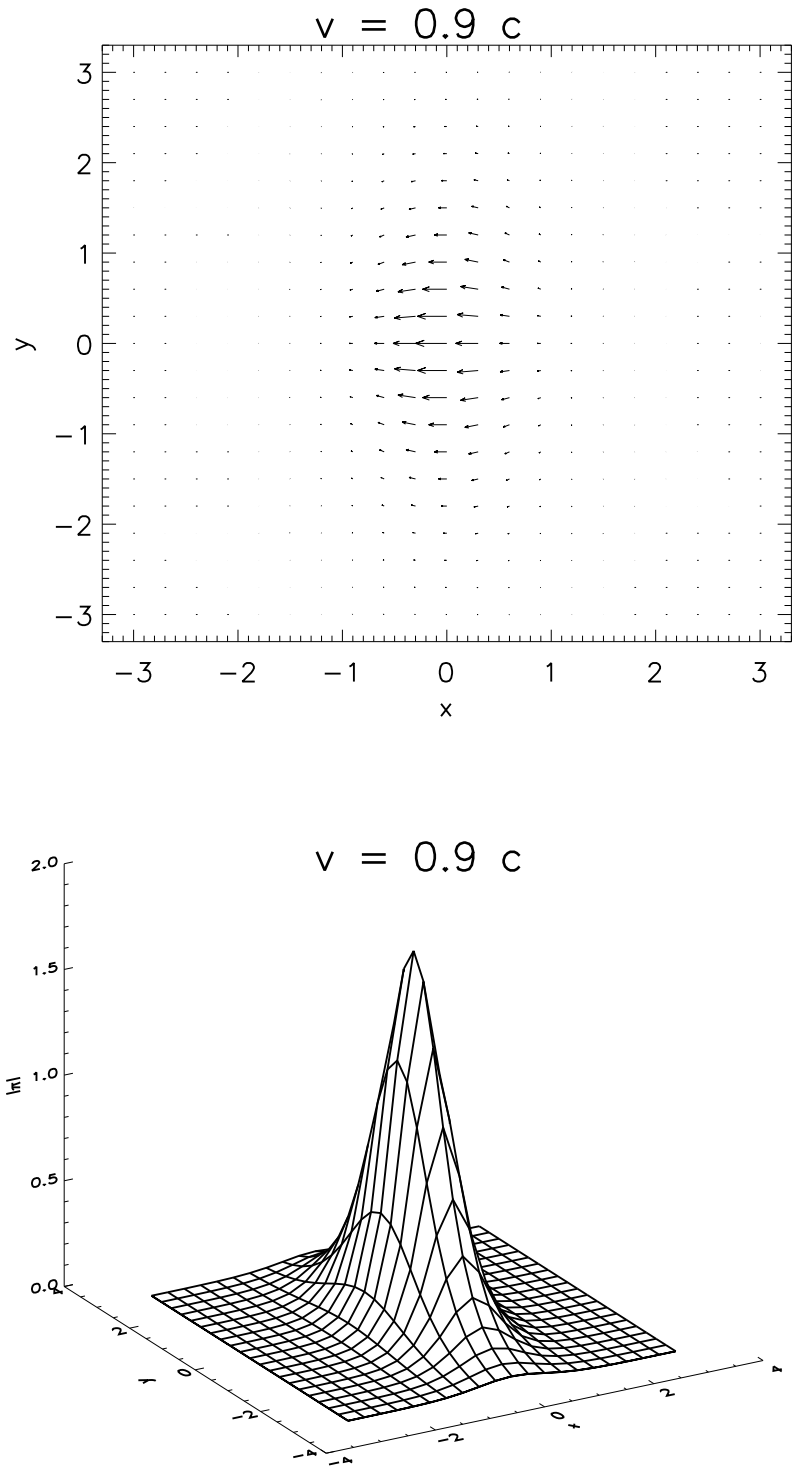

Figure 3.8: The momentum π (conjugate to the Higgs field) of a string that is parallel to the z-axis, moving with speed $v = 0.9$ in the positive x-direction. We show the momentum represented by arrows (top) and the absolute value of the momentum (bottom) in a slice of constant z coordinate. The configuration above corresponds to a model with $e = \eta = 1$ and $\lambda = 2$. The units of the coordinates on the axes are physical (non-rescaled) units ($m^{-1} = 1/\sqrt{2}$ physical units).

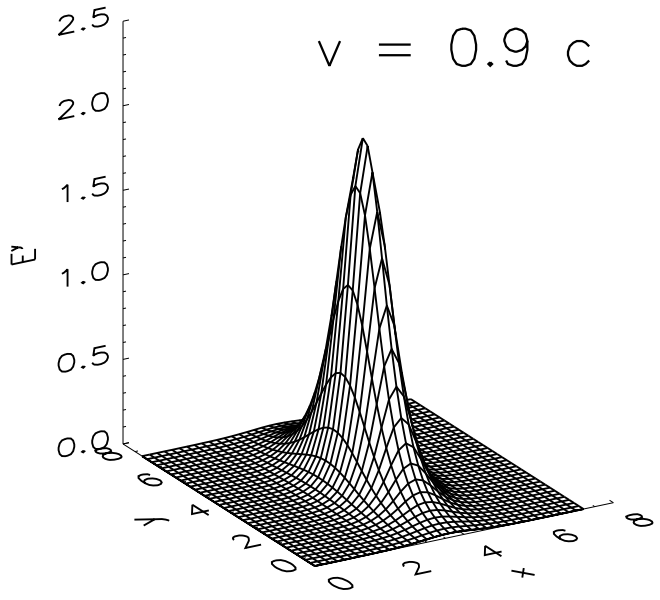

Figure 3.9: The electric field in the y-direction E^y, i.e. the y-component of the momentum conjugate to the gauge field, of a string that is parallel to the z-axis, moving with speed $v = 0.9$ in the positive x-direction. We show a slice of constant z. The other components of the electric field are equal to zero. $e = \eta = 1$ and $\lambda = 2$. Everything is again expressed in physical, non-rescaled units.

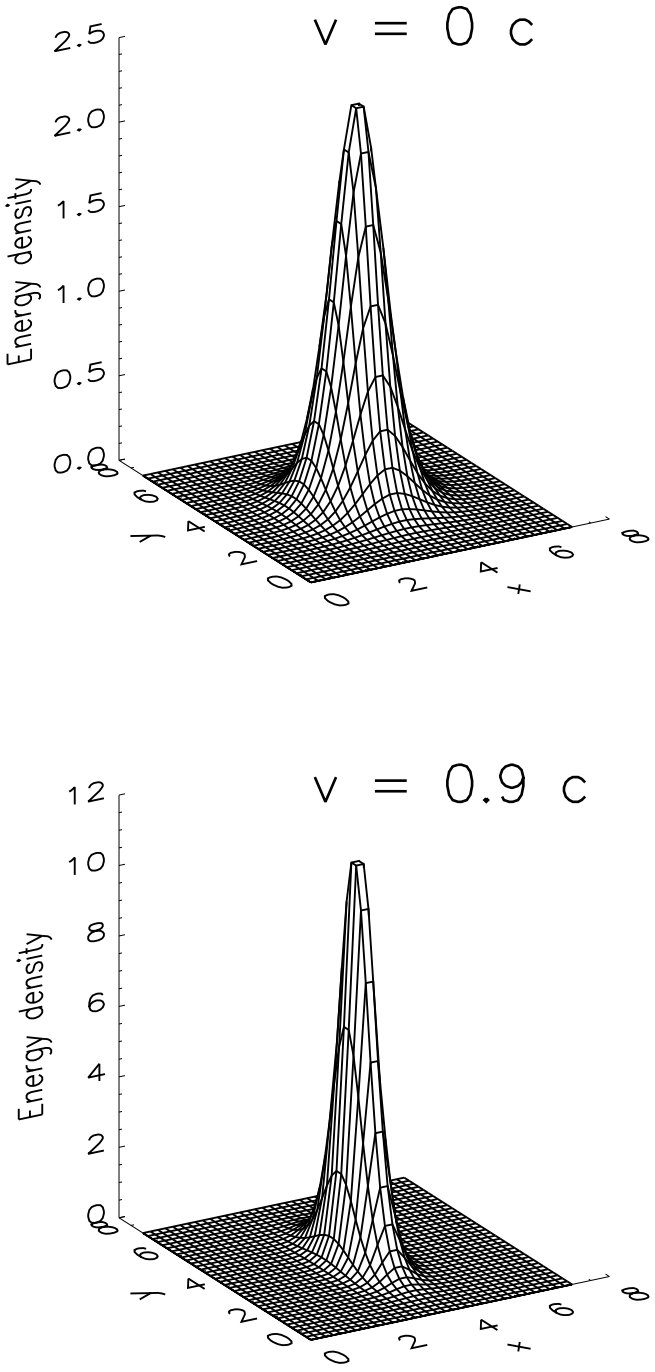

Figure 3.10: The energy per unit surface area of the strings described in the previous figures: a string parallel to the z-axis with $v = 0$ (top) and one with $v = 0.9$ (bottom). We show slices of constant z. Integration over the entire slice gives the energy per unit length of the string. For the static ($v = 0$) string, we get $\mu(0) \approx 6.3$ and for the string with $v = 0.9$, we get $\mu(0.9) \approx 14.3$ (physical units). Note that this is consistent with $\mu(v) = \gamma(v)\mu(0)$ because $\gamma(0.9) \approx 2.3$.

The momenta corresponding to the string described above are given by $\pi(t,\vec{r}) := \partial_t \phi^*(t,\vec{r}) = -v\partial_x \phi^*(t,\vec{r})$ and $E_i(t,\vec{r}) := -\partial_t A_i(t,\vec{r}) = v\partial_x A_i(t,\vec{r})$, because the string moves in the x-direction with velocity v. Applying some algebra to the expressions for the fields given above, we get, in terms of the coordinates $\vec{r}'$ and t' in the S' frame,

$$\begin{aligned} \pi(t',\vec{r}') &= -\eta \frac{v\gamma(v)}{r'} e^{-i(\theta' + y' I_2(x',y'))} [x' X'(r') + i\frac{y'}{r'} P(r') X(r')], \\ \vec{E}(t',\vec{r}') &= -\frac{v\gamma(v)}{er'} P'(r') \begin{pmatrix} 0 \\ \cos\alpha \\ -\sin\alpha \end{pmatrix}. \end{aligned} \tag{3.32}$$

The equations (3.32) and (3.30) express the initial configuration of a single straight string in terms of known functions. In section 3.5, we will discuss how our code uses these expressions (together with the coordinate transformations (3.22) and (3.23)) to create two such configurations and superpose them by (3.17). We thus end up with the desired initial configuration of two moving local strings on a lattice. For a system of two global strings, the gauge fields are absent. In this case, the initial configuration of the Higgs fiels and its conjugate momentum are obtained in the same way as for local strings, with the gauge field set to zero everywhere. Equivalently, this system is described as a system of local strings in the limit $\beta \to \infty$.

3.4 Boundary conditions

A drawback of (lattice) simulations is that, where ordinary space is infinite, a lattice inevitably has boundaries. This might be a problem, because, after we have placed an initial configuration on the lattice, in order to evolve the fields at a certain point we need to know the values of the fields at neighboring points. The lattice points on a boundary of the lattice by definition do not have any neighboring lattice points on one side though. The boundary conditions (BC) specify which field values represent those non-existent lattice points just across the boundary. For a big enough simulation volume (box), the choice of boundary conditions does not influence the interaction in the center of the box because information cannot travel faster than the speed of light. This means that, if available memory and computation time were not an issue, we could always perform the simulations in a box that is big enough for the boundaries not to influence the fields in some central region of interest during the entire simulation. In this case, the simulation results will be completely independent of the choice of BC and really represent the interaction of infinite strings. However, in practice, especially for simulations in which the fields are evolved over a long time (for example in the case of very slowly moving strings), it is not attainable, or at least very time consuming, to simulate such a big volume. Hence, it is useful to take a look at some physically reasonable ways of treating the boundaries, such that the influence of the BC on the simulation does not cause problems. We will discuss three types of BC, all three of which have been used in our simulations (and in those of others) at some point. We will assume a volume with dimensions $aN_1, ..., aN_n$ (in our case, n will be either two or three) to be represented by a lattice with vertex coordinates $(x_1, ..., x_n) = a(i_1, ..., i_n)$ and $i_1 \in \{1, ..., N_1\}$, $i_2 \in \{1, ..., N_2\}$, etc. This box is filled with an initial configuration corresponding to a system of two straight strings (see previous section). The BC must then describe how to find the field values corresponding to points that lie just past the boundaries of this box, i.e. the fields corresponding to coordinates $i_k = 0$ or $i_k = N + 1$ (for any $k \in \{1, ..., n\}$). As was previously stated, knowledge of these field

values is necessary when we wish to evolve the fields *on* the boundaries ($i_k = 1$ or $i_k = N$), as can be seen from the equations of motion (3.15) and (3.16). The boundary conditions will be discussed in terms of the continuous field theory.

3.4.1 Periodic boundary conditions

Periodic BC (see for example [21]) are very useful for two dimensional simulations. In three dimensional simulations, they can only be applied to the boundaries on which the fields are initially in, or close to, the vacuum. When the boundary conditions are periodic, the fields just past a boundary are considered to be equal (up to a gauge transformation) to the fields at the boundary on the other side. One would naively expect periodic BC in the 1-direction to mean that

$$\begin{aligned} \phi(x_1 + L_1, x_2, .., x_n) &= \phi(x_1, x_2, ..., x_n) \\ A_\mu(x_1 + L_1, x_2, .., x_n) &= A_\mu(x_1, x_2, ..., x_n). \end{aligned} \tag{3.33}$$

However, if we apply this to our initial configuration described in the previous section, we would find that the fields are discontinuous at the boundary . This is the case because for our initial configuration, $\phi(0, x_2, ..., x_n) \neq \phi(L, x_2, ..., x_n)$. This can be solved by demanding that the fields are periodic up to a gauge transformation $\alpha(x_2, ..., x_n)$ that "patches" the fields at the two boundaries together. We then get

$$\phi(x_1 + L_1, x_2, .., x_n) = e^{ie\alpha(x_2,...,x_n)}\phi(x_1, x_2, ..., x_n), \tag{3.34}$$

$$A_\mu(x_1 + L_1, x_2, .., x_n) = A_\mu(x_1, x_2, ..., x_n) - \partial_\mu\alpha(x_2, ..., x_n). \tag{3.35}$$

The "patch function" α is determined from the initial configuration ϕ_i by

$$e^{ie\alpha(x_2,...x_n)} := \frac{\phi_i(L, x_2, ..., x_n)}{\phi_i(0, x_2, ..., x_n)}. \tag{3.36}$$

Note that the 1-component of the gauge field, and in general the component of the gauge field normal to the boundary, is purely periodic (i.e. no patch function). Since a gauge transformation does not change the physical properties of the fields, (3.36) defines a configuration that is (physically) periodic in the 1-direction. Periodicity in the other directions is defined analogously. The lattice formulation becomes

$$\phi_{(i_1+N_1,i_2,..,i_n)} = e^{ie\alpha(i_2,...,i_n)}\phi_{(i_1,i_2,...,i_n)} \tag{3.37}$$

$$A_{\mu(i_1+N_1,i_2,..,i_n)} = A_{\mu,(i_1,i_2,...,i_n)} - \partial_\mu\alpha(i_2, ..., i_n), \tag{3.38}$$

and α is found by initially also calculating the values the fields would have at the points with $i_1 = N + 1$ (which are considered to lie just outside the lattice) and using

$$e^{ie\alpha(i_2,...i_n)} := \frac{\phi_i(N + 1, x_2, ..., x_n)}{\phi_i(1, x_2, ..., x_n)}. \tag{3.39}$$

Periodic BC are possible because in the initial configuration, the fields at the boundaries are in (or close to) the vacuum. If this is not the case, there may not exist a gauge transformation that patches the fields on opposing boundaries, because the Higgs fields on opposing boundaries may not have the same absolute value (gauge transformations only change the phase). For this reason, periodic boundary conditions cannot be used on a boundary that has a string passing through it. In three dimensional simulations of straight strings, such boundaries always exist and therefore we need to find alternative BC for at least one pair of boundaries.

3.4.2 Reflective boundary conditions

A very straightforward way of treating boundaries is to use extrapolation of the fields inside the box to obtain the fields just outside the box. This extrapolation can in principle be performed in several ways. When the gradient of the field normal to a boundary is assumed to be equal to zero, we speak of reflective boundary conditions, which is a rather popular choice. These BC are, for example, used in [28]. On the lattice, reflective BC mean that (for all fields) the field values just past the boundaries are considered to be given by

$$\begin{aligned} \varphi_{(0,i_2,\ldots,i_n)} &= \varphi_{(1,i_2,\ldots,i_n)} \\ \varphi_{(N+1,i_2,\ldots,i_n)} &= \varphi_{(N,i_2,\ldots,i_n)}. \end{aligned} \tag{3.40}$$

Reflective BC are used in a number of our own simulations (see chapter 4).

3.4.3 "Free string" boundary conditions

The other type of BC that we choose to use for many of our three dimensional simulations assume that the fields just past the boundaries behave like they would if the strings did not interact (see for example [19]). This is realized as follows. If we wish to know the fields across a boundary at a time t, we first calculate the x-coordinates the strings would have if they had moved with constant speed since the beginning of the simulation by $x_1(t) = x_1(0)+vt = x_1+vt$ and $x_2(t) = x_2(0) - vt = x_2 - vt$. We then calculate the field values at the desired points (the points that lie just past the boundary) by the same method we used to find the initial configuration (i.e. by superposition of two straight Abrikosov-Nielsen-Olesen strings), but this time the parameters describing the system are $x_1(t)$ instead of x_1, $x_2(t)$ instead of x_2, and α and v like before. This way, the fields across the boundaries represent strings moving with constant velocity that keep their original shape. For large enough box size and assuming the angle α is non-zero so that the strings will pass through the boundaries at different y-coordinates, this seems like a good approximation to the fields' behavior across the lattice boundaries in infinite space because, in this case, the parts of the strings at the boundaries will be sufficiently far apart to not notice each other's presence during the simulation, i.e. they indeed propagate as free strings. If there *is* sufficient time during the simulation for the string segments to feel each other's presence, the fields across the boundaries as found by the method described above will likely not be exactly what they should be for two *infinite* straight strings. However, for most simulations, the deviation will not be very big. When simulating the interaction of two slowly moving strings, the total simulation time can get rather large. In this case, the deviations can be big, and the simulation should not be interpreted as the interaction of two infinite straight strings, but rather as two straight string segments that are "driven" by some force exerted at the points where they intersect the boundary. The effect of this force is exactly to make the string segments at the boundaries move at constant velocity. In fact, such an approach is in a way more realistic than the scenario of two straight infinite strings, since in reality only segments of strings are straight and these segments are influenced by the rest of the string they are attached to. The disadvantage is that once we are no longer describing infinite straight strings, we introduce extra parameters because, in principle, the driving force representing the pull of the rest of the string is arbitrary. We will stick to the choice made above because these BC are closest to the case of infinite strings, but in theory one can for example replace the relations $x_1(t) = x_1 + vt$ and $x_2(t) = x_2 - vt$ by

any reasonable functions $x_1(t)$ and $x_2(t)$ to get different BC that might agree with another physical situation.

3.5 Code

In this section, we will discuss in some detail the code we used to perform our simulations. Readers not interested in these technical details might want to skip this section and go straight to the "Results" chapter. In principle, the most important basic aspects of how our simulations are run, were covered in the previous sections. The code is written in C and is available in full through `www.lorentz.leidenuniv.nl/~rdeputter`. The code can be found both both in plain text format (`sim.c`) and postscript format (`sim.ps`) with line numbering. The code describes a simulation of two local strings on a three dimensional lattice with, applied to all boundaries, either the boundary conditions described in section 3.4.2, or those described in section 3.4.3. We also performed some simulations that used two other codes: one simulating global strings in three dimensions and one simulating local strings in two dimensions. However, the first of these codes is exactly the same as the code we are discussing in this section, except that the gauge fields are removed. The second code is also the same in most ways (removing a dimension is trivial), but uses different boundary conditions (namely periodic). We will not go into the details of these two codes. In the following discussion, the names of variables, functions etc. that appear in the code are printed in boldface.

To increase the speed at which simulations can be run, we have written the code in such a way that it can simultaneously use multiple processors. This was made possible by the use of the MPI (Message Passing Interface) package. The advantage of using MPI is that the lattice (box) can be divided into a number of subboxes. Each process takes care of one such subbox and the processes communicate with each other about what happens at the boundaries. Naming the number of available processors **size**, our code divides the total box into **size** subboxes that are stacked upon each other vertically (figure 3.11), although other ways of dividing the simulation volume into subboxes would of course also have worked. If the time taken by the communication between processes is negligible, the simulation speed is proportional to **size** and hence we can gain a lot of time by running the code on a cluster of parallel processors. The code describes the actions that a single process, characterized by the integer **rank** (that has a value in the range from 0 to **size** -1), should carry out.

Before going into **main()**, let us first discuss some of the most important variables and constants that appear in the code, most of which are defined as global variables at the very beginning of the code (lines 15 to 111). Starting with the parameters describing the lattice, a is called **latticespacing** and the dimensions of one subbox in terms of lattice sites are given by **isize_net**, **jsize_net** and **ksize_net**, such that the total boxsize is **isize_net** $\times$ **jsize_net** $\times$ (**size** $\cdot$ **ksize_net**) (the physical sizes are found upon multiplication by the lattice spacing). The parameter **timestep** corresponds to Δt. The code decribes the abelian Higgs model with $\eta = 1$, which is why this parameter does not appear anywhere in the code. The parameters e and λ are called **e** and **lambda** respectively. Furthermore, **alpha1** is α_1, i.e. the angle that string 1 makes with the z-axis, **alpha2** is α_2 and **v0** will be used for both the velocity of string 1 as that of string 2. The fields are put into three dimensional arrays with the size of a subbox plus one lattice site past the boundaries, i.e. (**isize_net**+2) $\times$ (**jsize_net**+2) $\times$ (**ksize_net**+2). The actual subbox is considered to be the part of the array with coordinates [i,j,k] $i = 1, ...,$**isize_net**, $j = 1, ...,$**jsize_net** and $k = 1, ...,$**ksize_net** and the points on the

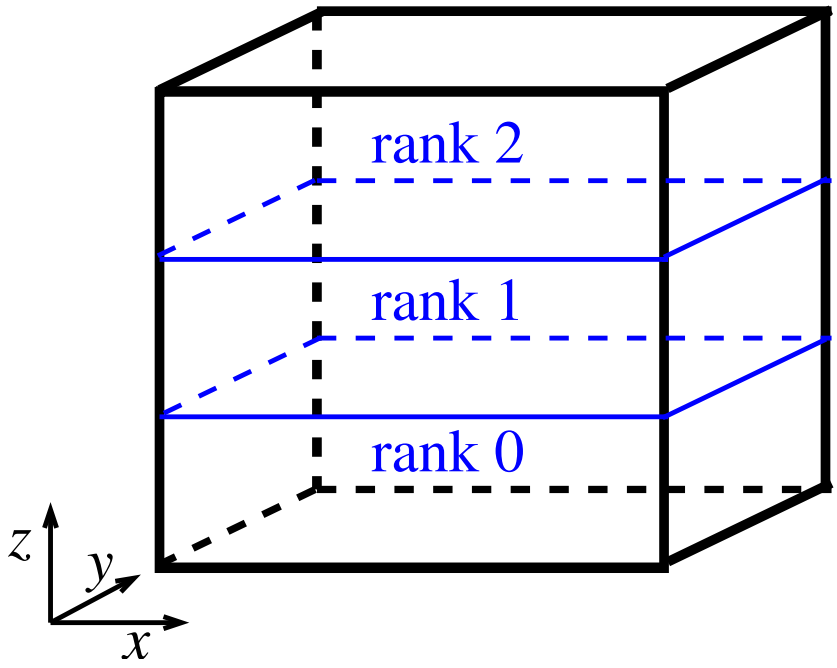

Figure 3.11: The simulation volume (the big box) is divided into a number of subboxes as shown above. Each subbox is handled by a separate process and the processes exchange information about what happens at the subbox boundaries. Which subbox is handled by each process is determined from the rank of the process. The subbox at the bottom of the big box corresponds to rank zero, the one above it corresponds to rank one, etc. In the situation shown here, three processors are used. Running simulations in parallel can save a lot of time. Ideally, i.e. if the time it takes to exchange information between processes is negligible, the speed of the code is proportional to the number of used processors.

boundaries of the array ($i = 0$,**isize_net**+1, etc.) are considered to lie just past the boundary of the subbox. If a boundary lies next to another subbox handled by another process, i.e. the subbox boundary is an internal boundary, these points are considered to lie inside that other subbox. If a boundary lies on the outside of the total box, in which case it is called an external boundary, the points lie just outside the simulation volume. The reason we include the external lattice points in our arrays is that the field values at these points are needed to evolve the momenta on the boundary of a subbox. Their valus will be obtained either by communication with the process describing a neighboring subbox (for internal boundaries), or by applying the boundary conditions described in 3.4.2 or 3.4.3 (for external boundaries). The names of the arrays and their relation to the field definitions in this thesis, are
Higgs = ϕ,
Higgsmomentum = π,
xlinks = eaA_x,
Ex = eaE^x,
ylinks = eaA_y,
Ey = eaE^y,
zlinks = eaA_z,
Ez = eaE^z.
We also define an array the size of a subbox, called **Energy**, that contains the energy density according to equation (3.14). In addition to the arrays described above, we also define two dimensional arrays with size **Nslice** $\times$ **Nslice** that will contain a two dimensional slice of the field configuration of a single string. These slices will be used to create a three dimensional configuration relatively fast. We also create a number of auxiliary arrays like **Higgs2**, **Higgsmomentum2**, etc., that will for example be used to temporarily store a configuration. Other relevant quantities will be discussed as we encounter them in the code.

main(), starting on line 1669, can be divided into three blocks. The first block (line 1686 to 1790) can be seen as preparation for the actual calculations and is used among other things to initialize parameters. In the second block (line 1791 to 2085), an initial configuration of two strings on a lattice is created and the third block (line 2086 to 2136) takes care of the evolution of the fields. The code is commented, but we will here explain the basic steps that are taken and make some remarks on things that are important.

3.5.1 Initialization of parameters

At the very beginning of the main code, a number of parameters is initialized. Throughout, η is chosen to be one and therefore this parameter does not occur in the code at all. Although e does occur explicitly in the code, we will always choose it to be equal to 1 too. The parameter β is varied by changing λ (and thus the characteristic Higgs radius $m^{-1} = \frac{1}{\eta\sqrt{\lambda}}$). For example, in the online version of the code, we have $\lambda = 2$ so that $\beta = 1$. The string profiles X and P are loaded from files and their derivatives are calculated. We use the profiles corresponding to the right value of β. In the case of the code that can be found online therefore, the profiles of a $\beta = 1$ string are loaded. When the simulation is carried out for another value of λ (and therefore of β), we need to load different profiles. We described how to create these profiles for any value of β in section 3.3. One of the other things that are done in the first block is that the positions of the subboxes within the total simulation volume are determined so that a process knows the absolute coordinates of its lattice points and so that it knows with which other processes to communicate about the boundaries. The lattice spacing a is chosen

small enough for the lattice to represent a continuum. By small enough, we mean that it is (much) smaller than the relevant physical scales of the system, in this case the typical Higgs and gauge radii. Note that, for high velocities Lorentz contraction makes these scales smaller and we need to reduce the lattice spacing a accordingly. The timestep Δt is chosen such that the Courant condition ([27]) is fulfilled: $\Delta t \leq \frac{a}{\sqrt{3}}$.

3.5.2 Creation of initial configuration

In block 2 (line 1791 to 2085), the initial configuration is constructed. The idea is to first construct constant z slices of the configurations of each individual string separately, and then to use these slices to create a superposition of the two strings in our (three dimensional) subbox. For each string (see figures 3.3 and 3.4), with velocity $\pm v$ and angle α_i with the z-axis, where $i = 1$ or $i = 2$, we fill a set of two dimensional arrays (one array for each field) with the configuration at constant z, around a string of velocity $\pm v$ and angle α_i with the z-axis. The fields on this slice are calculated using the expressions for the initial configuration in section 3.3. The fields (corresponding to one string) at any point (X, Y, Z) in the *three dimensional* (sub)box can then be found by first calculating the x- and y-coordinate of (X, Y, Z) relative to the point where the string intersects the $z = Z$ plane. We then find the elements of the constant z arrays described above close to these cordinates and use interpolation to find the desired field values. The fields corresponding to the complete two string system are found using the superposition rules (3.17).

In the code, this procedure is carried out as follows. First, a slice of the configuration of string 1, characterized by **alpha1** and **v0**, is created using **slices()**. Each process calculates a part of this slice after which all processes send their part of the slice to the process with **rank**= 0. This process then puts the parts together to create the full slice and afterwards sends it to all other processes. The end result is that all processes own a constant z slice (put in arrays with names **Higgsslice1**, **Higgsmomentumslice1**, etc.) with the configuration corresponding to string 1, which intersects the slice in its center. After this, the same is done for string 2, which is characterized by **alpha2** and **-v0**, but this time the fields are put in arrays with names **Higgsslice2**,**Higgsmomentumslice2**, etc. Note that in **slices()**, the electric field on a link is calculated at the point halfway this link (see also [22]). For the gauge field on a link, we take the average over the link it is defined on, i.e. we integrate the gauge field over this link numerically and subsequently divide by the length of the link. When the slices are available to each process, the three dimensional initial field configuration can be constructed for each subbox. This is done by the function **initial_configuration()**, as described in the previous paragraph.

3.5.3 Evolution

In the third part of the code (line 2086 to 2136), the fields are evolved in small timesteps Δt. The fields are evolved using a so called leapfrog algorithm. This means that, starting from the initial configuration, we first evolve the momenta forward in time by half a timestep, then evolve the fields over a full timestep, then the momenta over a full timestep, then the fields over a full timestep again, etc. The function that evolves the fields over one timestep of size **timestep** using equations (3.15) and (3.16) is called **evolve()**. It first uses the conjugate momenta to evolve the fields by one timestep, then finds the values of the fields just passed the subbox boundaries, i.e. the array elements with $i = 0$,$i =$**isize_net**+1, ..., or

k =**ksize_net**+1, and then evolves the momenta. The field values just past the boundaries are obtained using the function **Boundaries()**. For internal boundaries, this function exchanges information with the process that deals with the relevant neighboring subbox, while for external boundaries, the field values are calculated using the boundary conditions in section 3.4.2 or 3.4.3. If **SHELLARD** is defined in line 13 when the code is compiled, the BC from section 3.4.2 are used and if **SHELLARD** is not defined, the BC from section 3.4.3 are automatically used.

Since we wish to use a leapfrog algorithm, we first evolve the momenta forward *half* a timestep using the function **Half_step()**. After this, a for loop is started that runs **evolve**. This way, the fields are evolved from $t = 0$ to $t =$ **simtime** (which is a parameter that is passed to the function by the user). The fields can be saved at desired moments. Also, the energy density can be calculated and saved.

Chapter 4

Results

4.1 Introduction

In this chapter, we investigate the interaction of strings for high speeds v (see figure 3.3). Both the numerical work in [28] (for global strings) and the analytic arguments in [8] and [12] (for both global and local strings), suggest that strings intercommute for speeds v up to a certain threshold velocity v_t. Above this velocity, strings would not exchange ends, but simply move through each other. Throughout this chapter, the term "threshold velocity" will exclusively be used for the specific type of threshold velocity discussed above. In [19], which describes simulations of local strings, intercommutation is found in all investigated cases (except when the strings are either exactly parallel or exactly anti-parallel). In this chapter, we present the results of our own simulations. We investigate the high v intercommutation behavior of both local (for different values of β) and global strings. We find that strings intercommute for speeds up to at least $v = 0.99$ and thus find no evidence for the existence of a threshold velocity. It does occur in some cases that strings first intercommute once, and then later intercommute again, in which case the net result is that the strings move through each other, i.e. there is no exchange of ends.

The typical string configuration considered in this chapter will be as discussed in the beginning of section 3.3 (specifically figures 3.3 and 3.4) and we will use the parameters defined there to describe these systems. We will always have $\alpha_1 = \frac{\pi}{2} - \frac{\alpha}{2}$ and $\alpha_2 = \frac{\pi}{2} + \frac{\alpha}{2}$, such that intercommutation corresponds to annihilation in the $z = z_0$ plane. The central point of the box, i.e. the point with coordinates (x_0, y_0, z_0), will be referred to as the "intersection point". The process of intercommutation takes place in the region around this point. The time at which the two strings come to intersect will be called t_0. The strings are located by looking at the configuration of the Higgs field in a number of (two dimensional) slices and locating points around which the Higgs field has non-zero winding number. This is always done "by hand", as opposed to automatically. As before, all quantities are in units $c = \hbar = 1$.

In principle, it may happen that two strings do not intercommute because they simply never come to intersect. More specifically, this will occur when the strings repel. However, this only happens either for low initial speeds, or for values of β much bigger than one (or both). In this thesis, we will restrict ourselves to the study of the high velocity intercommutation behavior and the existence of a threshold velocity. In our discussions, we will always implicitly assume β and v to be such that the strings *do* come to intersect after some (finite) time. What happens next (intercommutation or non-intercommutation) is what we are interested in here.

If the strings do not move apart far after intercommutation, it can happen that they exchange ends again after some time, so that the final state corresponds to non-intercommutation. However, in this thesis, the main question we will be concerned with is whether or not the strings *initially* intercommute. Hence, when we say that two strings intercommute, it might still be that a while after intercommutation the strings intercommute again due to attractive interaction between the strings after the first intercommutation. In fact, we have seen this happen in several simulations of local strings (see section 4.6). We will also always implicitly assume that the angle α between the strings is not equal to 0^o or 180^o. The type of system described by $\alpha = 0^o$ or $\alpha = 180^o$ is essentially two dimensional and has been studied extensively by others (see for example [23]).

The simulations we refer to in this chapter all use the codes (or straightforward modifications thereof) discussed in the previous chapter. The parameters of the abelian Higgs model will from now on be set to $e = 1$ and $\eta = 1$. β then depends on λ through $\beta = \lambda/2$. As we discussed, the intercommutation behavior of strings only depends on β. Changes in the parameters that keep β constant would only amount to a change in the scales of the system. Hence, when studying intercommutation, there is no loss of generality in fixing e and η. The choice $e = \eta = 1$ means that the gauge mass is given by $M = \sqrt{2}$ and the Higgs mass by $m = M\sqrt{\beta} = \sqrt{2\beta}$. This means that the physical, non-rescaled coordinates (r) we always use in this chapter are related to the rescaled coordinates ($r_{\rm rescaled}$) of inverse Higgs mass by: $r_{\rm rescaled} = \sqrt{2\beta}\, r$. All simulations referred to were performed on the Maris cluster of the Lorentz Institute for Theoretical Physics in Leiden. In most cases, simulations were run in parallel on five processors. The typical running time was of the order of an hour.

This chapter is organized as follows. In section 4.2, we discuss the numerical intercommutation of two local strings characterized by $\alpha = 90^o$, $v = 0.5$. We find that the process of intercommutation is very rapid and that during this process, the strings can for a while not be considered to be Nambu-Goto strings. This is consistent with earlier results found by others. In section 4.3, we present an argument that suggests that a threshold velocity does not exist and that, in fact, intercommutation takes place for all (sufficiently high) velocities of approach. We know of two analytic arguments ([8, 12]) that suggest the contrary. These arguments will be the topic of section 4.4. We will point out possible errors (using our conclusions from section 4.2) that could change their conclusion that above some threshold velocity, intercommutation does not occur. We wish to note though that we do not consider the arguments in section 4.3 and 4.4 to be proof of the non-existence of a threshold velocity. However, the results presented in section 4.5 (for global strings) and 4.6 (for local strings) do convincingly show that, if a threshold velocity exists, its value must be higher than 0.99 (at least for the values of β and α that we investigated). We also discuss the formation of a loop after intercommutation in these sections.

4.2 A closer look at intercommutation ($\beta = 1$)

As we discussed before, it is clear from previous studies that, for not too high velocities, intercommutation takes place whenever two strings come to intersect. For high velocities ($v \sim 0.9$), a number of studies ([8, 12, 28]) suggest that there exists a threshold velocity, above which strings no longer intercommute, but simply pass through each other instead. Before we investigate (the existence of) this threshold velocity, it is useful to first study in some detail what the interaction of two strings that *do* intercommute typically looks like.

To this purpose, we simulate the evolution of a system of two local strings, characterized by $v = 0.5$, $\alpha = 90^o$, $\beta = 1$ and an initial separation of 12 (physical) units. This configuration is evolved on a lattice of size $150 \times 150 \times 250$, with lattice spacing $a = 0.2$, such that the physical size of the simulation volume is $30 \times 30 \times 50$. We use the boundary conditions discussed in section 3.4.3. The configuration is evolved in time steps of size $\Delta t \approx 0.09$. The initial positions and orientations of the strings are sketched in figure 4.1. The initial configuration of the Higgs field on the slices given by $z = z_0$ and $y = y_0$, and the energy density on the slice given by $z = z_0$, are depicted in figures 4.2 and 4.3 respectively.

When this configuration is evolved, the strings remain straight and move with constant velocity for a long time. If the strings were to move with $v = 0.5$ the entire time until their cores intersect, intersection would take place at $t =$"initial separation"$/(2v) = 12$ units. We find that, not long before this time, at $t = 10.39$, the strings still practically have the same shape and the separation of the cores in the $z = z_0$ plane is about 1.2 units. We conclude that, until this time, the strings have hardly interacted. Soon after this time, the intercommutation process starts. This process, where the vortices annihilate in the $z = z_0$ plane, and move apart vertically in the $y = y_0$ plane, goes remarkably fast, something that was also noted in [28] (for global strings) and in [23] (for 90^o scattering of parallel local strings). At $t = 10.65$ already, the cores more or less overlap in the $z = z_0$ plane, i.e. the strings intersect. At $t = 10.91$, intercommutation has taken place and the zeroes are already separated by a distance of about 1.6 units (figure 4.4). After intercommutation, the strings keep moving away from each other in the z-direction at a velocity slightly bigger than $v = 0.5$. Quite a lot of energy is left behind in the region surrounding the intersection point. The shape of the strings after intercommutation is sketched in figure 4.5. We evolve the strings until $t = 24$ units and find that nothing new happens: the vertical distance between the two strings simply continues to increase (until the boundaries are reached by the strings). Note that the behavior of the fields in the center of the box can in principle be influenced by the boundaries from $t = 15$ onwards because of the finite box size. Other parts of the simulation volume can be influenced by the boundaries at even earlier times. However, we checked that the results presented above are independent of box size by running the same simulation in a box twice as big in all directions (by doubling the lattice spacing to $a = 0.4$). We also performed the simulation described above with different BC, namely the ones discussed in section 3.4.2. We are confident that the influence of the boundaries on the results presented in this section is negligible.

We perform another simulation to look at the actual process of intercommutation in more detail. For this simulation, we use a smaller lattice spacing, namely $a = 0.1$, and a time step $\Delta t = 0.05$. The lattice again has size $150 \times 150 \times 250$, which this time corresponds to a physical size of $15 \times 15 \times 25$ units. The other parameters are the same as in the first simulation. In figure 4.6, we show the Higgs field close to the intersection point in the $z = z_0$ plane at different times and in figure 4.8, the field in the $y = y_0$ plane is shown. We find that around the time of intercommutation ($t_0 \approx 10.61$ units) the absolute value of the Higgs field is very small in a region around the intersection point. For that reason, the vortex positions are not well defined for a short time. We again wish to stress how fast the process of intercommutation works. At $t = 10.4$, the strings have not yet intercommuted and the distance in the $z = z_0$ plane is roughly one unit. At $t = 10.6$, the strings almost exactly overlap, and at $t = 10.8$, the strings have exchanged ends and are already separated by a distance of about 1.4 units in the z-direction. This means that, if one were to calculate the average speed of each string in the $z = z_0$ plane just before intercommutation (over a period of time of about 0.2 units), one would find $v \approx 2.5$, and for the average speed in the $y = y_0$ plane (the speed at which

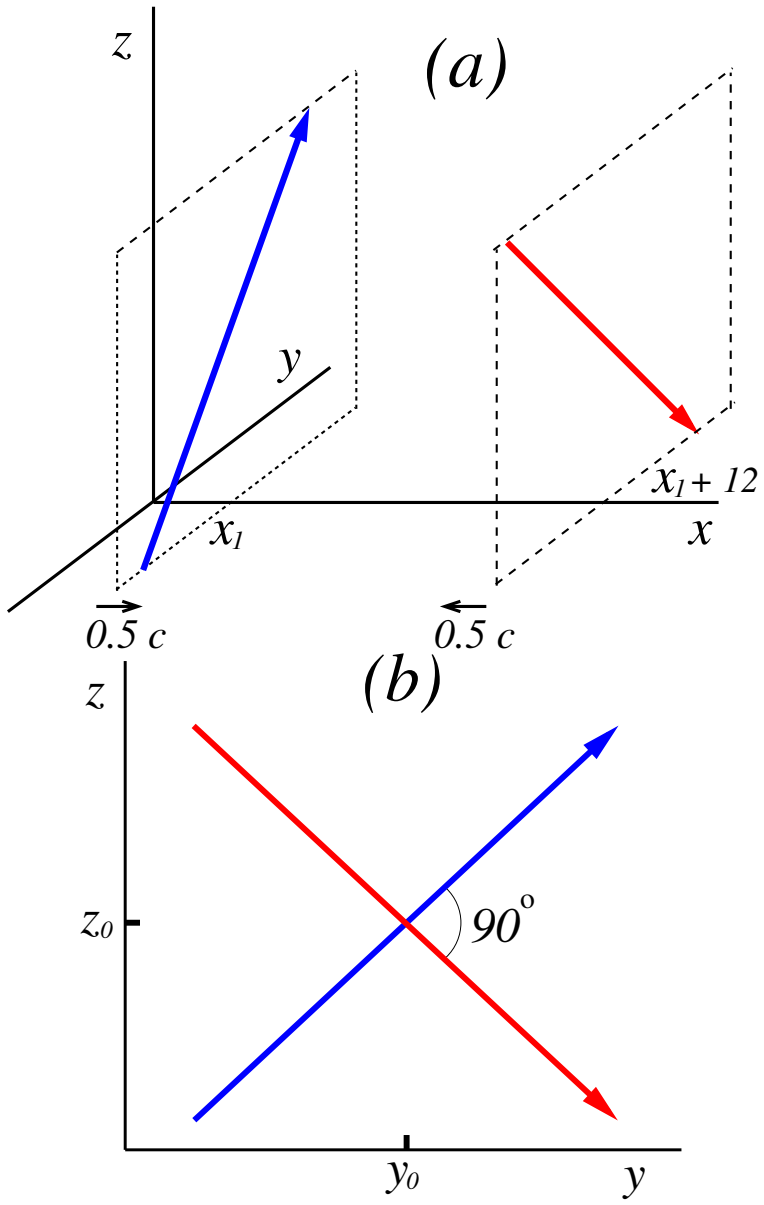

Figure 4.1: The initial positions and orientations of the strings in the system described in section 4.2 in three dimensions (a) and a projection of this configuration on the yz-plane (b). The direction of an arrow indicates the direction of increasing phase of the Higgs field by the right hand rule.

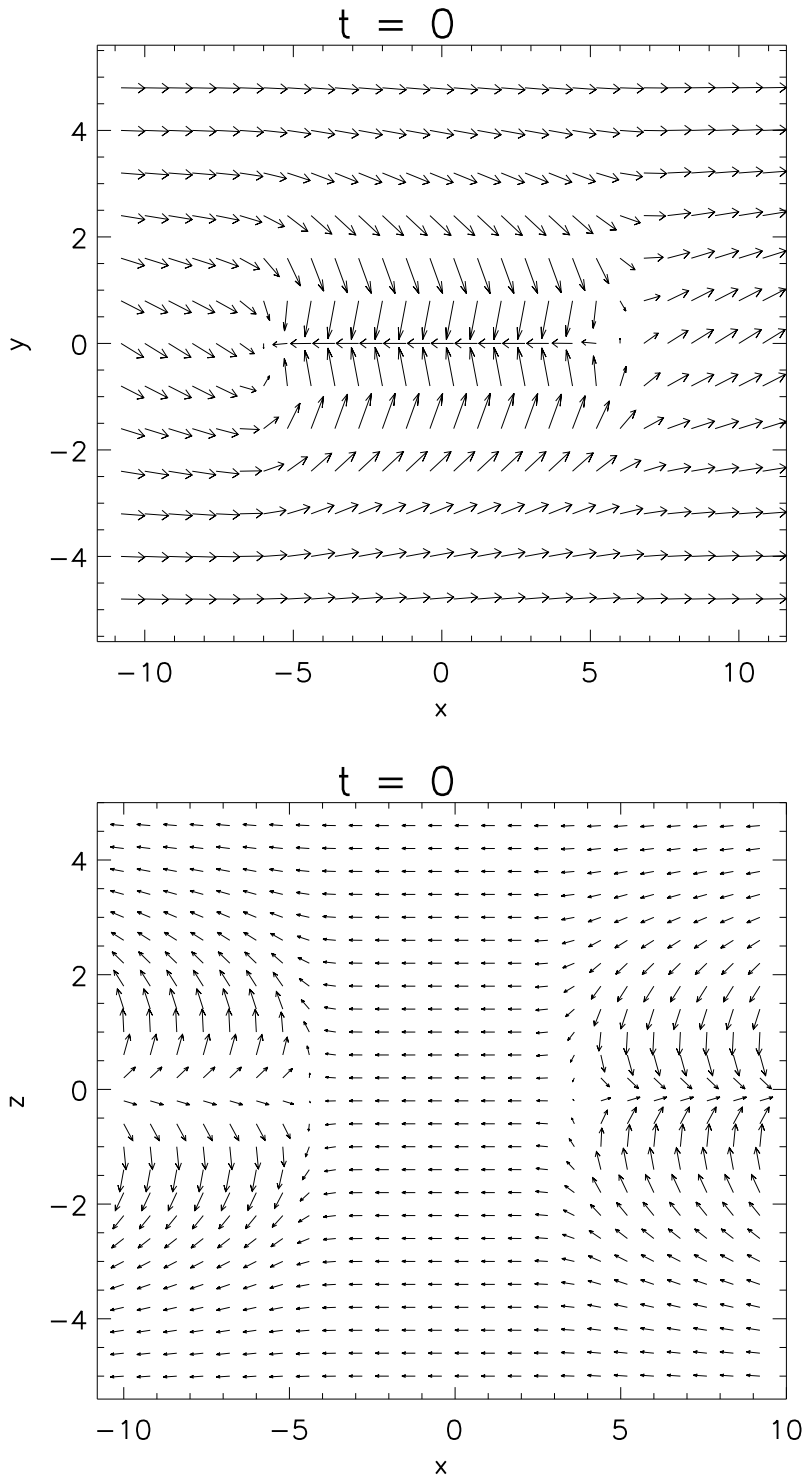

Figure 4.2: The configuration of the Higgs field corresponding to the situation sketched in figure 4.1 is shown both on the $z = z_0$ plane and the $y = y_0$ plane. Of each plane, only a central region is shown. The coordinates are given relative to the intersection point (x_0, y_0, z_0). The units have not been rescaled: $m^{-1} = \frac{1}{\sqrt{2}}$ units. Note that, in the $z = z_0$ plane, the winding number around the string on the left is equal to one (the phase increases by 2π when following one counter clockwise rotation around the vortex), and the winding number around the string on the right is equal to minus one. In the $y = y_0$ plane, both strings have winding number minus one.

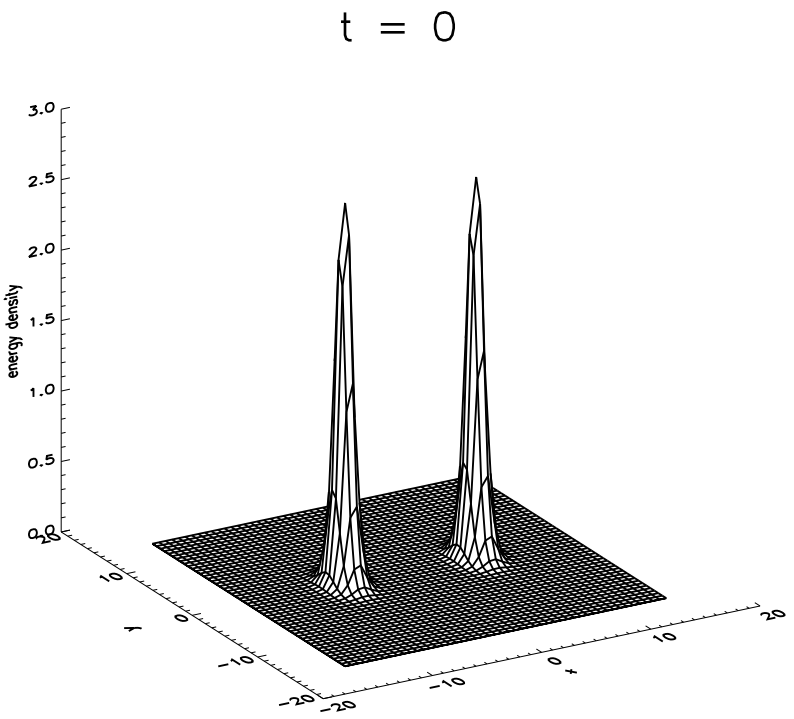

Figure 4.3: The energy density in the $z = z_0$ plane corresponding to the situation sketched in figure 4.1. The coordinates on the axes are given relative to the intersection point. The units have not been rescaled: $m^{-1} = \frac{1}{\sqrt{2}}$ units. The energy has peaks at the points where the strings intersect the $z = z_0$ plane.

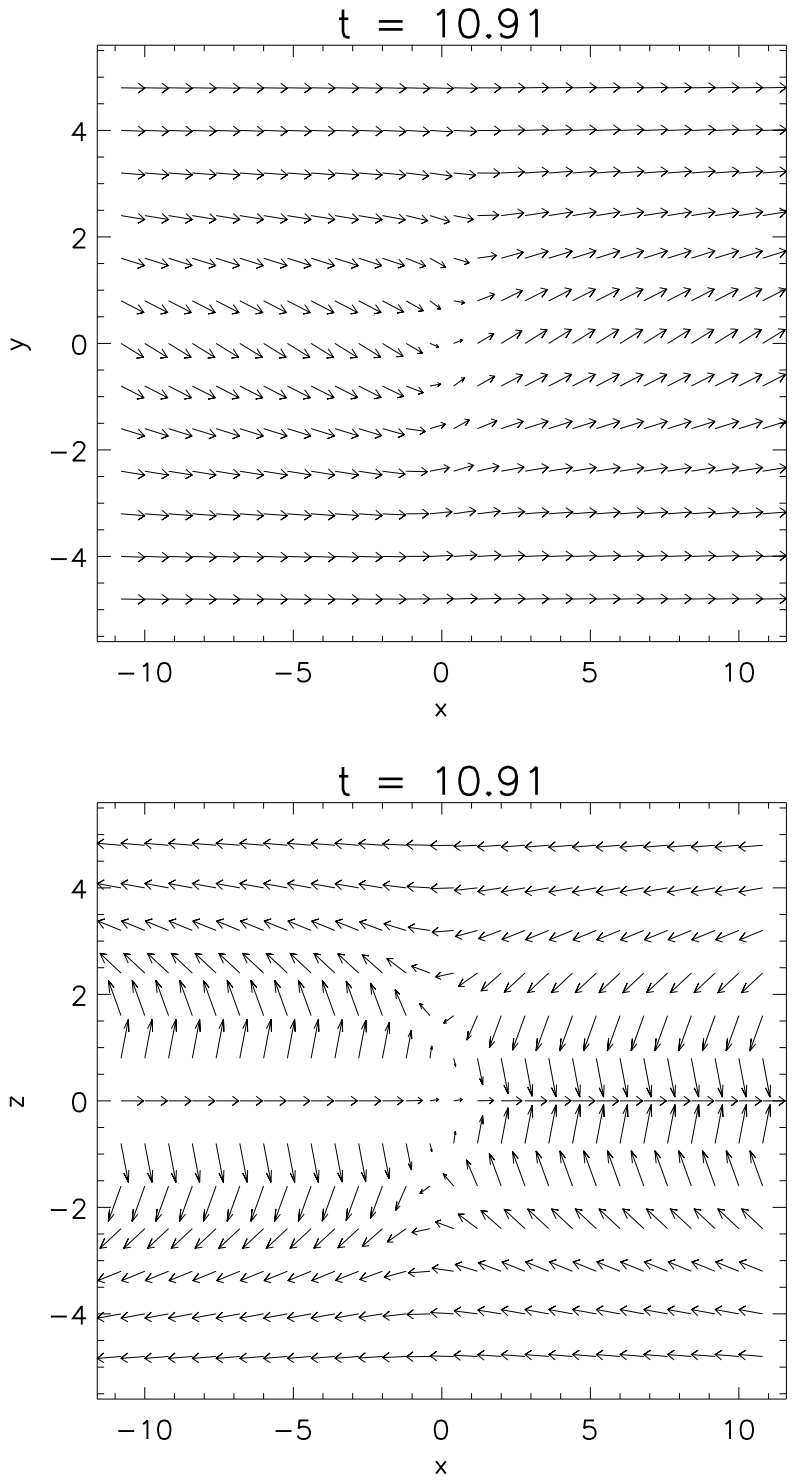

Figure 4.4: The Higgs field configuration at $t = 10.91$, right after intercommutation has taken place. In the $z = z_0$ plane (top), annihilation has taken place and in the $y = y_0$ plane (bottom), the strings have moved apart in the z-direction a considerable distance (the coordinates of the zeroes are given approximately by $(0, \pm 1)$). The coordinates on the axes are given relative to the intersection point. The units have not been rescaled: $m^{-1} = \frac{1}{\sqrt{2}}$ units.

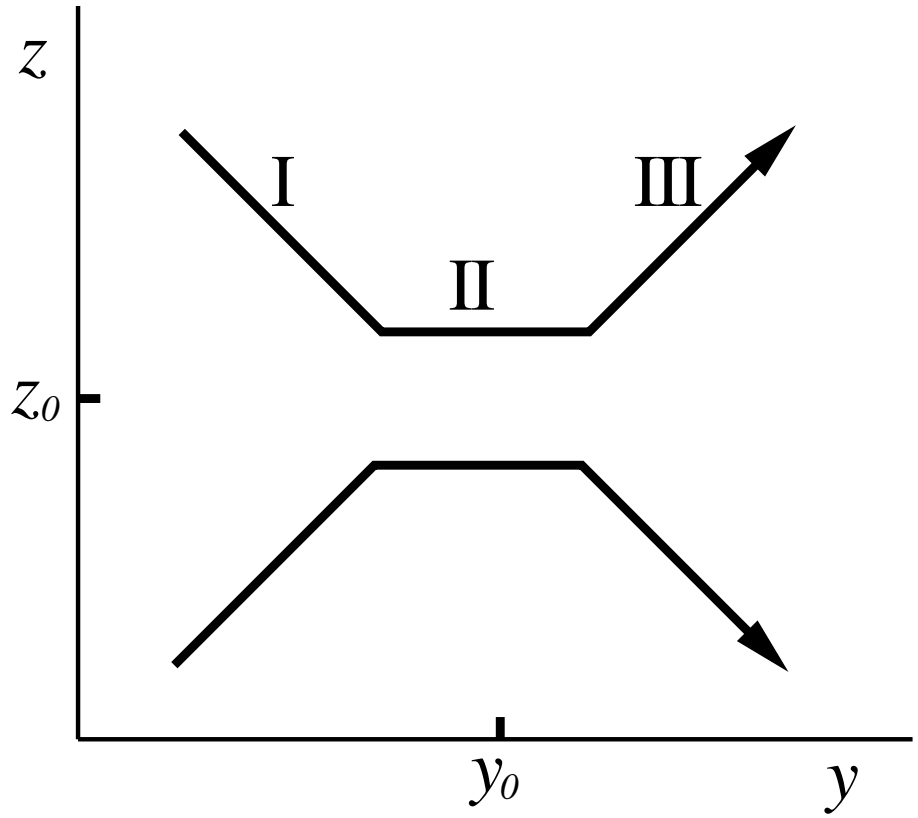

Figure 4.5: The approximate shape of the strings after intercommutation has taken place, as projected on the yz-plane. Each of the two strings can be considered to consist of three different, relatively straight parts. The parts I and III are far away from where the interaction has taken place and therefore still look the same as they would if no intercommutation had taken place. After a short period in which the strings move apart at a speed $v > c$, the distance between the horizontal parts (II) grows at a rate corresponding to string velocities slightly larger than $v = 0.5$, while the basic string shapes stay the same.

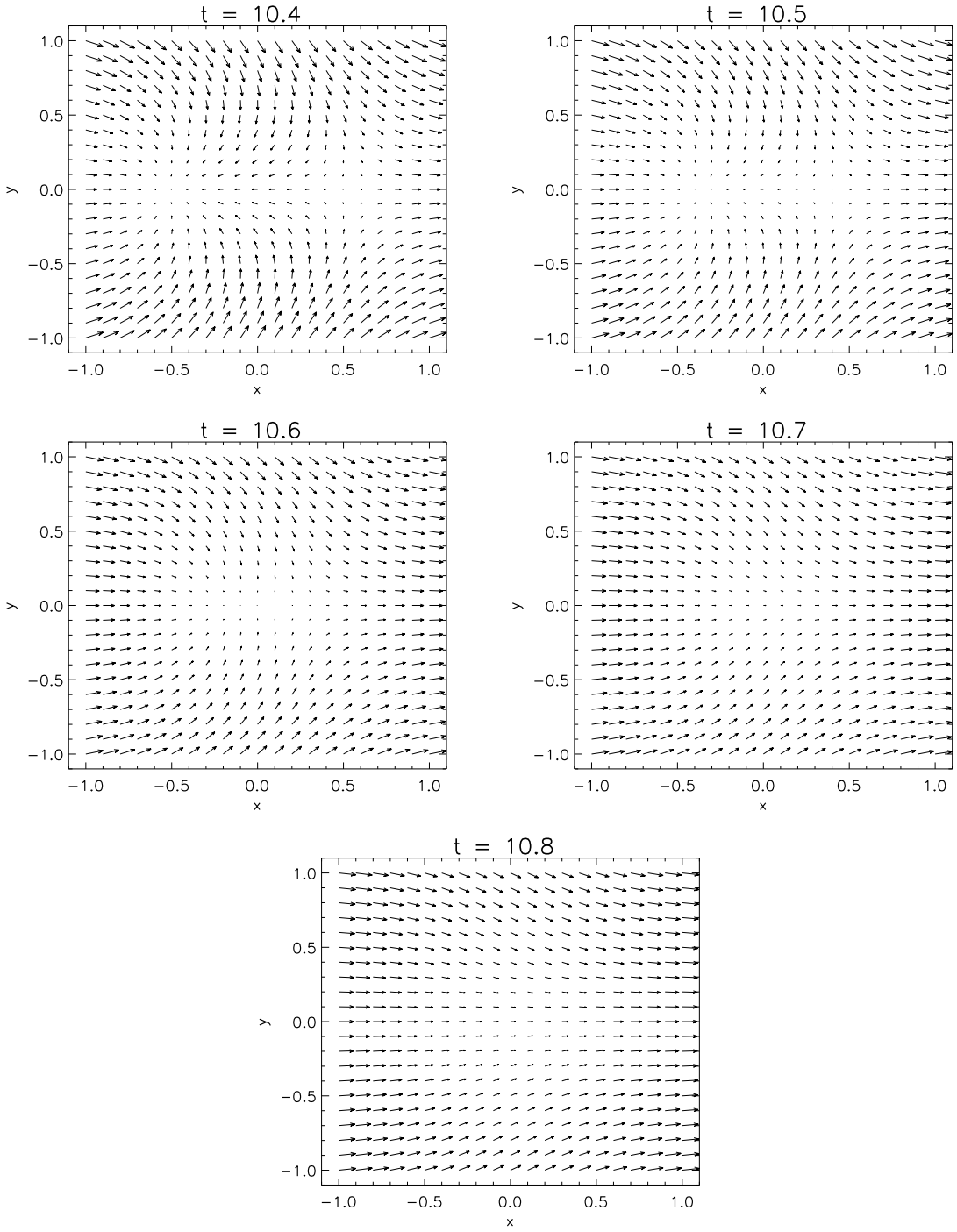

Figure 4.6: The Higgs field configuration at different times during the process of intercommutation. We show the Higgs field in the $z = z_0$ plane in a small region around the intersection point. Coordinates are relative to the intersection point. The units have not been rescaled: $m^{-1} = \frac{1}{\sqrt{2}}$ units. At $t = 10.6$, the zeroes basically overlap (the value of the Higgs field at the intersection point $(0, 0)$ is equal to -0.01). After this time, annihilation takes place in the $z = z_0$ plane and hence the strings exchange ends. It is important to note that the process is very fast. If one were to assign a velocity to the zeroes in the $z = z_0$ plane right before intercommutation, it would be much $(2 - 3$ times) bigger than the speed of light.

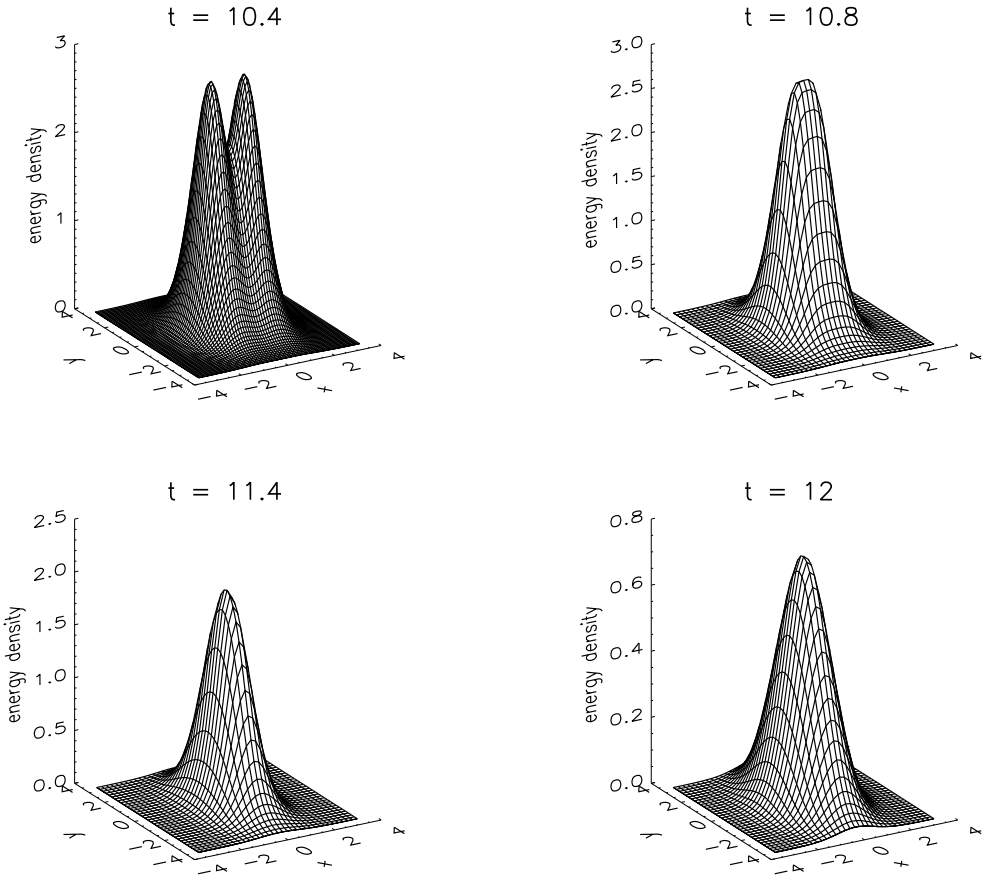

Figure 4.7: The energy density in the $z = z_0$ plane, i.e. the plane of annihilation, during the process of intercommutation (cf. figure 4.6). Closer inspection of the location of the energy peaks at $t = 10.4$, show that the distance between the peaks is about 1.6 physical units, which is larger than the distance between the zeroes of the Higgs field at that time (about 1 unit). Apparently, the energy peaks leg behind the Higgs zeroes before intercommutation. This confirms that, during intercommutation, the positions of the zeroes are energetically not that important. At $t = 10.8$, annihilation has taken place, but there is still quite a lot of energy left in the center of the $z = z_0$ plane. Afterwards, the energy peak in the center gets smaller and smaller as the strings move away in the z-direction.

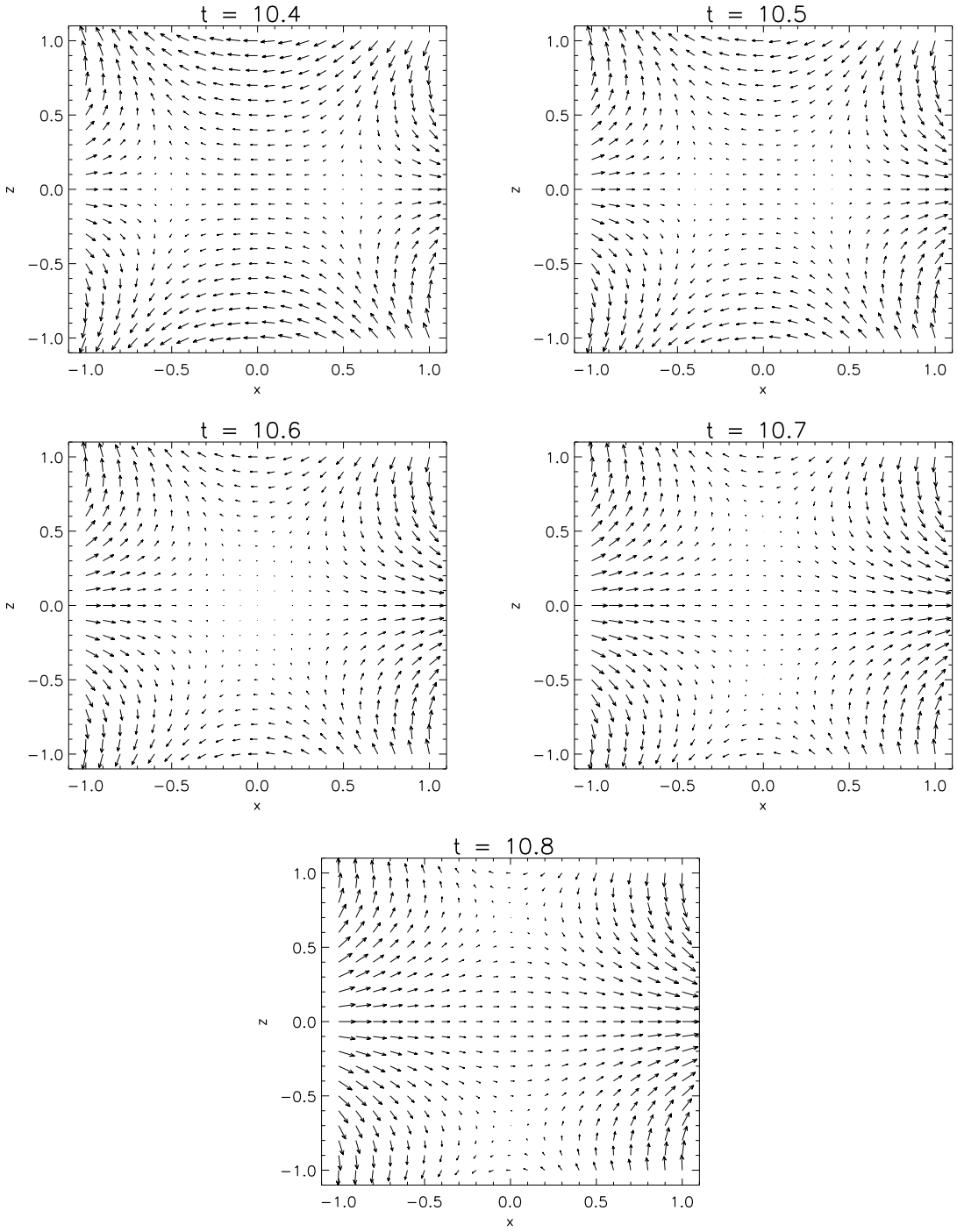

Figure 4.8: The Higgs field configuration at different times during the process of intercommutation. We show the Higgs field in the $y = y_0$ plane in a small region around the intersection point. Coordinates are relative to the intersection point. The units have not been rescaled: $m^{-1} = \frac{1}{\sqrt{2}}$ units. At $t = 10.6$, the zeroes basically overlap (the value of the Higgs field at the intersection point $(0, 0)$ is equal to -0.01). After this time, the zeroes move apart in the z-direction and hence the strings have exchanged ends. These figures again show that the process is very fast. If one were to assign a speed to the zeroes after intercommutation, it would be much bigger than the speed of light.

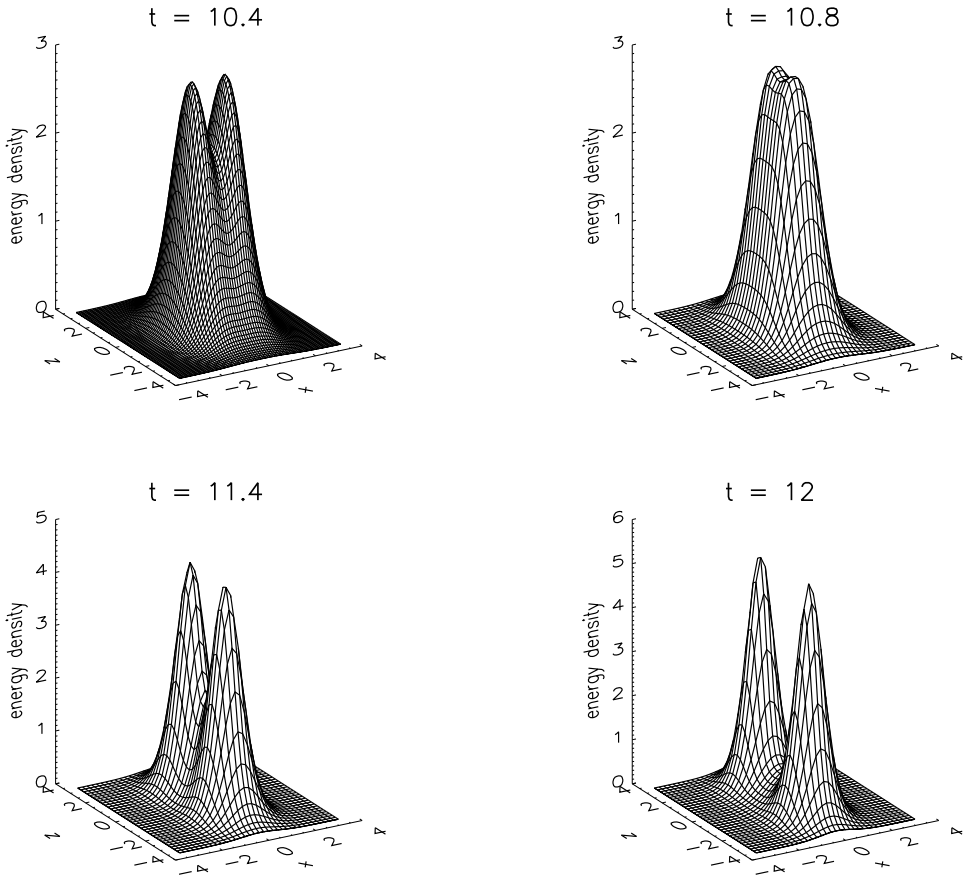

Figure 4.9: The energy density in the $y = y_0$ plane, i.e. the plane in which the strings scatter at 90^o, during the process of intercommutation (cf. figure 4.8). At $t = 10.8$, the strings have intercommuted and are moving away from each other in the z-direction.

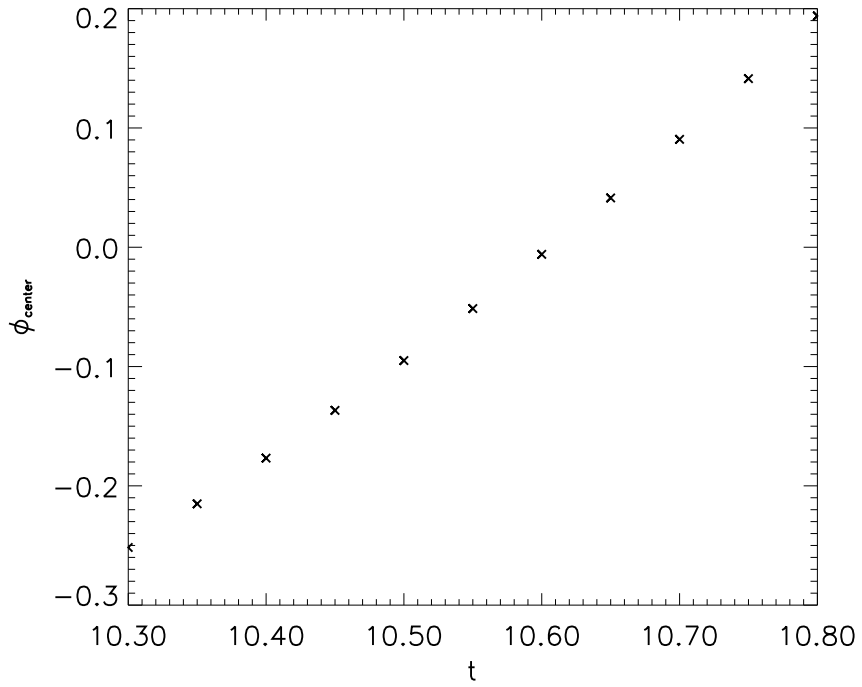

Figure 4.10: The value of the Higgs field ϕ at the "intersection point" (x_0, y_0, z_0) as a function of time. $\phi = 0$ corresponds to the exact moment when the vortices annihilate in the $z = z_0$ plane, or equivalently, the moment the strings intercommute. By interpolation, this occurs at $t_0 \approx 10.61$, at which time the time derivative of the field at the intersection point is about 1.0.

the strings move away from each other), right after intercommutation (again over a period of time of about 0.2 units), one would find $v \approx 3.5$. It might seem that an important law of nature is violated here, but this is not the case: no actual information or energy travels faster than the speed of light ! The velocity of the zeroes may be compared to the phase velocity of a wave packet. This velocity too, can be larger than the actual wave propagation speed without any information actually traveling faster than this speed. The high speed of the zeroes just before and just after the strings intersect, does tell us that, around this time, in the central region, the strings can definitely not be considered to be Nambu-Goto strings, not even approximately. A better way to describe the process could be to say that, until the cores are separated by a distance of perhaps $1.0 - 1.5$ units (roughly the characteristic string radius), the strings approximately move as free strings (with some interaction). Then, an almost instantaneous process of intercommutation takes place, after which the strings are separated by a distance of again $1.0 - 1.5$ units, but this time in the z-direction, and can approximately be described as free strings again. We also show plots of the energy density during intercommutation, both in the $z = z_0$ plane (figure 4.7) and in the $y = y_0$ plane (figure 4.9). It is interesting to note that right before intercommutation, in the $z = z_0$ plane, the energy peaks do not exactly follow the zeroes of the Higgs field, but leg behind a little bit. This is perhaps not too surprising, since one does not expect the energy peaks to travel faster than the speed of light. After intercommutation, an energy peak remains in the center of the box. The height of this peak does get smaller over time. The evolution of the energy density in the $y = y_0$ plane is exactly what one would expect for intercommutation: the peaks scatter at 90^o.

In conclusion, the two main points that we wish to make based on the simulations discussed in this section, are the following: 1. The actual intercommutation process is extremely fast. For a short time, the zeroes of the Higgs field move with a speed much faster (by at least a factor $2 - 3$) than the speed of light. 2. During this intercommutation process, the string segments in the region where intercommutation takes place, cannot be considered to be Nambu-Goto strings, at least not if we define the strings by the positions of the zeroes of the Higgs field. We wish to point out that these two points are not entirely new. A similar description of intercommutation in three dimensions is given in [19]. In [23], it was found that the 90^o scattering of vortices in two dimensions is also a very fast process. In this light, our description of the speed of the intercommutation process is perhaps not too surprising, because in the $y = y_0$ plane, intercommutation is nothing but the 90^o scattering of two vortices. Also, in [21], it is shown that during the 90^o scattering of two dimensional vortices, the energy density is concentrated in a ring around the intersection point and it is concluded that the zeroes of the Higgs field are energetically not that important during intercommutation. This is consistent with our observations in three dimensions (see figure 4.7) and supports the view that, during intercommutation, the parts of the strings close to the intersection point should not be described as Nambu-Goto strings.

4.3 Does intercommutation also occur for very high speeds ?

In section 4.5 and 4.6, we present simulation results that show that intercommutation takes place for speeds up to (at least) $v = 0.99$. This shows that, if a threshold velocity exists, its value must be higher than $v = 0.99$. We have reason to believe that, in fact, intercommutation will also occur for all speeds above $v = 0.99$. In other words, we do not expect a threshold

velocity to exist. In this section, we will present the argument on which this belief is based. It is not a proof by any means, but it at least *suggests* that intercommutation takes place for all (high) values of v. Remember that by intercommutation we mean *initial* intercommutation. We make no claims here about whether or not the strings reintercommute a while later.

Our approach is to consider what happens in the $z = z_0$ plane as two strings intercommute (see also section 2.6.2). In this plane, intercommutation corresponds to the annihilation of a vortex anti-vortex pair. Two dimensional simulations of vortex interactions in the abelian Higgs model ([21, 23]) provide no evidence that above some threshold velocity, vortices do not annihilate. As far as we know, annihilation occurs in all investigated cases. For high initial speeds ($v \gtrsim 0.9$), it *is* possible that the vortices reemerge after annihilation. We will come back to this phenomenon, and identify its three dimensional analog (the formation of a loop after intercommutation), in section 4.5. For now, the only thing that matters is that, initially, the vortices annihilate: if reemergence occurs, it occurs a while after annihilation. Of course, it is not certain that the two dimensional simulation results mentioned above, can be applied to a two dimensional plane of a three dimensional system. Also, the two dimensional simulations that we are aware of do not investigate values of v much higher than 0.9. Hence, the argument presented above, based on two dimensional results, is not a very solid one. In the rest of this section, we will consider what actually happens, in the three dimensional case, to the Higgs configuration in the $z = z_0$ plane when two strings come to intersect. In particular, we will argue that (at least for high values of v) the evolution of the Higgs field at the intersection point, i.e. $\phi(x_0, y_0, z_0)$, is such that annihilation in the $z = z_0$ plane, and hence intercommutation of the strings, is inevitable.

We first describe the *initial* configuration of the Higgs field in the $z = z_0$ plane. In figure[1] 4.2 (top), it is shown that initially, in the $z = z_0$ plane, far away from the vortices, in all directions, ϕ is real and positive (arrow pointing to the right). If we write $\phi = |\phi|e^{i\theta}$, this corresponds to $\theta = 0$. In between the two vortices on the other hand, ϕ is real and *negative* (arrow pointing to the left, $\theta = \pi$), i.e. the phase is opposite here. In the region surrounding the region where the Higgs field is negative, i.e. the central region in figure 4.2 (top), the phase changes gradually from $\theta = \pi$ to $\theta = 0$ in such a way that the winding number around the string on the left equals one and the winding number around the string on the right equals minus one.

We wish to know what happens when this initial configuration is evolved. We assume that the initial speeds of the strings are such that the strings come to intersect at some finite time t_0. As the strings approach each other, the region described above, where the phase of the Higgs field is *not* equal/close to $\theta = 0$, becomes smaller and smaller. It follows from symmetry that, during the approach, the phase of the Higgs field at the intersection point (x_0, y_0, z_0) remains unchanged, i.e. $\theta = \pi$. Since the two zeroes will eventually meet at the intersection point, at which time $|\phi(x_0, y_0, z_0)| = 0$ by definition, the absolute value of $\phi(x_0, y_0, z_0)$ tends to zero as the strings approach each other. When $\phi(x_0, y_0, z_0)$ reaches zero, the strings intersect and the first time derivative of $\phi(x_0, y_0, z_0)$ is either real and positive, or zero: $\dot{\phi}(x_0, y_0, z_0) > 0$ or $\dot{\phi}(x_0, y_0, z_0) = 0$ (any other value of $\dot{\phi}(x_0, y_0, z_0)$ is not possible because the field is negative before it reaches zero). What happens to $\phi(x_0, y_0, z_0)$ after this time, determines whether or not the strings intercommute. If $\dot{\phi}(x_0, y_0, z_0) > 0$ at t_0, $\phi(x_0, y_0, z_0)$ becomes positive and there is no winding left in the $z = z_0$ plane. In other words, in this case, the strings

[1] In figure 4.2, we use the system from the previous section to illustrate our explanation, i.e. $\beta = 1$, $\alpha = 90^o$ and $v = 0.5$, but the initial configuration is "qualitatively" the same for other values of β, v and α.

intercommute. This is what happens in the system simulated in the previous section, where $\dot{\phi}(x_0, y_0, z_0) \approx 1$ (see figure 4.10). In principle, it might also be that $\dot{\phi}(x_0, y_0, z_0) = 0$ at t_0, in which case the subsequent evolution of $\phi(x_0, y_0, z_0)$ depends on its second time derivative and could lead to intercommutation, if $\phi(x_0, y_0, z_0)$ becomes positive, or non-intercommutation, if $\phi(x_0, y_0, z_0)$ becomes negative. However, for high approach velocities, we do not expect this to occur. In fact, it makes a lot more sense for $\dot{\phi}(x_0, y_0, z_0)$ at t_0 to grow larger with v than the other way around. Hence, we expect that, for high velocities, $\phi(x_0, y_0, z_0)$ always becomes positive after the strings intersect, thus creating a configuration with no winding of the Higgs field in the $z = z_0$ plane: intercommutation.

In conclusion, the argument presented above suggests that it might be that there exists some (β and α dependent) minimum velocity, *below* which there is no intercommutation[2], but that, above this minimum velocity, the strings always intercommute. In other words, the argument leads us to believe that there is no maximum intercommutation velocity (threshold velocity). In section 4.5 and 4.6, we will present numerical evidence that intercommutation takes place for speeds up to at least $v = 0.99$. In the next section, we will first discuss two analytic arguments that predict that there *is* a threshold velocity.

4.4 Two arguments in favor of the existence of a threshold velocity

In [8], it is argued that above a threshold velocity v_t, given approximately by[3]

$$v_t = \sqrt{\frac{4\kappa(1-\cos\alpha)}{1+4\kappa(1-\cos\alpha)}}, \tag{4.1}$$

no intercommutation will take place. Here, κ is a parameter assumed to be close to unity. This result is first derived for global strings (v is understood to be the speed of the strings shortly before intercommutation) and later it is argued that it should hold for local strings as well, because when the strings intersect, the gauge fields can be ignored. The threshold velocity is derived by comparing a characteristic time scale for the intercommutation of two strings with zero velocity to the time a string needs to travel a distance of two string radii. When this latter time is bigger than the first, which is the case for $v > v_t$, it is expected that no intercommutation takes place. Here, it is implicitly assumed that the time a string needs to travel a distance of two string radii is a characteristic time for non-intercommutation. The characteristic time for intercommutation is calculated by starting from an ansatz describing two intersecting strings with zero velocity. In this configuration, the second time derivative of the Higgs field at the point of intersection is calculated. From the value of this second derivative, it is concluded that the strings will exchange ends and move away from each other and, more quantitatively, what the typical time taken by this process is. What is wrong with this calculation of the typical time for intercommutation is that for non-zero velocities, as we have shown, the field at the point of intersection has a non-zero *first* time derivative and it is this first derivative that makes sure that intercommutation occurs, not the second. In fact,

[2] Another reason for introducing a minimum velocity for intercommutation was discussed in the introduction: for "low" speeds, repulsion between strings may prevent them from ever meeting at all. This may in particular be relevant for values of β much bigger than one.

[3] The parameters have different names in the actual preprint. What we call α is called θ and what we call κ is called α.

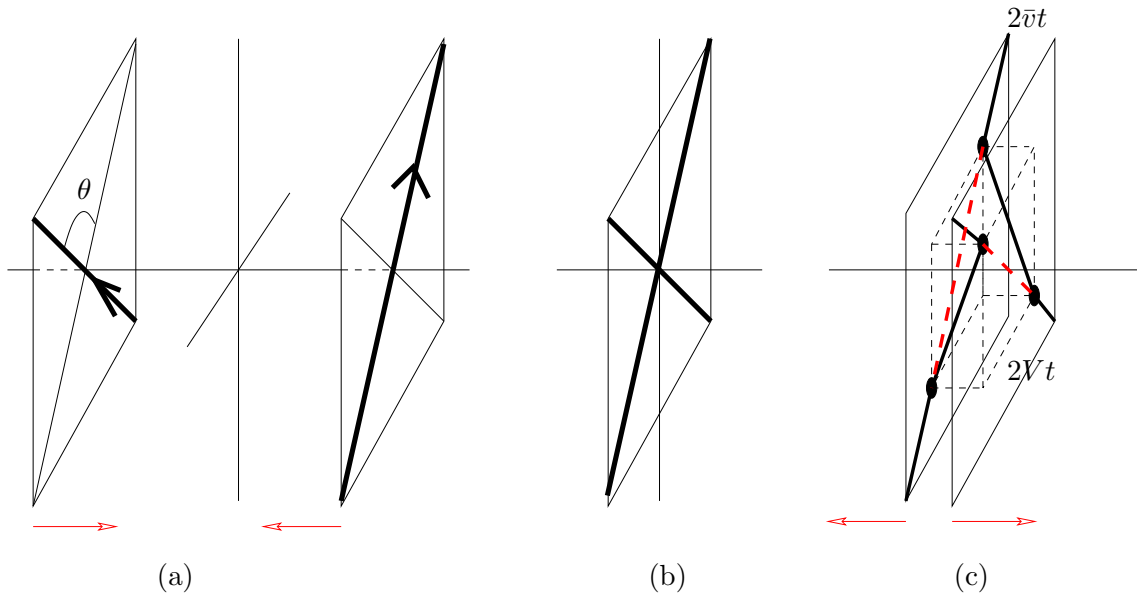

Figure 4.11: "Schematic figure of reconnection of vortex strings. (a) Two vortex strings (thick lines) are colliding. Small arrows indicate the directions of the string motion. (b) They collide at $t = 0$. (c) They reconnect with each other. The shape after the reconnection is assumed in such a way that the reconnected part is on a dashed box which expands. The blobs represent kink points. The thick dashed lines are the strings which would have been present if the reconnection didn't occur." Figure and caption text in quotes taken from [12]. The assumptions described here are used to derive the existence of a threshold velocity for intercommutation (see equation (4.3)).

it is because the two strings approach each other that the first derivative is positive. Hence, the assumption made in [8] that somehow the time needed by a string to travel a distance of two string radii is a characteristic time for non-intercommutation, is wrong. This is the main reason why we think the argument presented in [8] is incorrect.

In [12], the existence and value of a maximum speed for intercommutation is derived using an argument based on energy considerations. Again, we will first explain the basic argumentation followed and then discuss what we think is wrong with it. It starts with two intersecting straight strings with center of mass speed v (see figure 4.11) at $t = 0$. It is assumed that the energy of a string segment with length L and speed v is given by

$$E = \mu\gamma(v)L, \tag{4.2}$$

where μ is the energy per unit length of a string that is not moving. The energy of the system at a time t is then calculated, both in case the strings simply move through each other and in case the strings intercommute. In the latter case, after intercommutation, the strings are assumed to have the shapes shown in figure 4.11, and to move away from each other at a speed V. The speed V is assumed to be bound from above by $\sqrt{1-v^2}\sin(\alpha/2)$ because otherwise the kink points (see figure) move faster than the speed of light. From figure 4.11, it is clear that, if $V > v$, the total string length at time t, if intercommutation does take place, is smaller than the string length at the same time if intercommutation does not take place. The

higher V is made, the bigger the difference will become. On the other hand, increasing the value of V also increases the energy per unit length of the strings, as follows from the factor $\gamma(v)$ in (4.2). In other words, any reduction in length is coupled to an increase in energy per unit length. If a final speed V (within the allowed range) can be found such that the total energy after intercommutation is less than the energy after non-intercommutation for all t, i.e. $\delta E := E_{\rm int.} - E_{\rm non-int.} < 0$, it is concluded that intercommutation must take place. If no such V can be found, it is concluded that the strings move on without exchanging ends. This way, it is found that strings do not intercommute above a threshold velocity given by

$$v_t = \frac{\sin(\alpha/2)}{\sqrt{1+\sin^2(\alpha/2)}}. \tag{4.3}$$

Remarkably, this exactly coincides with the result found in [8], if we choose the parameter $\kappa = 1/8$ in (4.1).

What is wrong with this argument is that, as our simulations show (see section 4.2), during a short period of time, the strings can actually move away from each other at speeds much higher than the speed of light. Because of this, the string length can be reduced a great deal in a very short time if the strings intercommute. In the argument presented above, the reduction in string length due to high string velocities, is coupled to an increase in kinetic energy. However, during the short time when the zeroes move at superluminal speeds, the positions of the zeroes are energetically not that important and we can definitely not use (4.2) for the energy (if only because $\gamma(v)$ is not well defined for $v > 1$). Unfortunately, we do not know what would be a good alternative expression for the energy during this short period, so we cannot give an alternative argument that shows that the energy is reduced by intercommutation for *all* times[4] t. However, it is clear that intercommutation can always reduce the energy after a *finite* time. If we define t to be the (finite) time after intercommutation at which the strings move at a speed V smaller than the speed of light again, and are again approximately descibed by (4.2), then it is clear that intercommutation can always reduce the energy at t. The reason for this is that the speed V at t is not coupled to the string separation at that time in the same way as before (i.e. distance $= 2Vt$), because before t, the strings could have moved with an average speed much faster than V and even faster than the speed of light. In other words, the energy reduction due to the string length being shorter is not compensated by an increase in kinetic energy.

4.5 Numerical intercommutation of global strings and loop formation

We investigated numerically whether or not strings intercommute at high velocities, by simulating string interactions for various different sets of parameter values. To start with global strings, we found that intercommutation occurs in all cases, where we went up to speeds as high as $v = 0.99$. We did not simulate higher speeds, partly because the Lorentz contraction at high speeds makes simulations increasingly difficult to carry out (because the lattice spacing needs to be made increasingly small and therefore, to keep the total physical size of the box constant, it is necessary to increase the grid size) and partly because you have to stop

[4] In particular, a good argument based on reduction of energy should show that the energy is reduced by intercommutation after an infinitesimal time.

somewhere. The interaction proceeds roughly in the same fashion as the intercommutation process described in section 4.2. In all cases, the strings move away from each other very fast after intercommutation, leaving a lump of energy behind in the center. The simulation results can be found in figure 4.13.

We used a code that is basically the same as the one described in section 3.5, except without the gauge fields. As parameters of the Higgs model, we used $\eta = 1$ and $\lambda = 2$, such that the typical string core size is given by $m^{-1} = 1/\sqrt{2}$. As far as we can tell, these are the same conventions as were used in [28]. Most simulations were done on a $150 \times 150 \times 250$ lattice, with lattice spacing $a = 0.1$, and time step $\Delta t = 0.05$. The initial separation was taken to be 6 (physical) units. In a number of cases, we simulated the same system twice, once with the BC from section 3.4.2, which we think were also used in [28], and once with the BC from section 3.4.3, which were used in [19]. In all cases, the main results were the same for both types of BC. After sufficient time, there were differences in the field values, but these differences were very small. Over time, we have performed enough checks (varying grid size, lattice spacing, etc.) to be confident that we simulated continuum physics. The main conclusion of the simulations is that we found no evidence for the existence of a threshold velocity[5].

Besides this, we also found in some cases with high v, that a while after intercommutation has taken place, something else interesting happens (see figure 4.12). Out of the energy left behind in the center of the box after intercommutation, a new string *loop* forms. This loop lies entirely in the $y = y_0$ plane and initially grows. After a while, it stops growing, starts shrinking and finally self-annihilates in the center of the box again. All this happens when the strings that have intercommuted are already far away, since these strings move apart at high speeds after intercommutation. Spontaneous loop formation after intercommutation has been observed for local strings in [19]. We can again understand the process a little better if we focus on the $z = z_0$ plane and compare the situation with what we know about vortex interactions in two dimensions. As we discussed before, intercommutation corresponds to the annihilation of a vortex anti-vortex pair in this plane. For vortices in the two dimensional abelian Higgs model, we mentioned in section 4.3 (see for example [23]) that when a vortex anti-vortex pair have high enough initial speeds, the vortices reemerge after annihilation. After reemergence, the vortices either move in exactly the same directions as before (forward reemergence), as if they passed through each other, or they both move in the exact opposite directions (backward reemergence), as if they bounced back. The direction of motion after reemergence turns out to depend on β. In [23], it was found that for a number of values $\beta \geq 8$, forward reemergence occurs and for a number of values $\beta \leq 4$, backward reemergence occurs. We are not aware of any simulations that explicitly show reemergence for vortices in a model without the gauge field, i.e. $\beta \to \infty$ (corresponding to global strings), but the results for finite β suggest that, in this case, the vortices emerge in the forward direction, i.e. as if they passed through each other. If we translate this to the $z = z_0$ plane in the three dimensional case, the reemergence corresponds to the creation of a growing loop in the $y = y_0$ plane, which is perpendicular to the plane in which annihilation takes place when the strings intercommute. Forward reemergence corresponds to the loop orientation sketched in figure 4.12, which is indeed what we find in our numerical simulations. In other words, if we look at the loop in the $z = z_0$ plane, we see a vortex moving in the positive x-direction and an

[5]Technically, it is still possible that there is a threshold velocity, but with a value higher than the velocities we have probed.

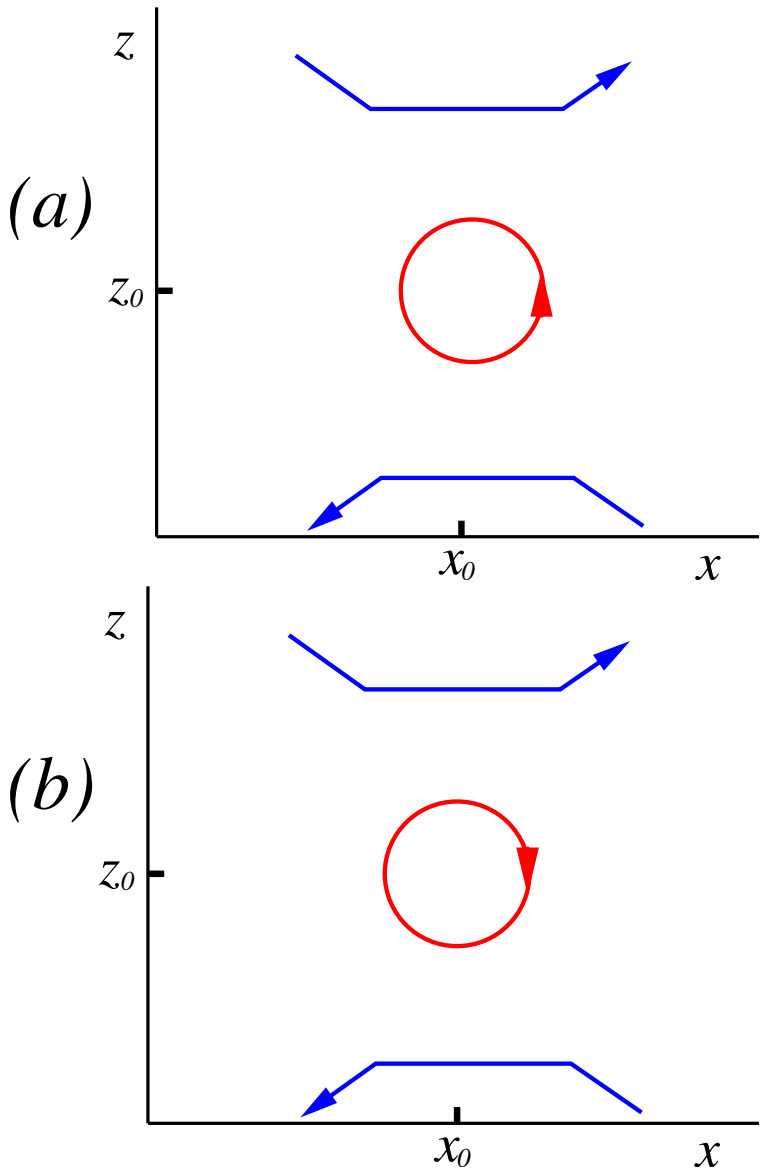

Figure 4.12: For high speeds of approach, it can happen that a string loop forms in the center of the box a while after intercommutation. The loop lies in the $y = y_0$ plane and can in principle have two different orientations. For global strings, the loop orientation turns out to be as sketched in figure (a). For local strings, we have also observed loop formation. Here, the orientation depends on the value of β. It seems that for high values of β, the orientation if given by figure (a), while for values of β below some threshold value close to $\beta = 4$, the orientation is given by figure (b). The blue strings in the figures represent the two original strings that have intercommuted. Note that these strings do not exactly lie in the $y = y_0$ plane (rather, they intersect this plane), so in that sense the figures are not entirely correct. For local strings, in some cases, the loop that is formed after intercommutation catches up with the two original strings and plays a role in the *re*intercommutation of these strings.

α	v	**intercommutation ?**	loop seen ?
45^o	0.99	yes	no
90^o	0.99	yes	yes
120^o	0.9	yes	yes
120^o	0.95	yes	yes
120^o	0.99	yes	yes
135^o	0.99	yes	yes

Figure 4.13: All simulations of global string systems resulted in intercommutation. Afterwards, the strings move away from each other in the z-direction very rapidly. In some cases, we observed the formation of a loop in the center of the box a while after intercommutation. Although we did not check this explicitly in all cases, we do not expect such a loop to grow fast enough to catch up and interact with the two original strings that have intercommuted. The table shows the parameters of the different simulations we carried out. We also indicate whether or not we found loop formation.

anti-vortex moving in the negative x-direction.

The formation of a loop may also explain some of the results in [28]. Here (see also section 2.6.2), the intercommutation of global strings is investigated by the same type of lattice simulations as we used. The boundary conditions are, as far as we can tell, as described in section 3.4.2. It is claimed in this paper, that a threshold velocity v_t does exist. In terms of the initial speeds, v_t would be in the range $0.7 - 0.97$, depending on α. The corresponding velocities just before intercommutation are also estimated and in terms of these speeds, the threshold value is in the range $0.9 - 0.97$. According to [28], above these velocities, the strings pass through each other when they meet. Particular attention is paid to a simulation characterized by initial speed $v = 0.9$ (the strings start at a distance of roughly 6.5 units) and angle $\alpha = 120^o$. It is shown that (long) after the strings intersect, the energy has two separated peaks in the plane given by $z = z_0$. From this, and from projections of the energy on the xz-plane of the energy, it is concluded that the strings have not intercommuted, but instead have moved through each other.

To see what is going on here, we performed several simulations using the same initial string separation of $x_2 - x_1 \approx 6.5$ units and the same values of v and α as the simulation in [28] described above. We performed simulations with several values of the lattice spacing and the box size to check that the results are not a lattice artefact. We also performed the simulations for both the boundary conditions described in section 3.4.2 and those in section 3.4.3. The former are the same boundary conditions that we think were used in [28]. The main result was the same for all simulations: first, the strings intercommute after about 3 units of time, after which the strings move apart in the z-direction. Then, a loop is formed around $t = 5.5$. The loop grows for a while and then starts shrinking again until it disappears some time before $t = 24$. We checked that the loop never grows big enough to "catch up" with the original strings. The process is illustrated in figure 4.14 and 4.15.

It might be that in [28], the loop was mistaken for the original strings. After all, in the $z = z_0$ plane, the growth of a loop looks exactly the same as the two original straight strings moving apart after non-intercommutation. In both cases, two energy peaks moving away from each other in the x-direction are observed. If we are right, a more detailed inspection

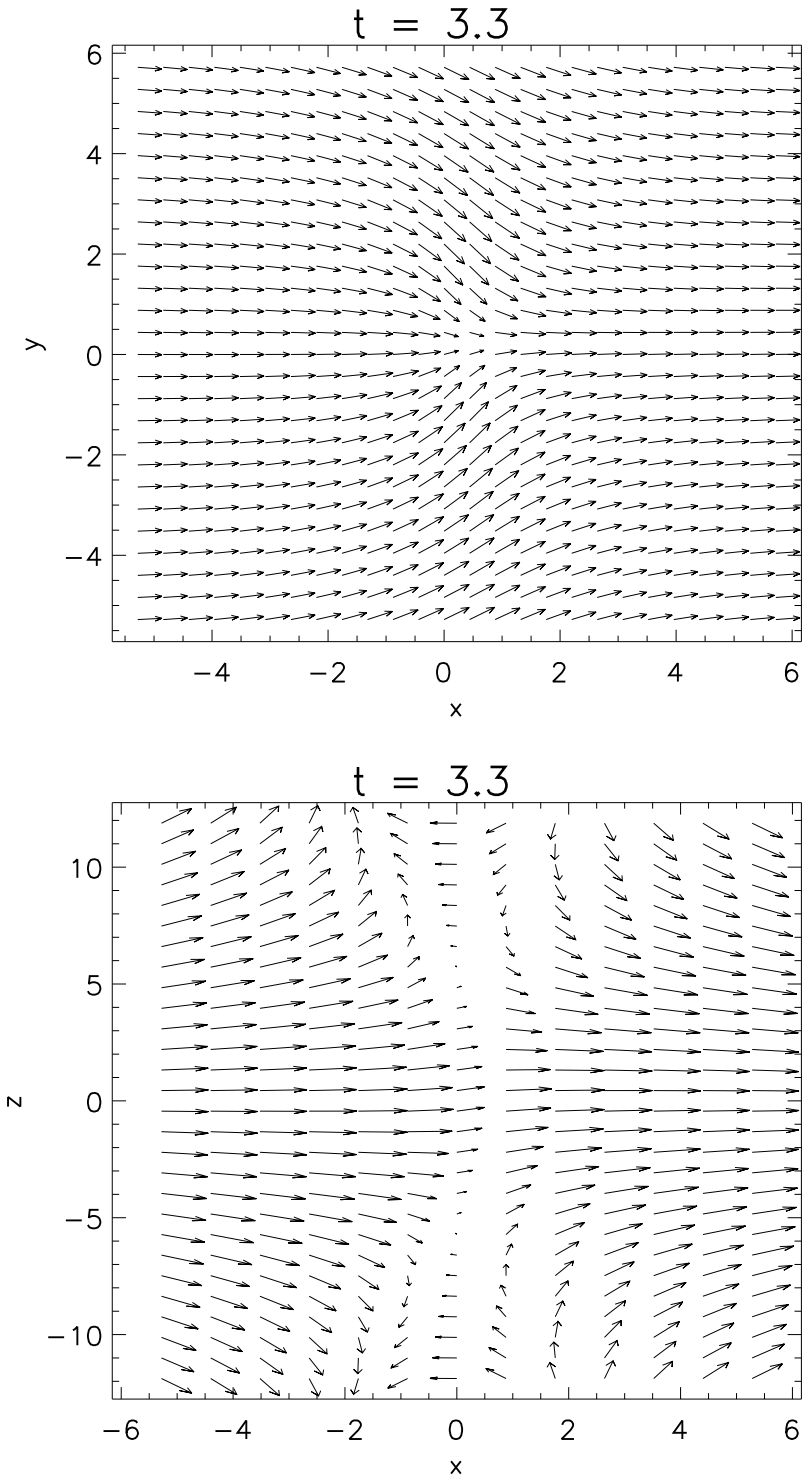

Figure 4.14: Interaction of global strings: $v = 0.9$, $\alpha = 120^o$ and initial distance $x_2 - x_1 = 6.5$ units. The simulation uses lattice spacing $a \approx 0.22$, boxsize $\approx 33 \times 33 \times 55$ (physical size) and $\Delta t = 0.1$. Coordinates are relative to the intersection point. The units have not been rescaled: $m^{-1} = \frac{1}{\sqrt{2}}$ units. At $t = 3.3$, intercommutation has just taken place, as can be seen from the $z = z_0$ plane (top) and the $y = y_0$ plane (bottom). No string passes through the former plane and the distance between strings in the latter plane is about 10 units.

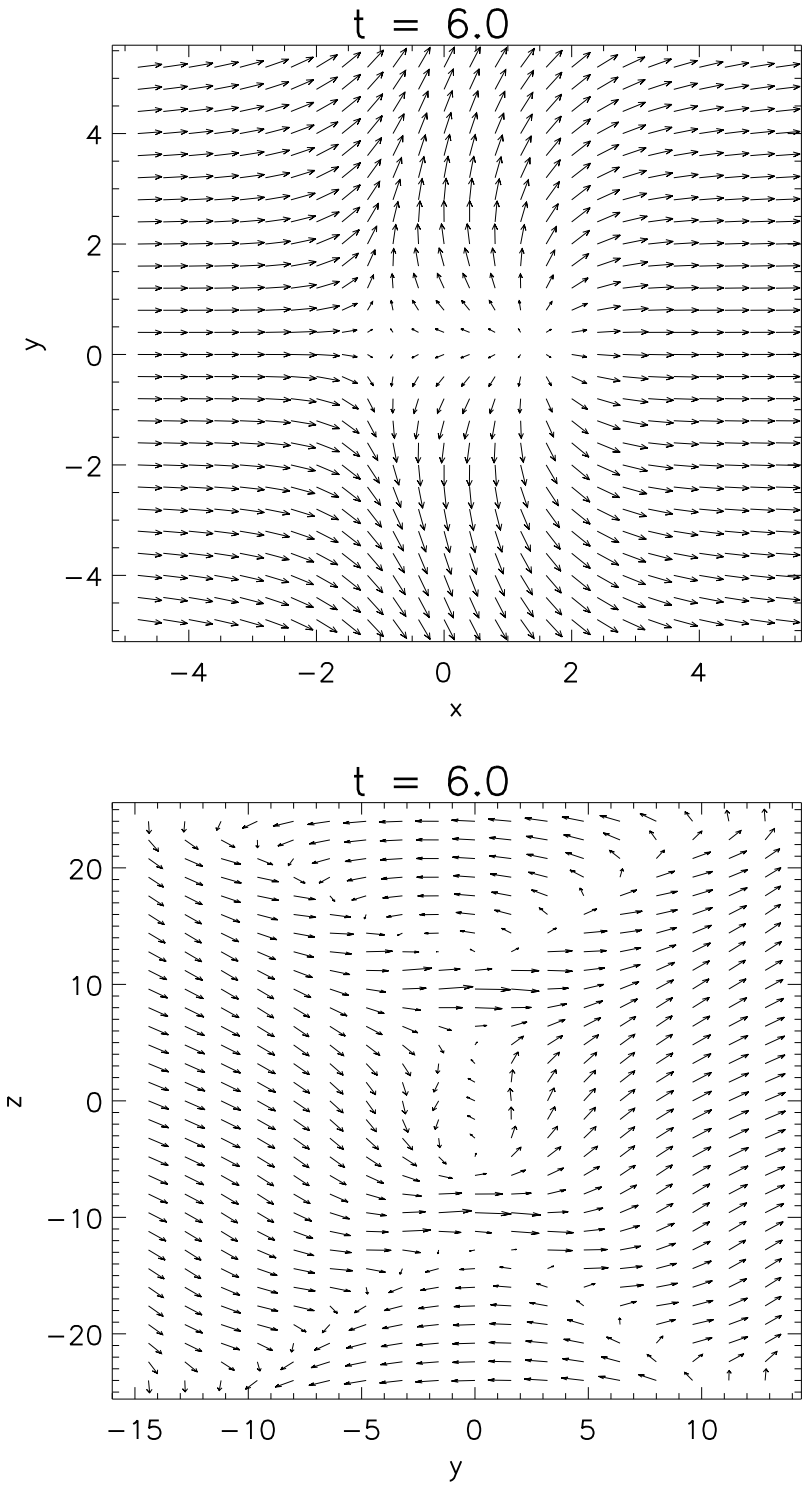

Figure 4.15: Same system as in previous figure, but with $t = 6.0$. Coordinates are relative to the intersection point. The units have not been rescaled: $m^{-1} = \frac{1}{\sqrt{2}}$ units. A string loop has formed in the center of the box. We show the $z = z_0$ plane (top) and the $x = x_0$ plane (bottom). In the latter plane, the Higgs field has four zeroes: the two closest to the edge correspond to the original strings that have intercommuted and are now moving away from each other. The other two zeroes correspond to the string loop passing through the $x = x_0$ plane. The loop grows, but never comes close to the strings. After a while, the loop starts shrinking and eventually disappears.

of the positions of the zeroes of the Higgs field throughout the three dimensional volume in the simulation in [28], would have revealed that the two original strings had intercommuted and moved apart a long time ago and that a loop had formed in the center.

4.6 Numerical intercommutation of local strings

The next step is to investigate numerically whether or not *local* strings intercommutate at high velocities. For $\alpha = 90^o$, equation (4.1) suggests that above a speed of about $0.6 - 0.94$, for values of κ in the interval $1/8 - 2$ ($\kappa = 1/8$ corresponds to the result (4.3)), strings do not intercommute. However, we performed several simulations for values of β in the range from $\frac{1}{64}$ to 64 (see figure 4.16) and found in all cases that intercommutation takes place for values of v up to at least $v = 0.99$. If a threshold velocity does exist, its value must be higher than this. The simulations of local strings were performed using the code described in section 3.5. All of the results presented in figure 4.16, are based on simulations on a $150 \times 150 \times 250$ lattice. For $\beta = 1$, we used a lattice spacing $a = 0.1$ and timestep $\Delta t = 0.05$, while the initial separation was taken to be 6 (physical) units. For different values of β, these parameters were changed in some cases because as[6] $\beta = \frac{\lambda}{2}$ is increased, the typical Higgs core size $m^{-1} = \lambda^{-\frac{1}{2}}$ gets smaller. We again made use of both the BC described in section 3.4.2 and those in section 3.4.3. In several cases, we checked our results by running the same simulation with both types of BC described, and by varying the initial separation. As expected, the results were always the same and we feel confident that our results are not in some way a lattice artefact.

The main conclusion is again that, initially, the strings intercommute in all cases. Afterwards, the strings are always separated by a considerable distance so that it is entirely clear that intercommutation has indeed occurred and that the strings do not simply overlap. We wish to stress again, that we consider the strings to intercommute if they intercommute *initially*, regardless of what happens afterwards. In the case discussed in section 4.2, i.e. local strings with relatively low velocities ($v = 0.5$), as well as in the cases discussed in the previous section about global strings, the distinction is not necessary because after intercommutation, the strings move apart fast and never see each other again. However, for high speeds ($v \approx 0.99$), the behavior of the system after intercommutation is sometimes more complicated.

The question of what happens to the strings after intercommutation in the long run is an interesting one. It is also a question that is harder to answer than the question that we posed ourselves (whether or not strings intercommute *initially*). The main reason for this is that the configuration needs to be evolved for a longer time to find out what happens. Hence, bigger simulation volumes need to be used. For these longer simulation times, it is also worth rethinking the approximation of string segments by straight strings. In practice, interacting string segments are parts of strings that are far from straight. Say for example, that in a simulation it is found that two straight strings, characterized by v and α, intercommute once initially, but a while later intercommute again. The net result would in this case be no exchange of ends. In the more realistic case of two string *segments* of the same string approaching each other (with the same v and α) however, it may very well be that after the first intercommutation the string segments are pulled away from each other by the rest of the strings they are attached to, thus causing the strings never to meet and intercommute

[6] Remember that we fix $e = \eta = 1$ and change β by changing λ.

β	α	v	**inter - commutation ?**	running time	initial separation	a	comments
1/64	90^o	0.99	yes	160	64	0.8	
1/4	45^o	0.99	yes	7	6	0.1	
1/4	90^o	0.9	yes	7	6	0.1	
1/4	90^o	0.99	yes	7	6	0.1	
1/4	135^o	0.99	yes	7	6	0.1	
1	45^o	0.99	yes	7	6	0.1	R (around $t = 7$)
1	90^o	0.5	yes	7	6	0.1	
1	90^o	0.95	yes	7	6	0.1	
1	90^o	0.99	yes	7	6	0.1	
1	120^o	0.95	yes	7	6	0.1	
1	120^o	0.99	yes	14	6	0.1	
1	135^o	0.99	yes	7	6	0.1	L
4	45^o	0.99	yes	7	6	0.1	R (around $t = 5$)
4	90^o	0.9	yes	7	6	0.1	
4	90^o	0.99	yes	7	6	0.1	R (around $t = 5$)
4	135^o	0.99	yes	7	6	0.1	
8	90^o	0.99	yes	7	6	0.1	R (around $t = 5$)
8	90^o	0.99	yes	4	3	0.05	R (around $t = 2.5$)
16	90^o	0.99	yes	5	3	0.05	R (around $t = 2.5$)
64	90^o	0.99	yes	2	1.6	0.02	L, R (around $t = 1.6$)

Figure 4.16: All simulations of local strings initially resulted in intercommutation. After intercommutation, the strings are clearly separated. We also took a look at what happens afterwards. In a lot of cases, it is hard to tell and longer simulations are necessary to find out what happens. In some other cases, we have observed loop formation in the center of the box. These loops always lie in the $y = y_0$ plane and the loop orientation depends on the value of β. Also, we found in some cases that strings intercommute a second time. In these cases, the net results is that no ends are exchanged. For some of the simulations where it is very clear that a loop (L) is formed or reintercommutation (R) occurs, we added a note in the "comments" column. This does not mean that no reintercommutation or loop formation occurs in the other cases. We simply did not investigate this (well enough). The loop with $\beta = 64$ mentioned in the table has the same orientation as the loops found in global string simulations, while the loop with $\beta = 1$ has opposite orientation. Note that the running time, the initial separationand the lattice spacing a are varied with β because the characteristic Higgs core size depends on β through $m^{-1} = \frac{1}{\sqrt{2\beta}}$ ($e = \eta = 1$). The gauge core size is kept constant, $M^{-1} = 1/\sqrt{2}$. The typical time step in our simulations was taken to be $\Delta t = a/2$.

a second time. Hence, in this case, only the first intercommutation would matter and the realistic net result would be the exchange of ends and formation of a loop. In other words, the long term behavior of straight strings after intercommutation might not have much meaning when applied to the interaction of realistically shaped strings. In the end of section 3.4.3, we suggested a way to incorporate the influence of the rest of the string on a string segment in the boundary conditions of the simulation.

We now wish to make some remarks on the behavior of the system after (the first) intercommutation in our simulations. The most interesting observation is that it sometimes indeed happens (see figure 4.16) that the strings exchange ends a second time a while after the first intercommutation. In these cases, the net result is that there is no exchange of ends and the strings move away from each other in the x-direction afterwards as if they had simply passed through each other. Since we know from section 4.2 that this does not happen for low velocities, it seems that (at least for certain values of β) there *is* a threshold velocity for reintercommutation.

Also, like in the case of global strings, we found that a loop (lying in the $y = y_0$ plane, perpendicular to the plane in which annihilation takes place when the strings intercommute) can be formed in the center of the box after intercommutation (see figure 4.12). It is interesting to note that the loop orientation depends on the value of β. Roughly speaking, it seems that for small β, the vortex anti-vortex pair in the $z = z_0$ plane reemerges in the backward direction, and for high values of β, they reemerge in the forward direction. In other words, the orientation of the loop is the same as for global strings for large β and opposite for small β. It is hard to say what the exact value of β is that separates these two regimes because, in a lot of cases, it is hard to tell what the orientation of a loop is because the loop lies in a region of very small $|\phi|$. However, it is clear that this critical value of β is larger than one and it is probably close to $\beta = 4$. This means that for critically coupled strings ($\beta = 1$), the loop orientation is the opposite of the loop orientation in the case of global strings. Qualitatively, this agrees nicely with the two dimensional results in [23], that were briefly discussed in section 4.5 ($\beta \leq 4$ implies backward reemergence). Finally, we note that, in the cases where strings intercommute a second time, the string loop (if there is one) often plays a role. Typically, what happens in these cases is that first, two straight strings intercommute and move apart. Then, a loop is formed in the center of the box. Next, this loop grows bigger fast and "catches up" with the two original strings. Finally, the two strings exchange ends through the loop and then move on in the x-direction as if nothing has happened. It seems that this process is easier if the loop has the orientation corresponding to high values of β.

4.7 Conclusions and outlook

We investigated the intercommutation behavior of straight global and local strings (in the abelian Higgs model). We focussed on claims of the existence of a threshold velocity, above which the strings do not intercommute, but simply pass through each other. We analyzed one particular case of intercommutation in detail and found that the intercommutation process proceeds extremely rapidly, with the zeroes of the Higgs field moving at superluminal speeds. We concluded that, during intercommutation, the strings should definitely not be considered Nambu-Goto strings. We also found that, if the strings initially have sufficiently high kinetic energy, a string loop can be formed and we gave a rationalization of this process in terms of the two dimensional interactions of vortex anti-vortex pairs. The formation of a loop has

been shown in earlier numerical work too ([19]). We investigated whether or not strings intercommute at very high velocities by performing numerical simulations. For both global strings and local strings with various values of β, we found intercommutation for velocities of approach up to $v = 0.99$, thus finding no evidence for the existence of a threshold velocity. We did find in a number of cases that strings intercommute a second time, such that the net result is the same as if there was no intercommutation at all.

As was discussed in chapter 2, the main reason for studying the intercommutation behavior of cosmic strings, is that the evolution of a cosmic string network depends strongly on the intercommutation pobability p. If $p \approx 1$, a string network can lose energy by forming loops sufficiently fast to reach a scaling solution ([16, 17, 18, 20, 28]). The conclusion from earlier studies that indeed $p \approx 1$, is not altered by our work. If anything, it is supported, because now we know that even for very high velocities, intercommutation takes place.

Since it might still be that, for certain values of β, intercommutation does not happen for *low* velocities, an interesting future project could be to investigate the low velocity intercommutation behavior of cosmic strings. We can think of two main reasons for non-intercommutation to occur for low approach velocities. First of all, it could be that the repulsion between strings is so strong that the strings will not come to intersect for a significant range of initial approach velocities. In particular, we expect that this might occur for high values of β. Two dimensional simulations of vortex vortex interaction ([23]) for example show that for large β, parallel strings need to approach each other with speeds $v > 0.55$ in order to come to intersect. This suggests that the repulsion of strings could have a considerable effect on the intercommutation probability. A second low velocity process that might affect the intercommutation probability is the formation of an $n = 2$ bound state. In [6], it is shown that nearly parallel strings with $\beta < 1$ could form a bound state when they meet. Investigation of the low velocity intercommutation behavior of strings might therefore result in the conclusion that p is significantly lower than 1 for values of β either much higher or much lower than 1. If this is the case, the evolution of a network of cosmic (abelian Higgs) strings might have an important dependence on β. This would be an interesting result because, to our knowledge, all simulation of string network evolution are based on β close to one and/or $p \approx 1$. Of course, we are speculating here and new simulations need to point out whether or not p is really affected by non-intercommutation at low velocities for certain values of β. These simulations would be more difficult than the ones discussed in this thesis in the sense that they probably need to run for longer times and thus require larger simulation volumes.

Finally, we wish to remind the reader that our results apply to strings in the abelain Higgs model, but that the types of strings relevant to cosmology could well be of another type. In particular, there is much recent interest in cosmic superstrings, which are macroscopic strings occurring in string theory. The interaction of these strings is known to be much different than the interaction of the strings that we have been studying ([26]).

Bibliography

[1] Albrecht A. and Turok N., *Evolution of cosmic strings*, Phys.Rev.Lett. **54** (1985), 1868–1871.

[2] A.A. Abrikosov, *Quantitative string evolution*, Zh. Eksp. Teor. Fiz. **32** (1957), 1442.

[3] M. Anderson, F. Bonjour, R. Gregory, and J. Stewart, *Effective action and motion of a cosmic string*, Phys.Rev.D **56** (1997), 8014–8028, hep–ph/9707324.

[4] M. A. Armstrong, *Basic topology*, 1st ed., Springer, 1983.

[5] D.P. Bennett, *Evolution of cosmic strings*, Phys.Rev.D **33** (1986), 872–888.

[6] L.M.A. Bettencourt, P. Laguna, and R.A. Matzner, *Nonintercommuting cosmic strings*, Phys.Rev.Letters **78** (1997), 2066–2069.

[7] P. Coles and F. Lucchin, *Cosmology - the origin and evolution of cosmic structure*, 2nd ed., Wiley, 2002.

[8] E. Copeland and N. Turok, *Cosmic string interactions*, Fermilab preprint **86/127-A** (1986).

[9] M. Creutz, L. Jacobs, and C. Rebbi, *Monte Carlo computations in lattice gauge theories*, Physics Reports **95** (1983), 201–282.

[10] de Vega H.J. and Schaposnik F.A., *Classical vortex solution of the abelian Higgs model*, Phys.Rev.D **14** (1976), 1100–1106.

[11] L. Dolan and R. Jackiw, *Symmetry behavior at finite temperature*, Phys.Rev.D **9** (1974), 3320.

[12] A. Hanany and K. Hashimoto, *Reconnection of colliding cosmic strings*, JHEP **0506** (2005), 021.

[13] M.B. Hindmarsh and T.W.B. Kibble, *Cosmic strings*, Rept.Prog.Phys. **58** (1995), 477–562, hep–ph/9411342.

[14] J.B. Kogut, *The lattice gauge theory approach to quantum chromodynamics*, Rev.Mod.Phys. **55** (1983), 775–836.

[15] F. Lenz, *Topological concepts in gauge theories*, Lectures given at Autumn School 'Topology and Geometry in Physics' in Heidelberg (2001), hep–th/0403286.

[16] C.J.A.P. Martins and E.P.S. Shellard, *Quantitative string evolution*, Phys.Rev.D **54** (1996), 2535–2556, hep–ph/9602271.

[17] C.J.A.P. Martins and E.P.S. Shellard, *Extending the velocity-dependent one-scale string evolution model*, Phys.Rev.D **65** (2002), 043514, hep–ph/0003298.

[18] C.J.A.P. Martins, E.P.S. Shellard, and J.N. Moore, *Unified model for vortex-string network evolution*, Phys.Rev.Lett. **92** (2004), 251601, hep–ph/0310255.

[19] R.A. Matzner, *Interaction of U(1) cosmic strings: Numerical intercommutation*, Computers in Physics **2** (1988), 51–64.

[20] J.N. Moore, E.P.S. Shellard, and C.J.A.P. Martins, *On the evolution of abelian-Higgs string networks*, Phys.Rev.D **65** (2002), 023503, hep–ph/0107171.

[21] K.J.M. Moriarty, E. Myers, and C. Rebbi, *Dynamical interactions of cosmic strings and flux vortices in superconductors*, Phys.Lett.B **207** (1988), 411–418.

[22] K.J.M. Moriarty, E. Myers, and C. Rebbi, *A vector code for the numerical simulation of cosmic strings and flux vortices in superconductors on the ETA-10*, Computer Physics Communications **54** (1989), 273–294.

[23] E. Myers, C. Rebbi, and R. Strilka, *Study of the interaction and scattering of vortices in the abelian Higgs (or Ginzburg-Landau) model*, Phys.Rev.D **45** (1992), 1355–1364.

[24] H.B. Nielsen and P. Olesen, *Quantitative string evolution*, Nucl. Phys. B **61** (1973), 45.

[25] L. Pogosian, M. Wyman, and I. Wasserman, *Observational constraints on cosmic strings: Bayesian analysis in a three-dimensional parameter space*, JCAP **0409** (2004), 008, astro–ph/0403268.

[26] J. Polchinski, *Introduction to cosmic F- and D-strings*, Lectures presented at the 2004 Cargese Summer School (2004), hep–th/0412244.

[27] W.H. Press, B.P. Flannery, S.A. Teukolsky, and W.T. Vetterling, *Numerical recipes in C*, 1st ed., Cambridge University Press, 1988.

[28] E.P.S. Shellard, *Cosmic string interactions*, Nuc.Phys.B **283** (1987), 624–656.

[29] Vachaspati T. and Vilenkin A., *Formation and evolution of cosmic strings*, Phys.Rev.D **30** (1984), 2036–2045.

Acknowledgements

The author wishes to thank prof. Ana Achúcarro, who supervised the research presented in this MSc thesis and was always available to answer my questions and to explain the physics behind the mathematical expressions I encountered in my work. I am also grateful to Jon Urrestilla for his useful advice during the early stages of this research project. This project was carried out during part of the year 2005 in the student room of the Lorentz Institute in Leiden. During this time, I was in the good company of a group of fellow students, who all had a part in making this a pleasant time for me. Their names are Timon Idema, Leo van Nierop, Jorrit Glastra, Jan Willem van de Meent, Luuk Ament and Rutger van Haasteren. In particular, the discussions about high energy physics with Leo, the help from Timon and at a later stage Jan Willem with many a computer problem and the musical contributions from Jorrit should not be left unmentioned. Besides these people there is of course a whole list of people, family and friends, who in some way helped me get to this point, but it takes too far to mention all those people here.

Roland de Putter,
Oktober 2005